The 2018 Europhysical Conference on Defects in Insulating Materials

8–13 July, 2018

EURODIM'18

BYDGOSZCZ
POLAND

BOOK OF ABSTRACTS

Contents

SCIENTIFIC PROGRAM
I. Oral presentations

Monday, 09.07.2018

S1 Fundamental physical phenomena. Dedicated to Fritz Luty memory

MoS1-P1	**P. Dorenbos**	***The levels of lanthanide point defects in inorganic compounds and deliberate design of electro-optical properties***
MoS1-K1	**M. Peng**	***A tango with bismuth***
MoS1-O1	F. Bridges	*Meta-stable dopant/compensator configurations and local distortions in optical crystals*
MoS1-O2	H. Vrielinck	*What paramagnetic vanadyl probe Ions tell us about framework transformations in metal-organic frameworks*

S2 Electronic excitations, excites state dynamics, radiative and non-radiative relaxations - 1

MoS2-K2	**G. Corradi**	***Excitonic scenarios of hopping, pinning and recombination in $LiNbO_3$***
MoS2-O3	S. Messerschmidt	*Temperature-dependent transient absorption and luminescence due to self-trapped excitons in Fe and Mg-doped $LiNbO_3$*
MoS2-O4	M. Bazzan	*Polaron physics in lithium niobate: theory vs experiments*
MoS2-O5	R.T. Williams	*Self-trapped excitons and Ce excited states studied by picosecond absorption spectroscopy in $La_{(1-x)}Ce_xBr_3$ with $0 < x \leq 1$*
MoS2-O6	M. Grinberg	*Luminescence quenching mechanisms in $Gd_3Al_2Ga_3O_{12}:Ce^{3+}$ and $Gd_3Ga_5O_{12}:Ce^{3+}$ phosphors*
MoS2-O7	V. Nagirnyi	*The role of lattice relaxation in the processes of luminescence, energy transfer and storage in doped lithium tetraborate*

S3 Point and extended defects in wide band-gap systems

MoS3-K3	**M. Kitaura**	***Mg^{2+} codoping effect on shallow electron traps in Ce:$Gd_3Al_2Ga_3O_{12}$ crystals***
MoS3-K4	**A.I. Popov**	***Thermal annealing of F-type centers in irradiated solids: A critical analysis of experimental and theoretical studies***
MoS3-O8	B. Berzina	*Luminescent nitrogen vacancy type defects in III group element nitrides AlN and hBN*
MoS3-O09	A. Suchocki	*Controlling luminescence of transition metal and rare-earth dopands using high pressures*
MoS3-O10	L. Flores	*Study of near infrared photoluminescence in Yb^{3+}, Er^{3+} and Yb^{3+}, Tb^{3+} co-doped silicon oxycarbide thin films*
MoS3-O11	Y. Hizhnyi	*Optical properties and electronic structure of Te- and Al-doped ZnSe crystals*

S4 Thin film and composite scintillators and low-dimensional systems

MoS4-K5	**M. Kucera**	***Development of film garnet scintillators based on the garnet compounds***
MoS4-O12	J. A. Mares	*α- and gamma-rays characterization of single crystalline films and composite scintillators*
MoS4-O13	S. Witkiewicz -Łukaszek	*Composite scintillators based on the doped LuAG crystals and films for simultaneous registration of α-particles and γ-quanta*
MoS4-O14	T. Runka	*Raman spectroscopy of Ce^{3+} doped $Lu_3Al_5O_{12}$ single crystalline films grown onto $Y_3Al_5O_{12}$ substrate*
MoS4-O15	V. Gorbenko	*Efficiency of Bi^{3+}-Yb^{3+} energy transfer in luminescent materials based on the single crystalline films of $Y_{3-x}Lu_xAl_{5-y}Ga_yO_{12}$:Yb,Bi garnets*

Tuesday, 10.07.2018

S5 Defects at surfaces and interfaces

TuS5-P2	**I. Moreels**	***Defects, defect mitigation and doping in highly fluorescent colloidal nanoplatelets***
TuS5-K6	**P. Dereń**	***The role of defects in the stabilization of Eu^{2+} in dielectrics***
TuS5-O16	K. Fabisiak	*Study of defects in chemical vapor deposited diamond films*
TuS5-O17	P. Goswami	*Effect of magnetic Impurities on monolayer uniaxially strained graphene on TMD*
TuS5-O18	P. Galinetto	*Structural, electronic and magnetic properties of pure and poped $FeNb_{11}O_{29}$*

S6 Radiation effects, radiation induced defects, colour centers

TuS6-K7	**P. Bilski**	***Application of color centers in LiF crystals for fluorescent imaging of nuclear particles tracks***
TuS6- O19	R. M. Montereali	*Visible photoluminescence of colour centres in lithium fluoride detectors for low-energy proton beam Bragg curve imaging and dose mapping*
TuS6- O20	A. Lushchik	*Fast-neutron-induced and as-grown structural defects in Mg-Al spinel crystals with different Stoichiometry*
TuS6-O21	E. Friedland	*Influence of inelastic stopping on critical amorphization parameters of indium arsenide implanted with heavy ions*
TuS6-O22	J. Schuyt	*Radiation induced changes in the luminescent properties of Mn and Sm doped $NaMgF_3$ for non-destructive radiation dosimeter readout*
TuS6-O23	S. Kurosawa	*Scintillation and optical properties for Ce-doped $(Gd,La)_2Si_2O_7$ in Low Temperature*

S7 Defects and material preparation technology

TuS7-K8	**Z. Galazka**	***Defects in ultra-wide-bandgap oxide semiconductor β-Ga_2O_3***
TuS7-K9	**M. Batentschuk**	***Defects in light conversion phosphors with a high fluorescence quantum yield for white light emitting diodes and solar cells*** *(NANOLUX 2014 #286)*
TuS7-O24	L. Chepyga	*Investigation of the influence of Mg^{2+} and Si^{4+} substitution on the emission properties of $Y_3Al_5O_{12}:Ce^{3+}$ as luminescence converter for white light emitting diodes (NANOLUX 2014 #286)*
TuS7-O25	Yu. Zorenko	*Single crystalline films in investigation of the intrinsic and defect–related luminescence of garnet compounds (NANOLUX 2014 #286)*
TuS7-O26	M. Valerio	*Synthesis and characterization of pure and doped $BaAl_2O_4$ via a modified Sol-Gel route using PVA*
TuS7-O27	M. Guzik	*Transparent ceramics based on rare earth ions-doped cubic tungstate/ molybdate matrices: a challenge and prospect for new efficient optical materials?*

S8. Defect diffusion, ionic relaxations, ionic transport

TuS8-K10	**R. Merkle**	***Defects and transport in perovskites with protons, oxygen vacancies and electron holes***
TuS8-O28	S. Łoś	*The charge transport characterization of thin diamonds layer by impedance method*
TuS8-O29	P. Szroeder	*Impact of defects, strain, and magnetic field on electronic states in graphene and heterogeneous charge transfer kinetics*
TuS8-O30	Y.J. Wang.	*Hole trap process and highly sensitive optical thermometry, host-sensitized and IVCT interfered in Pr^{3+}-doped $Na_2La_2Ti_3O_{10}$ micro-crystals with layered perovskite structure*

S9 Luminescence spectroscopy of excitons, impurities, and defects, including using of synchrotron radiation – 1

WeS9-P3	**G. Boulon**	***Distribution of dopants in crystals/ceramics/glasses/glass-ceramics analyzed by the conjugation of TEM, EDX, XPS and optical spectroscopic tools***
WeS9-K11	**Z. Barandiarán**	***A new model to explain anomalous emission from CaF_2:Yb and other systems***

WeS9-O31	S. Feofilov	*Luminescence zero-phonon lines of $3d^3$ Ions in garnet solid solutions with disorder in different cation sublattices*
WeS9-O32	L. Seijo	*Exploring widespread hypotheses of luminescence with multiconfigurational ab initio calculations*
WeS9-O33	K. Lengyel	*Cooperative luminescence of Yb pairs in $Li_6Y(BO3)_3$ single crystals*

S10 Luminescence spectroscopy of excitons, impurities, and defects, including using of synchrotron radiation – 2

WeS10-K12	**M. Kirm**	***Relaxation of intrinsic and extrinsic excitations in nano- to micro-size alumina***
WeS10-O34	A. Voloshinovskii	*Relaxation of electron excitations in CeF_3 nanocrystals*
WeS10-O35	Y. Zhydachevskyy	*Quantum efficiency of the down-conversion process in some Bi^{3+}-Yb^{3+} or Ce^{3+}-Yb^{3+} co-doped oxide phosphors*
WeS10-O36	V. Tsiumra	*Localized excitons in Bi-doped YVO_4*
WeS10-O37	A. Andrade	*Luminescent mechanism of RE^{3+} -doped BaY_2F_8 single crystals (RE= Tb, Er, Nd, Pr and Tm)*

Thursday, 12.07.2018

S11 Defects modeling and computational methods

ThS11-P4	**E. Kotomin**	***Large scale first principles modeling of non-stoichiometric perovskites***
ThS11-K13	**M. Engel**	***Colloidal clusters from confined self-assembly***
ThS11-O38	A. Gadomski	*On grain-boundary fingerprint embodied in polycrystalline slowly evolving soft materials*
ThS11-O39	A. Shields	*Shining a light on amorphous UO_3: a computational and experimental approach to understanding amorphous uranium materials*
ThS11-O40	J. Siódmiak	*Modeling of hyaluronic acid in solution: parametrization of the biopolymer molecule in the coarse-grained representation*

S12 Scintillation, energy transfer and storage, carrier trapping phenomena – 1

ThS12-K14	**S. Tanabe**	***Rechargeable persistent phosphors for the first and third bio-imaging windows by traps redistribution***
ThS12-K15	**E. Zych**	***Double doping for energy storage. The case of Lu_2O_3-base ceramics***
ThS12-O41	S. Kim	*Anion vacancy as killer defect in $Cu_2ZnSnS(Se)_4$*
ThS12-O42	Z. Macedo	*Structure, defects, non-stoichiometry and ion migration in bismuth germanate: experimental and computer modeling approaches*
ThS12-O43	I. Venevtsev	*Afterglow decay curves modeled for mixed oxide garnets using TSL measurements*

S13 Scintillation, energy transfer and storage, carrier trapping phenomena – 2

ThS13-K16	**V. Laguta**	***Paramagnetic trapped-electron and trapped-hole centers in oxide scintillators***
ThS13- O44	A.N. Vasil'ev	*Energy transfer to RE Ions in scintillators with the account for excitation density effects*
ThS13-O45	A. Belsky	*Decay mechanisms in YAG-Ce,Mg fibers excited by γ- and X-rays*
ThS13-O46	F. Moretti	*Effect of Au codoping in BaBrCl:Eu scintillating single crystals*
ThS13-O47	Z. Mianowska	*Non-proportionality phenomenon in CsI:Tl scintillators – new observations*
ThS13-O48	K. Bartosiewicz	*Effect of Ce and Mg concentration ratio on the properties of $Gd_3Ga_3Al_2O_{12}$ single crystal scintillators*
ThS13-O49	G. Pilania	*Physics-informed machine learning for rapid screening of potential inorganic scintillator chemistries*

S14 Electronic excitations, excites state dynamics, radiative and non-radiative relaxations - 2

ThS14-K17	**S. Mahlik**	***Determination of the location of impurity and defect states with respect to the bands by high pressure spectroscopy***
ThS14-O50	J. Komar	*Energy transfer and down- and up-conversion phenomena in $Gd_3(Al,Ga)_5O_{12}$ crystals containing Pr^{3+} and Yb^{3+} impurities*
ThS14-O51	L-I. Bulyk	*Eu^{3+} luminescent centers in RE=Y, Gd, Tb aluminum perovskites under high pressure*
ThS14-O52	D. Włodarczyk	*Structural studies focused on $Ca_9R(VO_4)_7$ (R = La, Nd, Gd) whitlockites under elevated pressure*

Friday, 13.07.2018

S15 Nano-crystals, colloids and aggregates

FrS15-K18	**Y. Orlovskii**	***NIR fluorescence concentration self-quenching and quenching by OH- molecular groups in aqueous colloids of Nd^{3+} doped nanocrystals used for bioimaging***
FrS15-O53	A. Vedda	*Radio-luminescence spectral features and fast emission in hafnium dioxide nanocrystals*
FrS15-O54	T. Iwayama	*Optical properties of silicon nanocrystals synthesized by reactive pulsed laser deposition*
FrS15-O55	M. Gomes	*Temperature-sensitive luminescence of $Y_2O_3:Nd^{3+}$ nanocrystals produced by an eco-friendly route*
FrS15-O56	S. Fedorenko	*Luminescence impurity quenching and self-quenching in disordered systems: from bulk to nanoparticles*
FrS15-O57	M. Kushlyk	*Enhancement of YAG:Ce,Yb photoluminescence by Ag nanoparticles*

S16 Material preparation technology and technological applications

FrS16-K19	**E. Yukihara**	***Development of luminescent materials for new thermoluminescence (TL) and optically stimulated luminescence (OSL) applications***
FrS16-O58	T. D. Gustafson	*Progress and challenges towards the development of a new optically stimulated luminescence (OSL) material based on MgB_4O_7*
FrS16-O59	M. Gnyba	*Raman spectroscopic study of diamond foils synthesis*
FrS16-O60	L. Mosińska	*Diamond as a transducer material for the production of biosensors*

II. Poster session I

Tuesday, 10.07.2018

TuP1-1	A.V. Popov	*Concentration self-quenching of luminescence in LaF_3: Nd^{3+} crystals*
TuP1-2	V. Vistovskyy	*Diffusion of 5p-holes in BaF_2 nanoparticles*
TuP1-3	M. Bazzan	*Anomalous diffusion of small electron polarons in lithium niobate*
TuP1-4	V. Dyu	*Dynamics of changes in optical absorption in $Bi_{12}TiO_{20}$:Al crystal induced by nanosecond laser pulses*
TuP1-5	B. Berzina	*Luminescence of doped AlN nanopowders for marking of biological materials*
TuP1-6	E. Edinach	*High-frequency magnetic resonance study of non-Kramers Tb^{3+} ions in yttrium aluminum garnet crystals*
TuP1-7	L. Kovács	*OH^- defects in transition metal ion doped stoichiometric $LiNbO_3$*
TuP1-8	É. Tichy-Rács	*Optical spectroscopy of $Li_6Y(BO_3)_3$ single crystals doped with praseodymium*
TuP1-9	M. Gieysztor	*Time-resolved analysis of the NV centers' fluorescence dynamics*
TuP1-10	R. Merkle	*Proton uptake and mobility in (Ba,Sr,La)FeO_3 perovskites: DFT results*
TuP1-11	P. Szroeder	*Photoluminescence of single-walled carbon nanotube thin Films*
TuP1-12	Yu. Zorenko	*Eu^{3+} multicenter formation and luminescent properties of $Ca_3Sc_2Si_3O_{12}$:Eu and $Ca_2YScMgSiO_{12}$:Eu single crystalline films (NANOLUX 2014 #286)*
TuP1-13	T. Zorenko	*Growth and luminescent properties of $Ca_3Sc_2Si_3O_{12}$:Pr and $Ca_2YScMgSiO_{12}$:Pr single crystalline films (NANOLUX 2014 #286)*
TuP1-14	S. Witkiewicz -Łukaszek	*Luminescent properties of $Ca_3Sc_2Si_3O_{12}$:Mn and $Ca_2YScMgSiO_{12}$:Mn single crystalline films (NANOLUX 2014 #286)*
TuP1-15	B. Shibiri	*Lithiation induced structural changes in layered-spinel bulk and nanoporous Li-Mn-O electrode materials.*
TuP1-16	W. Gieszczyk	*Luminescent properties of undoped and Ce^{3+} doped Y_2O_3–Al_2O_3 double system crystals prepared by micro-pulling down method*
TuP1-17	A. Sulich	*High-resolution XRD study on selected Czochralski-grown rare-earth containing borates and gallates*
TuP1-18	L. Kocsor	*Preparation of $LiNbO_3$ nanocrystals and rare earth diffused layers for quantum optical experiments*
TuP1-19	M. Valerio	*Synthesis and characterization of hydroxyapatite nanoparticles produced via proteic sol-gel method*
TuP1-20	P. Popielarski	*Persistent photoconductivity in ZnO thin films grown on Si substrate by spin coating method*

III. Poster session II

Thursday, 12.07.2018

ThP2-1	M. Buryi	*Permanent and irradiation-induced point defects in molybdenum rich $PbMoO_4$ and their participation in charge trapping processes*
ThP2-2	V. Gorbenko	*Growth and luminescence properties of the β-Ga_2O_3 single crystalline films*
ThP2-3	J. Paterek	*YAG:Ce codoped with Ho^{3+}: energy transfer and acceleration of Ce^{3+} decay*
ThP2-4	M. Rathaiah	*Effect of Ca^{2+} and Si^{4+} co-doping on luminescence and scintillation properties of $Lu_3Al_5O_{12}$: Ce^{3+} epitaxial garnet films*
ThP2-5	S. Kim	*Fabrication and characterization of UV cured polyvinyl toluene based plastic scintillator for 3D printing applications*
ThP2-6	A. Platonenko	*Structural and electronic properties of β-$NaYF_4$ and β-NaYF4:Ce^{3+}*
ThP2-7	G. Pilania	*Materials theory and Informatics for the discovery and optimization of new radiation detector materials*
ThP2-8	B. Rikhotso	*Simulation of structural evolution and ion diffusion in LixTiO_2 nanosheet*
ThP2-9	D.-S. Chao	*Identification of antisite defects and transmuted impurities in gallium arsenide (GaAs) irradiated by fission neutrons*
ThP2-10	V. Gritsyna	*Radiation induced processes in spinel crystals doped with titanium*
ThP2-11	E. Nichelatti	*Modelling of photoluminescence from F_2 and F_3^+ colour centres in lithium fluoride irradiated at high doses by low-energy proton beams*
ThP2-12	D. Ananchenko	*ESR and luminescent properties of anion-deficient α-Al2O3 single crystals after high dose irradiation by pulsed electron beam*
ThP2-13	M. V. dos S. Rezende	*Effect of the amounts of Li^+ additive on the luminescence properties of $LiBaPO_4$:Eu phosphors*
ThP2-14	M. Kemere	*Energy Transfer in Dy^{3+}/Eu^{3+} co-doped glass-ceramics containing fluoride nanocrystallites*
ThP2-15	W. Jadwisienczak	*Synthesis, Characterization and Properties of Multifferroic $Na_{0.5}Bi_{0.5-x}Eu_xTiO_3$ Perovskite Red Phosphor*
ThP2-16	A. Belsky	*Free and bound excitons in ZnO at variable excitation density*
TuP2-17	Rossi M.C.	*Phase transition, structural defects and stress development in superficial and buried regions of femtosecond laser modified diamond*
TuP2-18	L. Mosińska	*The influence of the level of H-termination on wetting properties of CVD diamond surface*
ThP2-19	K. Paprocki	*Morphological and cathodoluminescence study of defects in diamond films grown by HF CVD technique*

ABSTRACTS
IV. Oral presentations

S1 Fundamental physical phenomena

The levels of lanthanide point defects in inorganic compounds and deliberate design of electro-optical properties

Pieter Dorenbos[1,*]

[1] *Delft University of Technology, Faculty of Applied Sciences, Dept. Radiation Science and Technology, section Luminescence Materials, Mekelweg 15, 2629JB, Delft, The Netherlands.*
[*] *Corresponding author*

Point defects in inorganic compounds, either present as contaminant or as deliberate dopant or of intrinsic origin created during the synthesis phase, can participate in optical and electronic phenomena. The energies involved in optical absorption, luminescence, electron or hole trapping in defects, photo- and electrochromic properties, defect valence changes all relate to the electron binding energy difference between the initial and the final state of the process. Such difference can be probed by various spectroscopic methods. Luminescence spectroscopy provides information on the energy level structure of the luminescence ion within its host. Thermoluminescence spectroscopy provides information on how deep an electron or a hole is trapped by a defect, and this relates to the energy differences between the defect ground state and the host valence and conduction bands. Similar information can be obtained from charge transfer bands that appear in spectra when electrons are excited from the valence band to a defect or from a defect to the conduction band [1].

Over the years above type of spectroscopic information for the important class of lanthanide dopants in about 2000 different inorganic compounds has been gathered. The lanthanides, either di- or trivalent, display very systematic properties with increasing number of electrons in the 4f-orbital. It has led to phenomenological models that predict luminescence properties, preferred valence, the depth of electron and or hole trap for all the lanthanides in a specific compound from the knowledge of just one of them [2]. Today schemes can be generated routinely that show the binding energy of electrons in lanthanide states with respect to the host bands but also with respect to the vacuum level [3]. This latter aspect is very important because it enables to compare defect level and host band energies of different compounds with respect to one common energy, i.e., the vacuum level [4].

In this lecture an overview is presented on the models available to determine lanthanide level and host band binding energies, and examples are provided to show how this all affects performance of e.g. luminescence and carrier storage phosphors. The knowledge on host band binding energies forms a solid basis to also derive the binding energies in electronic states of other elements like Bi, Pb, and Tl and transition metal elements, and the latest developments are presented. Finally, all compounds, all dopants, all data together form one unified picture.

[1] P. Dorenbos, *Opt. Materials* **69** (2017) 8.
[2] P. Dorenbos, *ECS Journal of Solid State Science and Technology* **2** (2013) R1.
[3] P. Dorenbos, *Phys. Rev. B* **85** (2012) 165107.
[4] P. Dorenbos, *Phys. Rev. B*. **87** (2013) 035118.

A Tango with Bismuth

Mingying Peng*

The China-Germany Research Center for Photonic Materials and Devices, State Key Laboratory of Luminescent Materials and Devices, School of Material Science and Engineering, South China University of Technology, Guangzhou 510640, China
**Corresponding author: pengmingying@scut.edu.cn*

A new family of laser materials activated by bismuth has aroused great attentions ever since the beginning of this century [1-11]. This is due to their intriguing luminescence broadly distributed from 1000 to 2000nm and therefore the potential applications in broadband optical amplifiers and novel lasers for future optical fiber communication [1-2]. In this talk, I will present our new findings on bismuth doped glasses, fibers and crystals, such as the unusual near to mid infrared luminescence at room temperature, the unexpected effects of glass components and thermal history on the optical properties and so on [1-11]. Following this, I will introduce our efforts to unravel the complex nature of the infrared luminescence, which has confused us for quite long time [2-7]. In the end, I will try to present our latest work on photothermal effects of Bi doped glass and their applications in bone tumor therapy and bone repair [11].

[1] M. Peng, J. Qiu, D. Chen, X. Meng, X. Jiang, and C. Zhu, *Opt. Lett.* **29**(2004)1998.
[2] R. Cao, M. Peng, L. Wondraczek, and J. Qiu, *Opt. Express* **20** (2012) 2562.
[3] J. Zheng, M. Peng, F. Kang, R. Cao, Z. Ma, G. Dong, J. Qiu, and S. Xu, *Opt. Express* **20** (2012) 22569.
[4] L. Wang, Y. Zhao, S. Xu, and M. Peng, *Opt. Lett.* **41**(2016)1340.
[5] F. Kang, H. Zhang, L. Wondraczek, X. Yang, Y. Zhang, D. Lei, and M. Peng, *Chem. Mater.* **28** (2016) 2692.
[6] F. Kang, M. Peng, D. Lei, and Q. Zhang, *Chem. Mater.* **28** (2016) 7807.
[7] J. Han, L. Li, M. Peng, B. Huang, F. Pan, F. Kang, L. Li, J. Wang, and B. Lei, *Chem. Mater.* **29** (2017) 8412.
[8] Y. Xue, J. Cao, Z. Zhang, L. Wang, S. Xu, , and M. Peng, *J. Am. Ceram. Soc.* **101** (2018) 624.
[9] X. Li, J. Cao, L. Wang, and M. Peng, *J. Am. Ceram. Soc.* **101** (2018) 1159.
[10] Z. Zhang, J. Cao, Y. Xue, L. Tan, S. Xu, Z. Yang, and M. Peng, *J. Am. Ceram. Soc.* **101** (2018) 1916.
[11] L. Wang, N. Long, L. Li, Y. Lu, M. Li, J. Cao, Y. Zhang, Q. Zhang, S. Xu, Z. Yang, C. Mao, and M. Peng, *Light: Science & Applications*, 2018, doi: 10.1038/s41377-018-0007-z.

Meta-stable dopant/compensator configurations and local distortions in optical crystals

Frank Bridges [1,*], Cameron MacKeen, [1], László Kovács [2], and Zoila Barandiarán [3]

[1]*Physics Department, University of California, Santa Cruz, California 95064, USA*
[2]*Institute for Solid State Physics and Optics, Wigner Research Center for Physics, Budapest, Hungary*
[3]*Departamento de Química, Instituto Universitario de Ciencia de Materiales Nicolás Cabrera, and Condensed Matter Physics Center (IFIMAC), Universidad Autónoma de Madrid, 28049 Madrid, Spain*
[*]*Corresponding author*

Dopants are incorporated into many crystalline materials to control a wide range of physical properties - here we focus more on optical properties. Even at relatively low impurity concentrations, significant changes can be induced in the optical absorption, photorefraction coefficient and other non-linear optical parameters. For non-isovalent dopants, charge compensating defects are needed, either as substitutional defects or as interstitials, and consequently there can be multiple distributions of the dopant/compensator combination. Here we consider two optical systems CaF_2 doped with Yb and $LiNbO_3$ doped with Zn, In, Er, and Hf. Both host crystals have very high melting points and for $LiNbO_3$ there are two possible substitution sites. An important question is whether the dopant/compensator distributions that form when the material crystallizes at high temperatures, are still in thermal equilibrium at room temperature. Based on EXAFS and XANES results for these systems we propose that in many cases the distributions are likely meta-stable, quenched in as the crystal cooled. For CaF_2:Yb the valence of Yb can be changed by exposure to high intensity x-rays at 200K and this leads to changes in the XANES and several distinct dopant/compensator distributions[1] with different properties. For $LiNbO_3$ the substitution site, extracted from EXAFS, does not always agree with calculations[2], and it is likely that different dopant/compensator distributions have different properties. Also the local distortions induced about the dopant cation vary significantly with the type of cation. Consequently learning how to control such distributions in a systematic way should provide new ways to control the properties of these systems.

[1] C. MacKeen, F. Bridges, L. Seijo, Z. Barandiarán, M. Kozina, A. Mehta, M. F. Reid, and J.-P. R. Wells, *J. Phys. Chem. C* **121** (2017) 28435; C. MacKeen, F. Bridges, M. Kozina, A. Mehta, M. F. Reid, and J.-P. R. Wells and Z. Barandiarán, *J. Phys. Chem Lett.* **8** (2017) 3313.
[2] F. Bridges, C. Mackeen, and L. Kovács, *Phys. Rev. B* **91** (2016) 014101.

What Paramagnetic Vanadyl Probe Ions Tell Us About Framework Transformations In Metal-Organic Frameworks

Henk Vrielinck [1,*], Irena Nevjestic [1], Kwinten Maes [1], Hannes Depauw [2], Pascal Van Der Voort [2] and Freddy Callens [1]

[1] *Ghent University, Dept. of Solid State Sciences, Krijgslaan 281-S1, B-9000 Gent, Belgium*
[2] *Ghent University, Dept. of Chemistry, Krijgslaan 281-S3, B-9000 Gent, Belgium*
[*] *Corresponding author*

MIL-53(Al) is a metal-organic framework (MOF) constructed from Al-OH metal-inorganic chains connected by benzene dicarboxylate (BDC) organic linkers. After synthesis the framework exhibits an orthorhombic crystal structure characterized by large pores, which are blocked by unreacted linker and solvent molecules. After removal of these molecules from the pores, this MOF exhibits breathing: temperature, pressure and exposure to guest molecules like CO_2 and H_2O trigger transformations between a closed pore state with monoclinic crystal structure, and an open pore state with orthorhombic crystal symmetry. In the closed pore state the degree of hydration of the framework has a marked influence on the lattice parameters. In the open pore state the framework is dehydrated. A multifrequency EPR study of paramagnetic vanadyl (VO) dopant ions replacing (AlOH) in MIL-53(Al) allowed to distinguish the as synthesized, hydrated and dehydrated closed pore and the open pore states of this framework [1] and the conditions for bringing the framework (nearly exclusively) in one of these states have been established. Moreover, we found that O_2 can enter the framework and broaden the VO EPR spectrum in the open pore state, but not in the closed pore states.

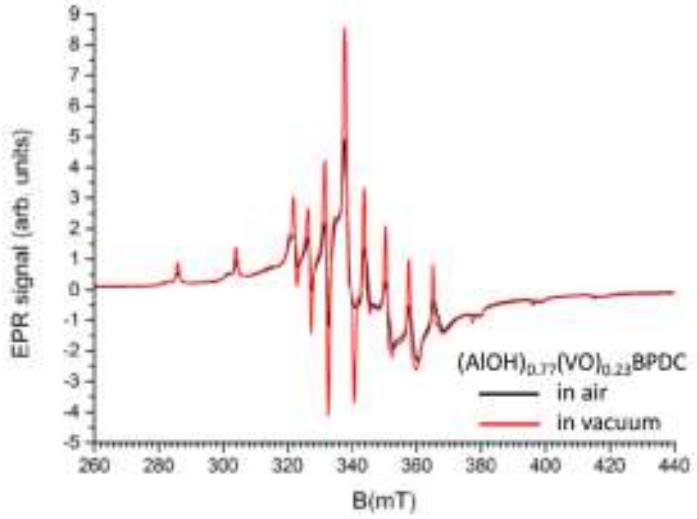

Figure 1: X-band (9.5 GHz) EPR spectrum of $(AlOH)_{1-x}(VO)_x$ BPDC, recorded at room temperature in ambient air and in vacuum.

We recently studied a mixed metal $(AlOH)_{1-x}(VO)_x$-BPDC (BPDC=biphenyl dicarboxylate) MOF series, isostructural to MIL-53(Al), but exhibiting a different type of breathing [2]. The EPR spectrum of VO dopant centres in these frameworks (see Figure 1) shows certain similarities with those in MIL-53(Al), but also remarkable differences.

[1] I. Nevjestić, et al., *Phys. Chem. Chem. Phys.* **19** (2017) 24545.
[2] H. Depauw, et al., *J. Mater. Chem. A* **5** (2017) 24580.

S2 Electronic excitations, excites state dynamics, radiative and non-radiative relaxations – 1

Excitonic Scenarios of Hopping, Pinning and Recombination in $LiNbO_3$

Gábor Corradi [1,2,*], Simon Messerschmidt [1], Andreas Krampf [1], Felix Freytag [1], Mirco Imlau [1], Laura Vittadello [3], Marco Bazzan [3]

[1] *School of Physics, Osnabrück University, Barbarastraße 7, D-49076 Osnabrück, Germany*
[2] *Institute for Solid State Physics and Optics, Wigner Research Centre for Physics, Hungarian Academy of Sciences, Konkoly-Thege út 29-33, H-1121 Budapest, Hungary*
[3] *Dipartimento di Fisica e Astronomia, Universitá di Padova, Via Marzolo 8, 35135 Italy*
[*] *Corresponding author*

Nb^{4+}– O^- relaxed pairs created at early stages of band-to-band pumping (called self-trapped excitons, STE), consisting of a hole and an electron polaron binding each other within a NbO_6 octahedron, were only treated as recombination centers in earlier photoluminescence (PL) studies and completely disregarded in the discussion of transient absorption (TA) experiments. However, fs-pulse-induced PL experiments in Mg-doped $LiNbO_3$ display low temperature decay times on the minute scale and survival of the emission up to room temperature in multi-domain samples (see [1] and references therein). Recent combined studies of ultrashort laser pulse induced TA and PL, carried out in $LiNbO_3$ doped with Fe or Mg in the 20-400 K temperature range, suggest a purely excitonic scenario to play an important role comparable to processes involving polaron hopping [2].

In this work STEs are suggested to be hopping entities capable to pinning on various defects which results in various radiative and non-radiative recombination paths, yielding in particular TA components of longer time scale than single-site polaronic processes without STE formation. Each transient component both in TA and PL can be described with a stretched exponential function with a lifetime $\tau(T)$ having an Arrhenius type temperature dependence down to a characteristic temperature T_c and a stretching factor $\beta(T)$ steeply changing near the same T_c. For faster processes, upon lowering the temperature, the observed decreasing β values can be ascribed to the increasing dominance of polaron hopping, while reverse $\beta(T)$ dependence observed for slower processes can be attributed to STE decay with increasingly mono-exponential character due to STE pinning. This fingerprint behavior of $\beta(T)$ is also supported by markedly different activation energies for STE and polaron decay.

Possible pinning defects including both intrinsic defects and impurities are considered, yielding a coherent description of various TA components in different $LiNbO_3$ systems. In particular, a two-step pinned-STE decay process on Fe is discussed explaining in a natural way all peculiarities of the TA in Fe doped $LiNbO_3$. Similar processes involving shallow pinning defects influencing STE hopping may be considered for PL. Defect models with different local distortions are discussed to connect local changes of the electron-phonon coupling to the lifetimes of various relaxation channels, contrasting also the hopping behavior of STEs and single-site polarons.

[1] T. Kämpfe, A. Haußmann, L. M. Eng, P. Reichenbach, A. Thiessen, T. Woike, R. Steudtner, *Phys. Rev. B*, **93** (2016) 174116.
[2] S. Messerschmidt, A. Krampf, F. Freytag, M. Imlau, L. Vittadello, M. Bazzan, G. Corradi, *submitted*

Temperature-Dependent Transient Absorption and Luminescence due to Self-Trapped Excitons in Fe and Mg-doped $LiNbO_3$

Simon Messerschmidt [1,*], Andreas Krampf [1], Felix Freytag [1], Mirco Imlau [1], Laura Vittadello [2], Marco Bazzan [2], Gábor Corradi [1,3]

[1] *School of Physics, Osnabrück University, Barbarastraße 7, D-49076 Osnabrück, Germany*
[2] *Dipartimento di Fisica e Astronomia, Universitá di Padova, Via Marzolo 8, 35135 Italy*
[3] *Institute for Solid State Physics and Optics, Wigner Research Centre for Physics, Hungarian Academy of Sciences, Konkoly-Thege út 29-33, H-1121 Budapest, Hungary*
[*] *Corresponding author*

Earlier room temperature results on the transient absorption (TA) in the near IR to near UV range in $LiNbO_3$ could be explained by the capture of polarons by Fe^{3+} and trapped-hole defects, leaving a number of open questions concerning the exact functional shape of the decay components, their spectral distribution, and the existence of TA even on the minute scale [1,2]. Photoluminescence (PL) and its temperature dependence on the other hand were attributed to the radiative decay of self-trapped excitons (STE) formed via polaron hopping, showing a marked dependence on crystal composition and doping [3].

To bridge the gaps between various interpretations, in this work combined TA/PL investigations comprising broad temperature (20-400 K) and temporal ranges and different dopings were carried out. Nanosecond pulses derived from a Nd:YAG laser were applied for time resolved measurements with λ=532 nm and *E*pulse <= 290 mJ for TA and λ=355 nm and *E*max = 120 mJ for PL, respectively. CW probe lasers selected from λ= 445 nm to 1310 nm and a digital oscilloscope were used to detect the dynamic transmission loss. Pulse induced PL dynamics were measured by spectrally selective photon counting. Emission spectra were recorded using a frequency-doubled Ti:Sapphire fs laser with λ=400 nm and E_{pulse} = 40 µJ.

TA results in 0.1 mol% Fe doped $LiNbO_3$ show, for decreasing temperatures, an increasing temporal separation of fast and slow stretched-exponential components, with contrasting behaviors of their $\beta(T)$ stretching factors. The longer scale TA in the blue region, especially for the wavelength λ= 445 nm, is dominated by an Fe-related component providing an interim maximum. In 6.5 mol% Mg doped $LiNbO_3$ a similar but weaker feature at λ= 445 nm is observed at room temperature due to background Fe impurities, while the shorter timescale in the latter case is characterized by a decreasing component for all probe wavelengths. PL in 6.5 mol% Mg-doped $LiNbO_3$ can be described by a single decaying component with a $\beta(T)$ fingerprint similar to that of long TA components. These findings can only be explained by considering, in addition to processes involving polaron hopping, the existence of long-lived excitonic states absorbing in the blue spectral range and decaying non-radiatively [4]. The involved STE-scenarios will be discussed in a separate contribution.

[1] P. Herth, D. Schaniel, T. Woike, T. Granzow, M. Imlau, E. Krätzig, *Phys. Rev. B* **71** (2005) 125128.
[2] D. Conradi, C. Merschjann, B. Schoke, M. Imlau, G. Corradi, K. Polgár, *Phys. Stat. Sol. (RRL)* **2** (2008) 284.
[3] D. M. Kroll, G. Blasse, *J. Chem. Phys*. **73** (1980) 163
[4] S. Messerschmidt, A. Krampf, F. Freytag, M. Imlau, L. Vittadello, M. Bazzan, G. Corradi, submitted.

Polaron Physics in Lithium Niobate: Theory vs Experiments

M. Bazzan [1,*], L. Vittadello [1], L. Guilbert [2], I. Mhaouech [2], M. Aillerie [2], S. Messerschmidt [3], M. Imlau [3], A. Danielyan [4] and E. Kokanyan [4]

[1]*Università di Padova - Physics and Astronomy Dept., Via Marzolo 8, Padova, Italy*
[2]*Université de Lorraine, LMOPS et CentraleSupélec, 2 rue E. Belin, F-57070 Metz, France*
[3]*School of Physics, Osnabrueck University, Barbarastrasse 7, 49076, Osnabrueck, Germany*
[4]*Armenian State Pedagogical University after Kh. Abovyan and Institute for Physical Research, National Academy of Science, Tigran Metsi Ave., 17, Yerevan, Armenia*
[*]*Corresponding author*

Lithium niobate ($LiNbO_3$, LN) is often taken as a paradigm for light-induced charge transport phenomena in oxide crystals. Understanding these phenomena is crucial for practical applications in the fields of nonlinear and ultra-fast optics [1], photorefractive holography [2], integrated optics [3] and ferroelectric photovoltaics [4]. It is nowadays accepted that the basic description of the experimentally observed behaviors must be attempted in terms of polarons hopping among regular or defective lattice sites. In this contribution it will be shown how this task can be successfully accomplished by Monte-Carlo methods based on the Marcus-Holstein model [5,6,7]. The basic parameters of the model can be determined either by independent spectroscopic measurements, either by comparing the simulation results with temperature dependent experiments, in particular time-resolved transient absorption spectroscopy [8] and photorefractive characterization. The simulations provide an insight on how the experimentally observed dependencies can be explained in terms of prevalence of one or another hop type and, by comparison with data, allow estimating some poorly known parameters related to the photo-excitation process.

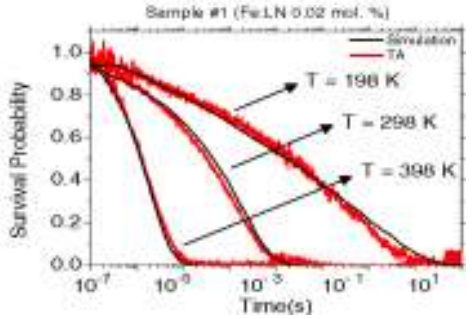

Figure 1: Comparison between experimental data and simulation of light-induced effects in Fe:LN. (Left) Transient absorption decays at 785 nm at different temperatures. (Right) Saturation space charge field as a function of temperature and for different trap concentrations.

[1] Imlau M., et al. 2015 *Appl. Phys. Rev*. **2** 040606
[2] Gunther P. and Huignard J.-P. *Photorefractive Materials and their applications,* 2006
[3] Bazzan M. and Sada C. 2015 *Appl. Phys. Rev*. **2**, 040603
[4] He, J.et al., J. M., *Chemistry of Materials*, 2016, **28**, 25-29
[5] Marcus, R. A., *The Journal of Chemical Physics*, 1956, **24**, 966-978
[6] Holstein, T. *Annals of Physics*, 1959, **8**, 343 – 389
[7] Mhaouech I. and Guilbert L., *Solid State Sciences*, 2016, **60**, 28 – 36
[8] Guilbert L., et al., *Journal of Physics: Condensed Matter*, 2018, **30**, 125701

Self-Trapped Excitons and Ce Excited States Studied by Picosecond Absorption Spectroscopy in $La_{(1-x)}Ce_xBr_3$ with $0 < x \leq 1$

Richard T. Williams [1,*], Peiyun Li [1], Sergii Gridin [1], K. Burak Ucer [1], and Peter R. Menge [2]

[1] *Department of Physics, Wake Forest University, Winston Salem, NC 27106, USA*
[2] *Saint-Gobain Crystals, 17900 Great Lakes Parkway, Hiram, OH 44234, USA*
[*] *Corresponding author*

Picosecond time-resolved optical absorption spectra induced by two-photon interband excitation of $LaBr_3$, $LaBr_3$:Ce(4.4% and 22.2%), and $CeBr_3$ are reported. The spectra are similar in general characteristics to self-trapped exciton (STE) absorption previously measured in alkali halides and alkaline-earth halides. A broad ultraviolet absorption band results from excitation of the self-trapped hole within the STE. A series of infrared and red-visible bands results from excitation of the bound outer electron within the STE similar to bands found in alkali halides corresponding to different degrees of "off-center" relaxation. Induced absorption in cerium-doped $LaBr_3$ after band-gap excitation of the host exhibits similar STE spectra, except decaying faster on the tens-of-picoseconds scale in proportion to the Ce concentration. This is attributed to dipole-dipole energy transfer from STE to Ce^{3+} dopant ions, and the measurements yield the concentration-dependent dipole-dipole transfer rate. The absorption spectra were also measured after direct excitation of the Ce^{3+} ions in $LaBr_3$:Ce with sufficient intensity to drive 2- and 3-photon resonantly enhanced excitation. In this case the spectrum attributed to STEs created adjacent to Ce^{3+} ions decays in 1 picosecond, attributed to dipole-dipole transfer from the nearest-neighbor separation. A transient absorption band at 2.2 eV growing with Ce concentration in $LaBr_3$ is found and attributed to a charge-transfer excitation of the Ce^{3+*} excited state responsible for scintillation in $LaBr_3$:Ce crystals. This study concludes that energy transport resulting in scintillation of $LaBr_3$:Ce proceeds mainly by STE rather than sequential trapping of holes and electrons on Ce^{3+} ions. While the time scale of these induced absorption measurements is shorter than the scintillation measurements in $LaBr_3$:Ce made by Bizarri and Dorenbos [1], the results are complementary and seem in basic agreement where they overlap. We suggest that dipole-dipole transfer from STEs at their point of creation (i.e. before hopping) is the main part of the "Prompt transfer" process identified in Ref. [1]. Furthermore the temperature-dependent change of emission/absorption overlap determining dipole-dipole transfer rate probably accounts for the "Fast Process II" of temperature-dependent STE/Ce transfer in the immediate neighborhood of Ce, having activation energy different from Slow Process II associated with STE diffusion [1]. With extension of the picosecond absorption measurements to $CeBr_3$, we have data to motivate contemplation of what happens when the activator becomes identical with the cation consitituent of the crystal in which the STE is still observed. On what time scale are STEs associated with a hole in the topmost filled halogen band, or the topmost filled Ce(4f) band? At what rate do they communicate? This is similar to the situation encountered and discussed earlier in LaF_3 and CeF_3 including their mixture [2]. In that time there were no picosecond absorption measurements in the subject system, but now there are in the bromide sister system.

[1] G. A. Bizarri, P. Dorenbos, *Phys. Rev. B* **75** (2007) 184302.
[2] A.N. Vasil'ev, Proc. SCINT99, ed. V. Mikhailin, Moscow State University (2000) 43.

Luminescence quenching mechanisms in $Gd_3Al_2Ga_3O_{12}:Ce^{3+}$ $Gd_3Ga_5O_{12}:Ce^{3+}$ phosphors

Tadeusz Lesniewski [1], Sebastian Mahlik [1], Kazuki Asami [2], Jumpei Ueda [2], Setsuhisa Tanabe [2], Marek Grinberg [1,*]

[1]Institute of Experimental Physics, Faculty of Mathematics, Physics and Informatics, Gdańsk University, Wita Stwosza 57, 80-308 Gdańsk, Poland
[2]Graduate School of Human and Environmental Studies, Kyoto University, Kyoto 606-8501, Japan

The photocurrent excitation (PCE) spectra were measured at temperature range of 140 – 400 K and 100 – 500 K, for $Gd_3Al_2Ga_3O_{12}:Ce^{3+}$ (GAGG:Ce^{3+}) and $Gd_3Ga_5O_{12}:Ce^{3+}$ (GGG:Ce^{3+}), respectively. The PCE bands were related to ionisation processes of Ce^{3+}, mediated by optical excitation to crystal field splitted levels of 5*d* excited state configuration: $5d_1$ and $5d_2$, which gives a qualitative resemblance of PCE spectra to photoluminescence excitation (PLE) spectra of Ce^{3+} $5d_1 \rightarrow 4f$ emission. A double structure of $4f \rightarrow 5d_1$ transition was observed in the PCE, which is not apparent in the PLE spectra, the origin of which is attributed to the splitting of the lowest level of the 5d electronic configuration due to spin-orbit coupling. As a complementary experiment, we have performed the temperature dependent photoluminescence (PL) kinetics of GAGG: Ce^{3+} as well as photoluminescence measurement of GGG:Ce^{3+} at elevated pressure supplemented by pressure-temperature dependence of PL kinetics. Differences in the mechanism of ionisation transition of excited 5*d* electron of Ce^{3+} in GAGG and GGG host were ascertained on the ground of distinct temperature dependence of photocurrent intensity. The latter system exhibits autoionisation, which occurs when all of the 5*d* excited configuration is degenerated with the conduction band (CB), whereas in the former system, the autoionization process is thermally assisted, which is recognized by strong, exponential temperature dependence of photocurrent signal.

A model describing the relaxation kinetics of excited Ce^{3+} ions, that includes the localized states of Ce^{3+}, CB edge, radiative transitions in Ce^{3+}, autoionization of Ce^{3+} and nonradiative processes in the excited states of the system was developed. Our work shown that in the case of GAGG: Ce^{3+}, where the lowest state of 5*d* electronic configuration is located below the CB, the model is fully consistent with the experimental data of both the PL spectroscopy and PCE spectroscopy. Specifically, the activation barrier for transition from the $5d_1$ to the CB was estimated to be around 1600 cm^{-1}, the same value was obtained from the photoluminescence quenching represented by temperature dependence lifetime. The character of Ce^{3+} ionisation in GGG:Ce^{3+} has been related to lowering of the edge of the CB of the host with increase of Ga content in the host composition. As the result of the degeneration of the $5d_1$ state with CB no Ce^{3+} luminescence is observed in GGG:Ce^{3+}. However, in this case the temperature dependence of PCE spectra cannot be explained without consideration of additional localized state that is located 630 cm^{-1} below the CB of GGG. We attributed this state to the impurity trapped exciton ITE [1].

[1] M. Grinberg, *Optical Materials* **35** (2013) 2006

The role of lattice relaxation in the processes of luminescence, energy transfer and storage in doped lithium tetraborate

Vitali Nagirnyi [1,*], Ivo Romet [1], Maksym Buryi [2], Gábor Corradi [3,1], Eduard Feldbach [1], Valentin Laguta [2], Éva Tichy-Rács [3],

[1]*Institute of Physics, University of Tartu, W. Ostwald Str. 1, 50411, Tartu, Estonia*
[2]*Institute of Physics of the Czech Academy of Sciences, Cukrovarnicka 10/112, 162 00, Prague, Czech Republic*
[3]*Institute for Solid State Physics and Optics, Wigner Research Centre for Physics, Hungarian Academy of Sciences, Konkoly-Thege M ut 29-33, H-1121, Budapest, Hungary*
**Corresponding author*

Due to numerous applications in various technological fields lithium tetraborate, $Li_2B_4O_7$ (LTB), doped and undoped, has been extensively studied for decades. In particular, it attracted attention as a potential tissue equivalent thermoluminescent radiation dosimeter with effective atomic number (Z_{eff} = 7.4) closely matching the Z_{eff} of soft human tissue. However, very peculiar crystal lattice features, such as low local symmetry of lattice sites, ionic mobility, flexible, temperature dependent lattice structure, as well as piezo- and pyroelectric effects made studies of luminescent and EPR spectroscopy difficult and hampered considerably the understanding of energy storage processes in the material.

In the present work, LTB crystals and ceramics doped by manganese alone or codoped by other metal impurities (Cu, Ag etc.) were studied using photoluminescence and thermostimulated luminescence techniques, and, for the first time, EPR measurements of manganese doped LTB were extended from the X band to the Q band for higher resolution. Mn^{2+} ions are shown to substitute dominantly at lithium sites charge compensated by a nearby lithium vacancy. Excitation spectra of the Mn^{2+} ion emission in the energy range of 2.5-20 eV have revealed the specific forbidden transitions within the $3d^5$ electronic configuration as well as allowed electronic transitions to the Mn^{2+} ^6D term split by crystal field into two sub-bands. Based on the EPR studies and the comparison of TSL spectra of irradiated crystals with spectra of photostimulated luminescence, models of energy storage and TSL processes are proposed for irradiated crystals. An efficient energy transfer between various dopant metal ions have been revealed in lithium tetraborate doped with several impurities.

It will be shown that recharging and energy transfer processes taking place in pairs of impurity centres play a crucial role in recombination processes responsible for energy storage and thermally stimulated luminescence in LTB exposed to ionizing radiation. A considerable influence of lithium mobility and local lattice relaxation on these processes in a wide temperature range will be demonstrated.

S3 Point and extended defects in wide band-gap systems

Mg^{2+} cooping effect on shallow electron traps in $Ce:Gd_3Al_2Ga_3O_{12}$ crystals

Mamoru Kitaura

[1]*Faculty of Science, Yamagata University, 1-4-12 Kojirakawa, Yamagata 990-8560, Japan*

Cerium doped $Gd_3Al_2Ga_3O_{12}$ (Ce:GAGG) is known a functional phosphor material widely used in various fields [1,2]. Especially, the high light output for high-energy photons such as X- and γ-rays implies that Ce:GAGG is suitable for the application of scintillator. There are a number of subjects to be solved for the improvement of scintillation performance of this material. One of the subjects is the suppression of crystal defects that are inevitably introduced during crystal growth. For this purpose, the nature of such crystal defects in Ce:GAGG have been studied so far. Thermally-stimulated luminescence (TSL) and photo-stimulated luminescence (PSL) spectroscopies revealed that shallow electron traps locate at around 0.3 eV below the conduction band [3,4]. The UV-induced infrared absorption spectroscopy pointed out that the shallow electron traps are due to defect complexes associated with oxygen vacancies [5].

Mg^{2+} codoping, which accelerates the shortening of the scintillation decay of Ce:GAGG crystals, has recently attracted much attention [6]. Mg^{2+} cooping remarkably weakens the TSL and PSL bands due to shallow electron traps. Also, the UV-induced infrared absorption band does not appears for Mg^{2+} codoped Ce:GAGG. It is, therefore, evident that Mg^{2+} codoping suppresses the formation of shallow electron traps including oxygen vacancies. Since oxygen vacancies are introduced as charge compensators for cation vacancies, the suppression of shallow electron traps by Mg^{2+} codoping is caused by the replacement of Mg^{2+} ions for cation vacancies [7].

The positron annihilation lifetime spectrum, which can prove the distribution of negatively charged lattice sites such as cation vacancies, was reproduced by the superposition of two exponential decay components with the lifetimes of 168 ps and 224 ps. The component with the lifetime of 224 ps was connected to cation vacancies in GAGG, and the integrated intensity was remarkably decreased by Mg^{2+} cooping. It is more likely that the replacement of Mg^{2+} ions for cation vacancies results in the suppression of shallow electron traps.

We could obtained understanding of the Mg^{2+} codoping effect on shallow electron traps in Ce:GAGG. However, the acceleration of scintillation decay due to Mg^{2+} codoping cannot be explained by considering the suppression of shallow electron traps only. Further investigations are now in progress, to find an important key for understanding of Mg^{2+} cooping effect on the improvement of scintillation response.

[1] K. Kamada *et al*., J. Cryst. Growth **352**, 88 (2012).
[2] M. Kitaura *et al*., J. Appl. Phys. **115**, 083517 (2014).
[3] A. Satoh *et al.*, Jpn. J. Appl. Phys. **53**, 05FK01 (2014).
[4] M. Kitaura *et al*., Appl. Phys. Lett. **211**, 031112 (2018).
[5] M. Kitaura *et al*., Appl. Phys. Express 9, 072602 (2016).
[6] K. Kamada *et al*. Opt. Mater. 41, 63 (2015).
[7] M. Kitaura et al., Appl. Phys. Lett. 110, 251101 (2017).

Thermal annealing of F-type centers in irradiated solids: A critical analysis of experimental and theoretical studies

A.I. Popov [1,*], E.A. Kotomin [1], V.N. Kuzovkov [1], A. Lushchik [2]

[1] *Institute of Solid State Physics, University of Latvia, 8 Kengaraga, Riga, LV-1063 Latvia*
[2] *Institute of Physics, University of Tartu, W. Ostwald Str. 1, 50411 Tartu, Estonia*
[*] *Corresponding author: popov@latnet.lv*

The radiation-resistant oxide insulators (MgO, Al_2O_3, $MgAl_2O_4$, BeO etc) are important materials for applications in fusion reactors. It is very important to predict/simulate not only the kinetics of diffusion-controlled defect accumulation under neutron irradiation, but also a long-time defect structure evolution including the thermal annealing of radiation-induced defects.
After introducing some basics on the radiation point defects in halides, binary oxides and oxide perovskites [1] as well as the mechanisms of point defect and metal colloid formation in thermochemically reduced (TCR) or particle irradiated (neutron, ion, proton, electron) samples, the current understanding of their thermal annealing processes will be briefly reviewed.
We will shortly describe the recently developed and successfully applied [2-4] theoretical approach based on the formalism of the correlation functions, describing spatial distribution of both similar (F-F centers) and dissimilar defects (a Frenkel pair of defects: an F center – an interstitial Oi ion) which allows us to study defect kinetics and aggregation much better than generally accepted rate equations or simple first order kinetics.

In particular, the kinetics of the F-type center annealing after electron, heavy ions or neutron irradiation was treated as the bimolecular process with equal concentrations of the complementary F and Oi defects. The process is controlled by the interstitial oxygen ion mobility, which is much higher than that of the F centers. It is demonstrated how the shape of the F-annealing curve is determined by the two control parameters: activation energy and effective pre-exponential factor, and strongly depends on irradiation fluence and other conditions.

The appropriate migration energies were obtained for available in the literature experimental annealing kinetics for electron, neutron and ion irradiated MgO, Al_2O_3, $MgAl_2O_4$, $Y_3Al_5O_{12}$, BeO, ZnO, YSZ, PLZT etc. The results obtained are used for the evaluation of interstitial oxygen migration parameters and are compared with the available *ab initio* calculations. Comparison with an another type of experiments, namely, F-type center annealing in TCR samples, will be also presented for MgO, BeO, $MgAl_2O_4$ and YSZ. The results obtained are used for the evaluation of the activation energies for the F center migration.
Special attention is paid to: (1) dose effects on F center annealing in neutron and fast electron irradiated MgO and MgF_2; (2) a detailed comparison of diffusion-controlled F center thermal annealing in neutron, electron and heavy-ion irradiated MgO, MgF_2, Al_2O_3.

[1] A.I. Popov, E.A. Kotomin, J. Maier, *Nucl. Instr. Meth. B* 268 (2010) 3084.
[2] E.A.Kotomin, V.N. Kuzovkov, A.I. Popov, R. Vila, *Nucl. Instr. Meth. B* 374 (2016) 107.
[3] E.A. Kotomin, V.N.Kuzovkov, A.I. Popov, J.Maier, R.Vila, *J. Phys Chem A* 122 (2018) 28.
[4] V.N. Kuzovkov, E.A. Kotomin, A.I. Popov, *J. Nucl. Mat.* 502 (2018) 295.

Luminescent Nitrogen Vacancy Type Defects in III Group Element Nitrides AlN and hBN

Baiba Berzina*, Laima Trinkler and Valdis Korsaks

Institute of Solid State Physics, University of Latvia, 8 Kengaraga Str., Riga, Latvia
**Corresponding author:Baiba Berzina; baiber@latnet.lv*

Aluminum nitride and hexagonal boron nitride are wide band-gap materials with band gap energy around 6 eV, characterized with wurtzit bulk and hexagonal layered crystalline structures, respectively. Different forms of these materials are available including small size single crystals, polycrystalline powders and various nanostructures. During last two decades these materials are attached interests of many researchers due to their promising optical properties allowing development of far ultraviolet light (FUV) emitters based on exciton processes [1]. We are working on research of these materials for many years using spectral methods of investigation based on luminescence [2].
The aim of the present report is research of spectral properties of AlN and hBN caused by luminescent native defects in order to reveal the luminescence processes and mechanisms together with the defect structure responsible for this luminescence. For this purpose AlN and hBN nanopowders with grain diameter of d ≈ 60 nm and macro-size powders (d >100 nm) were used. Photoluminescence (PL) spectra and luminescence excitation (PLE) spectra were studied within a wide spectral region at various fixed temperatures from an interval between 10 K and 300 K.
It was observed that for both AlN and hBN materials, the spectral characteristics are very close. If one of these materials is excited with UV light it results in blue luminescence (BL) emission. This BL is forming a wide and complex luminescence band peaking at its own spectral position for each material. Excitation spectra of the BL consist of several bands forming three distinct groups. The PLE bands from the far UV region can be related to absorption of the host material resulting in exciton processes but the two others – to native defect absorption.
Analysis of the results obtained allows evaluation of the defects which are responsible for the BL in AlN and hBN. Most probably these defects are nitrogen vacancies (v_N) and related Fcenter type defects. The sub-band structure of the BL can be caused by the varieties of these defects. There are revealed three mechanisms resulting in the BL, which are largely dependent on the wavelength of the exciting light. The BL can be caused through: *i)* energy transfer from the host lattice excitons, *ii)* recombination processes between host lattice defects, and *iii)* direct excitation of luminescent defects.
It was found that the v_N-type surface defects in AlN and hBN are sensitive to oxygen gas surrounding the material, which is partly quenching the BL, in the same time gas is not affecting the luminescence from the material volume. This phenomenon is especially pronounced for the nanomaterials where the ratio of surface to volume is considerably enlarged in comparison with that for the macro-structures. This feature allows ranking of AlN and hBN nanopowders among the materials prospective for development of oxygen gas sensors.

[1] K. Watanabe, T. Taniguchi, K. Miya, Y. Sato, et al., *Diam. & Relat. Mat.* **20** (2011) 849.
[2] B. Berzina, V. Korsaks, L. Trinkler, et al., *Diam. & Relat. Mat.* **68** (2016) 131.

Controlling Luminescence of Transition Metal and Rare-Earth Dopands Using High Pressures

A. Suchocki [1,2]

[1]*Institute of Physics, Kazimierz Wielki University, Weyssenhoffa 11, 85-072, Bydgoszcz, Poland*
[2]*Institute of Physics, Polish Academy of Sciences, Al. Lotnikow 32/46, 02-668, Warsaw, Poland*

Pressure is one of the fundamental thermodynamic variables, which allows for precise changing (decreasing) the interatomic distances of materials. Therefore the strength of the crystal field experienced by emitting ions can be this way effectively increased resulting in changes of electronic structures of host materials and dopant ions. This leads to transformation of luminescence spectra of phosphors. Several examples of such effects will be presented. It will be shown, for example, that pressure: (i) transforms a broad-band luminescence of Cr^{3+} ions in low-strength crystal-field materials (e.g., $LiNbO_3$:Cr) into a sharp line type spectrum, due to a replacement of the Cr^{3+} first excited state from the strongly coupled to the lattice $^4T_2$ state to weakly coupled ^2E state [1]; (ii) changes non-luminescent at ambient pressure materials doped with Ce^{3+} (e.g., GGG:Ce) into highly efficient emitting ones, which is associated with removal of degeneracy of the 5d Ce^{3+} level with conduction band of host [2]; (iii) causes quenching of Mn^{2+} luminescence in certain materials (e.g., $NaScSi_2O_6$:Mn) due to pressure–induced crossing between $^4T_{1g}$ and $^2T_{2g}$ excited states [3]; (iv) induces structural phase transitions, resulting in changes of optical properties of materials, as it occurs in $Y_4Al_2O_9$:Ce [4] . In this way high pressure, which can be applied in precise and controlled way, allows to check and establish the best conditions for obtaining the desired luminescence properties of the material for practical applications.

*Acknowledgements***:** The work was supported by the Polish National Science Center (project 2015/17/B/ST5/01658), and by the EU within the European Regional Development Fund through the Innovative Economy grant (POIG.01.01.02-00-108/09).

1. A. Kamińska, A. Suchocki, et al., *Phys. Rev. B*. 2000, **62**, 10802-10811.
2. A. Kamińska, A. Suchocki, et al. *Phys. Rev. B*, 2012, **85**, 155111.
3. J. Barzowska, Zhiguo Xia, A. Suchocki et al., *RSC Advances* **7**, 275 (2017)
4. Y.J. Wang, A. Suchocki, et al, to be published.

Study of Near Infrared Photoluminescence in Yb^{3+}, Er^{3+} and Yb^{3+}, Tb^{3+} co-doped Silicon Oxycarbide Thin Films

Loreleyn F. Flores [1,*], K. Y. Tucto [1], Rolf Grieseler [1,2], Jorge A. Guerra [1], Jan A. Töfflinger [1], Andres Osvet [3], Miroslaw Batentschuk [3], Albrecht Winnacker [3] and Roland Weingärtner [3]

[1]*Departamento de Ciencias, Sección Física, Pontificia Universidad Católica del Perú, Av. Universitaria 1801, Lima 32, Perú*

[2]*Chair Materials for Electronics, Institute of Materials Engineering and Institute of Micro and Nanotechnologies MacroNano, TU Ilmenau, Gustav-Kirchhoff-Str. 5, 98693 Ilmenau, Germany*

[3]*i-MEET, Department of Material Science and Engineering, University of Erlangen-Nürnberg, Martenstr. 6, Erlangen 91058, Germany*

[*]*flores.lf@pucp.edu.pe*

The use of rare earth ions offers an approach to improve the solar cells efficiency through the application of spectral converters, based on up- and down-conversion. Different hosts were reported and studied to find an enhancement in quantum efficiency. However, to succeed in the implementation of spectral converters in commercial systems solar cells it is necessary to improve the stability and also the resistant to degradation of these converter layers [1]. In this sense amorphous silicon oxycarbides (*a*-SiC_xO_y) have several potential applications due to their good properties such as thermal and photostability, as well as a high hardness [2]. Likewise, it has been shown that *a*-SiC_xO_y is a promising host material to activate optically rare earth ions [3,4]. Among different possible rare earth systems, those with content of Yb^{3+} ions seem to be the most promising for the efficiency improvement of silicon solar cells.

In this work we study the NIR emission of Yb^{3+} in thin films luminescence systems co-doped with the rare earth ion pairs of Yb^{3+}-Tb^{3+} and Yb^{3+}-Er^{3+} with *a*-SiC_xO_y as a host. Thin films were grown on silicon substrates using RF magnetron sputtering. Different concentrations of Yb in the co-doped samples were studied. In order to investigate the chemical composition of the host, energy dispersive spectroscopy (EDS) and Fourier transform infrared spectroscopy (FTIR) were applied. Photoluminescence spectroscopy (PL) and photoluminescence excitation (PLE) examine the efficient conversion or absorption of high energy photons. Finally, sequential post-deposition annealing treatments up to 850 °C revealed the photoluminescence performance of the Yb^{3+} in the luminescence systems Yb^{3+}-Tb^{3+} and Yb^{3+}-Er^{3+}. Emission depending on the annealing temperature and decay lifetime also have been investigated.

[1] M. B. De la Mora, O. Amelines-Sarria, B. M. Monroy, C. D. Hernández-Pérez, and J. E. Lugo, *Sol. Energy Mater. Sol. Cells* **165** (2017) 59.

[2] S. L. Shevchuk and Y. P. Maishev, *Thin Solid Films* **492** (2005) 114.

[3] S. Boninelli, G. Bellocchi, G. Franzò, M. Miritello, and F. Iacona, *J. Appl. Phys*. **113**, (2013) 143503.

[4] S. Gallis, M. Huang, and A. E. Kaloyeros, *Appl. Phys. Lett*. **90** (2007) 19.

Optical Properties and Electronic Structure of Te- and Al-doped ZnSe Crystals

Yuriy A. Hizhnyi [1,*], Sergii G. Nedilko [1], Viktor I. Borysiuk [1], Vitalii P. Chornii [2], Iryna A. Rybalka [3], Sergii M. Galkin [3] and Iryna A. Tupitsyna [3]

[1] *Taras Shevchenko National University of Kyiv, 64/13 Volodymyrska str., 01601 Kyiv, Ukraine*
[2] *National University of Life and Environmental Sciences of Ukraine, 5 Geroiv Oborony st., 03041 Kyiv, Ukraine*
[3] *Institute for Scintillation Materials of NAS of Ukraine, 60 Nauky ave., 61072 Kharkiv, Ukraine*
[*] *Corresponding author*

The crystals of zinc selenide ZnSe are perspective materials to be used in scintillation bolometers for studying of rare event processes in physics of high-energy particles. The ZnSe crystals possess very good thermal and mechanical properties. In addition, ^{82}Se isotope is a candidate for neutrino less double-beta decay, so ZnSe crystals (enriched with ^{82}Se) are very perspective for studying the mentioned rare event process. At present moment, special attention is paid to purity of the ZnSe synthesized raw materials and grown crystals, since the presence of various defects strongly affects the scintillation characteristics. Electronic band structure calculations provide an opportunity to estimate the effect of various defects on the optical properties of crystals. A combination of such calculations with experimental optical spectroscopy studies can clarify the question about influence of defects on the optical and scintillation properties of ZnSe crystals.

The ZnSe samples both pure and doped with controlled impurities Te (C_{Te} = 0.3 %) and Al (C_{Al} = 0.05 %), were grown by Bridgman method. As a raw material, we used ZnSe, obtained by gas-phase synthesis with 5N purity and CVD method with 6N purity. The X-ray luminescence spectra of the samples were measured at the room temperature. The optical transmission spectra of ZnSe, ZnSe(Al) and ZnSe(Te) samples in the visible and infrared spectral ranges were measured.

The geometry optimized calculations of the electronic band structures and optical constants of ideal and defect-containing ZnSe crystals were performed in a supercell approach using the FP-LAPW method [1]. The 3x3x3 supercells were chosen for calculations and the studied defects were: a) substitutional defects of Al atoms on Zn positions, Te or O atoms on Se positions; b) vacancies of Zn and Se; c) combinations of the abovementioned defects. The partial densities of states, the linear optical properties (including absorption and reflectance spectra) and transition levels of defects (defect ionization energies) were calculated and analyzed.

Comparative analysis of experimental and computational results allowed assignment of additional defect-related bands in the optical absorption spectra of ZnSe. The influence of point defects on the luminescence mechanisms of zinc selenide is discussed.

Acknowledgement. Publication is based on the research provided by the grant support of the State Fund for Fundamental Research of Ukraine (project № F76/115-2017).

[1] P. Blaha, et al, 2001. ISBN 3-9501031-1-2.

S4 Thin film and composite scintillators and low-dimensional systems

Development of film garnet scintillators based on garnet compounds

Miroslav Kucera [1,*], Zuzana Lucenicova [1], Martin Nikl [2]

[1]*Charles University, Faculty of Mathematics & Physics, 12116 Prague, Czech Republic*
[2]*Institute of Physics, CAS, 16000 Prague, Czech Republic*
[*]*Corresponding author*

At present, great efforts are being made to improve properties of new scintillation materials, mainly due to the rapid development of their applications in medical techniques or for high rate detection and imaging. For these applications high light yield and fast response, with short scintillation decay and rise times, are necessary. In this contribution we review particular achievements of the liquid phase epitaxial (LPE) technology which appeared, due to the technological breakthrough, very effective for material screening and provides scintillators with properties comparable to the bulk single crystal counterparts [1].

Here we focus on oxide scintillator films, primarily on garnets and perovskites doped with Ce^{3+} and Pr^{3+} ions prepared by the LPE. Particular attention will be paid to multicomponent garnets $(LuGd)_3(GaAl)_5O_{12}$:Ce (GAGG:Ce) due to their high light yield and good energy resolution [2]. The scintillation characteristics of this garnet system are further considerably improved by intentional co-doping by divalent Mg^{2+} or Ca^{2+} ions which brings about drastic decrease of the TSL signal, significant reduction of afterglow, and suppression of slow components in the scintillation response [3]. The divalent co-doping results alongside in substantial shortening of both the decay time and the rise time (< 50 ps) of the scintillation emission upon X-ray excitation. The results show on substantial suppression of shallow electron traps at divalent co-doping which otherwise gives rise to delayed emission or non-radiative recombination channels which negatively influence scintillation properties. The light yield of GAGG:Ce,Mg epitaxial films with optimized composition approaches that of the best bulk single crystals measured so far [3]. The luminescent and scintillation properties of co-doped GAGG:Ce,Mg will be reviewed and discussed in more detail.

[1] M. Kucera, P. Prusa, LPE-grown thin-film scintillators, in: M. Nikl (Ed.) *Nanocomposite, Ceramic, and Thin Film Scintillators*, Pan Stanford Publ., Singapore, 2017, pp. 155-226.
[2] K. Kamada, T. Endo, K. Tsutumi, et al., *Crystal Growth & Design*, **11** (2011) 4484.
[3] P. Prusa, M. Kucera, V. Babin, et al., *Advanced Optical Materials*, **5** (2017) 1600875.

α- and γ-rays Characterization of Single Crystalline Films and Composite Scintillators

J.A. Mares [1,*], M. Nikl [1], R. Kucerkova [1], A. Beitlerova [1], V. Gorbenko [2], S. Witkiewicz [2], T. Zorenko [2], Yu. Zorenko [2]

[1]*Institute of Physics AS CR, Cukrovarnicka 10, 162 53 Prague 6, Czech Republic*
[2]*Institute of Physics, Kazimierz Wielki University in Bydgoszcz, Powstańców Wielkopolskich str., 2, 85090 Bydgoszcz, Poland*
[*]*Corresponding author*

The latest development in X-ray imaging high resolution radiography allows imagining objects of a few μm size [1]. For such a high resolution even under 1 μm (microradiography) the luminescence light generated by the X-rays transmitted through thin single scintillation crystalline plates with thickness between 10 to 50 μm is detected (plates are glued on a substrate material) [1]. Recently, a new technological approach based on the liquid phase epitaxy (LPE) for production of film scintillators was developed and this method allows to prepare thin (5-60 μm) single crystalline films (SCF) on bulk single crystal substrates with 0.5-1 mm thickness [2-5]. Besides simple epitaxial structures (SCF and undoped substrate), the LPE method allows to prepare multilayer scintillators (a few SCF scintillators deposited onto one substrate) or even composite scintillators of "sandwich type" (SCF scintillators onto scintillation substrate) [3]. Multilayer SCFs and composite scintillators can be used to resolve different components of ionizing radiation beam (e.g. heavy particles and γ-quanta) [3].

To characterize and to measure scintillation properties (N_{phels} photoelectron or light yields (LY), energy resolution, shaping time dependence and scintillation decays) of SCFs or composite scintillators it is not possible to use only γ-rays because e.g. at 661.66 keV energy of ^{137}Cs radioisotope attenuation coefficient is low ~0.095 cm^2/g [6] resulting in very weak scintillation response in such SCF scintillators. Opposite to γ-rays, α-particles interact immediately with electrons of the layer ions and their penetration depth in the SCF of LuAG garnet is about of 10 μm [5]. Therefore, α-particles can excite only SCF scintillators while γ-rays excite either another thicker layer or the substrate. Usually ^{241}Am is used as the α-particle source (energy 5.4857 MeV) that of γ-rays is usually ^{137}Cs (energy 661.66 keV) [3-5]. iin this contribution, we will present and compare scintillation properties of substrates based on Pr or Sc-doped LuAG crystals and LuAG:Ce, LuAG:Pr and LuAG:Sc SCFs. Now, LuAG:Ce or LuAG:Pr crystals [7] are characterized by high LY (~26000 ph/MeV and ~20000 ph/MeV, respectively). In this talk we will present detailed scintillation characteristics of composite scintillators based on LuAG crystal as (SCF/substrate) LuAG:Pr/LuAG:Ce, LuAG:Sc/LuAG:Ce, LuAG:Sc/LuAG:Pr, LuAG:Ce/LuAG:Pr and LuAG:Ce,Tb/LuAG:Pr.

[1] J. Tous, K. Blazek, M. Kucera, M. Nikl, and J. A. Mares, *Rad. Meas.* **47** (2012) 311.
[2] Yu. Zorenko, V. Gorbenko, T. Zorenko, K. Paprocki, M. Nikl, J. A. Mares, et al. *IEEE Trans. Nucl. Sci.* **63** (2016) 497.
[3] S. Witkiewicz-Lukaszek, V. Gorbenko, T. Zorenko, O. Sidletskiy, et al., to be published in *Cryst. Growth Design* (2018).
[4] P. Prusa, M. Nikl, J. A. Mares, M. Kucera, K. Nitsch, and A. Beitlerova, *Phys. Stat. Sol.* **A 206** (2009) 1494.
[5] P. Prusa, J.A. Mares, M. Nikl, M. Kucera, K. Nitsch, M. Hanus, *Opt. Mat.* **32** (2010)1360.
[6] X-ray and Gamma-Ray Data (www.nist.gov/PhysRefData)
[7] M. Nikl, A. Yoshikawa, K. Kamada, K. Nejezchleb, C. R. Stanek, J. A. Mares, and K. Blazek, *Progr. Cryst. Growth Charact. Materials* **59** (2013) 47.

Composite scintillators based on the doped LuAG crystals and films for simultaneous registration of α-particles and γ-quanta

S. Witkiewicz-Lukaszek[1,*],V. Gorbenko [1], T. Zorenko [1], J.A. Mares [2], M. Nikl [2], Yu. Zorenko [1]

[1]*Institute of Physics, Kazimierz Wielki University in Bydgoszcz, Powstańców Wielkopolskich str., 2, 85090 Bydgoszcz, Poland*

[2]*Institute of Physics, AS CR, Cukrovarnicka str., 10, 16200 Prague, Czech Republic*

**s-witkiewicz@wp.pl*

In recent years, novel concepts of detectors for microtomography have been proposed [1]. This concept is based on using the multilayer films-crystal composite scintillator (CS) with a separate pathway for registration of the signal coming from each layers and final overlapping of the images coming from the different parts of the CS [1]. Such CS can be also used for the registration of the components of the mixed ionization radiation fluxes [2].

This work presents the results of creation of a new type of CSs based on the Sc^{3+} doped single crystal (SC) substrates and Ce^{3+} and Pr^{3+} doped single crystalline films (SCF) of LuAG. Namely, we have manufactured two types of SCs based on the LuAG:Ce SCF/LuAG:Sc and LuAG:Pr SCF/LuAG:Sc SC epitaxial structures. These CSs were produced by the liquid phase epitaxy method from melt solutions using $PbO\text{-}B_2O_3$ flux. For characterization of the luminescent and scintillation properties of SCFs and bulk SC parts of CSs, the absorption and cathodoluminescence spectra, scintillation light yield and decay kinetics under excitation by α–particles of ^{241}Am (5.5 MeV) source and γ quanta of ^{137}Cs (0.662 MeV) source were measured. We show the possibility of the simultaneous registration of α-particles and γ-quanta by means of separation of the decay kinetics of SCF and SC parts of such CSs.

Under γ-quanta and α–particles excitations, the notable difference in the scintillation decay kinetics of CSs is observed (Fig.1). Such a difference can be characterized by t_γ/t_α decay time ratio, which is measured at 1/e, 0.1 and 0.05 levels. Due to the relatively large t_γ/t_α values being equal to 2.6 and 1.5 for LuAG:Ce SCF/ LuAG:Sc and LuAG:Pr SCF/LuAG:Sc SC CSs on 0.5 level (Fig.1), respectively, these types of CSs can be successfully applied for separation of the signals coming from SCF and SC parts. For this reason, first type of CSs can possess even better results at registration of the mixed radiation fluxes containing α-particles and γ-quanta in comparison with previous analogues [1, 2].

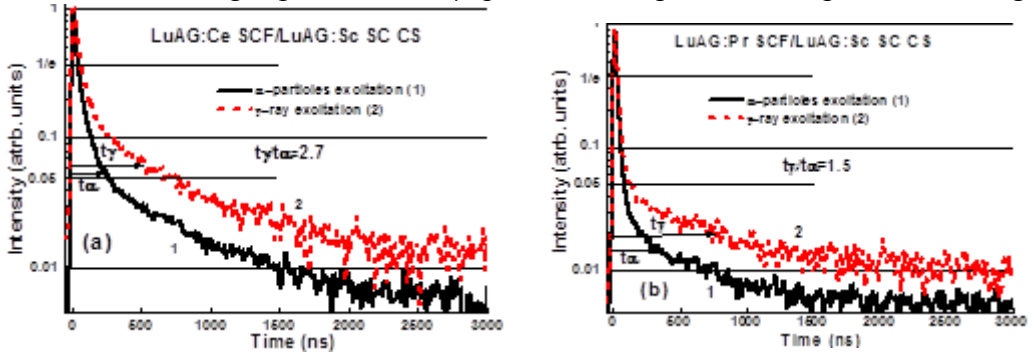

Fig.1. Scintillation decay of LuAG:Ce/LuAG:Sc (a), LuAG:Pr/LuAG:Sc (b) CSs under α-particles and γ-ray excitation by ^{241}Am and ^{137}Cs sources.

Acknowledgments: This work was supported by the Polish NCN 2016/21/B/ST8/03200 project.

[1] Yu. Zorenko, P.-A. Douissard, T. Martin, et.al, *Optical Materials* **65** (2017) 73-81.

[2] S. Witkiewicz-Lukaszek, V. Gorbenko, T. Zorenko, et.al, *Cryst. Growth Des.*, 2018, Article ASAP

Raman Spectroscopy of Ce^{3+} Doped $Lu_3Al_5O_{12}$ Single Crystalline Films grown onto $Y_3Al_5O_{12}$ Substrate

Wioletta Dewo [1], Yuriy Zorenko [2], Vitaliy Gorbenko [3] and Tomasz Runka [1,*]

[1]*Faculty of Technical Physics, Institute of Materials Research and Quantum Engineering, Poznan University of Technology, Piotrowo 3, 60-965 Poznań, Poland*
[2]*Institute of Physics, Kazimierz Wielki University in Bydgoszcz, Powstańców Wielkopolskich 2, 85-090 Bydgoszcz, Poland*
[*]*Corresponding author*

The RE^{3+} ion doped $Lu_3Al_5O_{12}$ (LuAG) single crystalline films (SCFs) grown using liquid-phase epitaxy (LPE) method on undoped $Y_3Al_5O_{12}$ (YAG) substrate have been found to be a materials with wide and promising applications, e.g. cathodoluminescent screens, scintillators, phosphors and laser media [1-4]. The optical image of the cross-section of the LuAG:Ce/YAG epitaxial structure is presented in Fig. 1a. The left part with yellow color with thickness about of 28 μm on the right side of the crystalline material is LuAG:Ce SCF.

In this paper, we present first time Raman spectroscopy investigations of cross-section of the LuAG:Ce SCF grown onto YAG substrate. As it is seen from Fig. 1b, the evolution of Raman spectra registered along the line leading through the interface between the layer and substrate is presented. We can distinguish between the signal from the layer and the substrate. Moreover, the Raman map collected from the area near the interface allows differentiating the Ce^{3+} doped LuAG crystalline film and YAG substrate.

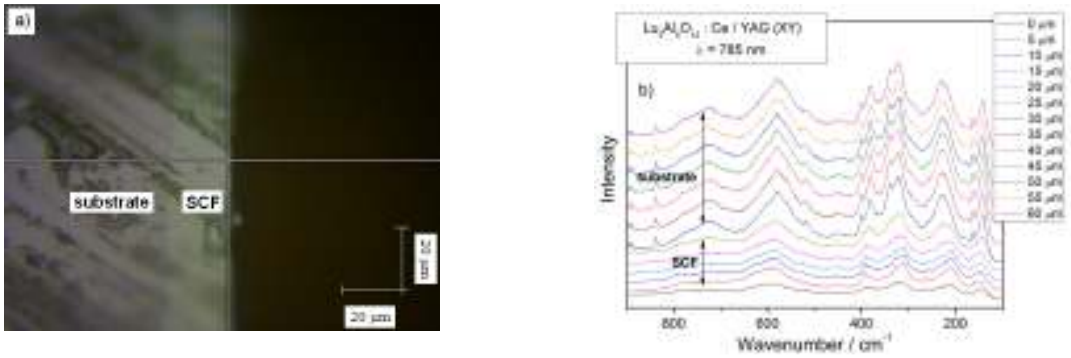

Fig. 1 The optical image (a) and the evolution of Raman spectra (b) through the cross-section of the LuAG:Ce/YAG epitaxial structure.

*Acknowledgments***.** This work was supported partially by the Research Projects of the Polish Ministry of Science and Higher Education 06/65/DSPB/5182 and the Polish NCN 2016/21/B/ST8/03200 project.

[1]. Yu. Zorenko, Pashkovsky M., Konstankevych I., Gorbenko V., Yurchyshyn P., Martynova V., Duziy *T. Proc. SPIE*. **3359** (1998) 256.
[2]. Yu. Zorenko, I. Konstankevych, M. Globus, B. Grinyov, V. Lyubinskiy, *Nucl. Instrum. Meth. A* **505** (2003) 93.
[3]. Yu. Zorenko, V. Gorbenko, I. Konstankevych, A. Voloshinovskii, G. Stryganyuk, V. Mikhailin, V. Kolobanov, D. Spassky, *J. Lumin*. **114** (2005) 85.
[4]. Yu. Zorenko, V. Gorbenko, I. Konstankevych, B. Grinev, M. Globus, *Nucl. Instrum. Meth. A* **486** (2002) 309.

Efficiency of $Bi^{3+}\rightarrow Yb^{3+}$ energy transfer in luminescent materials based on the single crystalline films of $Y_{3-x}Lu_xAl_{5-y}Ga_yO_{12}$:Yb,Bi garnets

V. Gorbenko *, T. Zorenko, K. Paprocki, K. Holovchenko, Yu. Zorenko

[1]*Institute of Physics, Kazimierz Wielki University in Bydgoszcz, 85090 Bydgoszcz, Poland*
**gorbenko@ukw.edu.pl*

The solar power is nowadays an important source of "green" and renewable energy. For this reason a considerable research has been focused recently on improving solar cell efficiency by better exploitation of the solar spectrum via photon conversion process. An efficient near-infrared (NIR) quantum-cutting for converting broadband ultraviolet (UV) into NIR luminescence via down-conversion (DC) processes has been demonstrated in Y_2O_3, Gd_2O_3, $Y_4Al_2O_9$, $Y_3Al_5O_{12}$, YVO_4 and other oxides [1-3]. Under excitation of UV photon in the 320–390 nm range, NIR emissions has been obtained from transitions of the Bi^{3+} ions to the Yb^{3+} ions. The efficiency of such energy transfer strongly depends on the energy of Bi^{3+} emission transitions with respect of Yb^{3+} electronic transitions and significantly varied on the different oxide host. For these reasons the room for the search of the efficient phosphors with $Bi^{3+}\rightarrow Yb^{3+}$ DC processes is still very large.

This our work is devoted to study of the $Bi^{3+}\rightarrow Yb^{3+}$ DC processes in the solid solution based on the $Lu_3Al_5O_{12}$ (LuAG) and $Y_3Al_5O_{12}$ (YAG) garnets, doped by Yb^{3+} and co-doped by Bi^{3+} ions. The solid solutions of $Lu_{3-x}Y_xAl_5O_{12}$:Bi,Yb garnets were obtained in the form of single crystalline films (SCF) using the liquid phase epitaxy (LPE) method. We search the conditions of heteroepitaxial LPE growth of the SCFs of $Lu_{3-x}Y_xAl_5O_{12}$:Yb, Bi garnets on YAG substrate using the Bi_2O_3-B_2O_3 based flux and found that the full set of $Lu_{3-x}Y_xAl_5O_{12}$:Yb,Bi SCFs with x values in x=0÷3.0 range can be crystallized onto the same YAG substrates. The SCFs were doped by Yb^{3+} and Bi^{3+} ions with a concentration of 1 at.% and 0.4-0.55 at. %, respectively.

We have found that the effective Bi^{3+}-Yb^{3+} energy transfer is realized in the $Lu_{3-x}Y_x$ Al_5O_{12}:Yb,Bi SCFs under e-beam high-energy excitation and excitation in the Bi^{3+} absorption bands. It was shown that increasing the Y^{3+} content **x** in these films causes the decrease of the luminescence efficiency of Bi^{3+} centers in the UV and visible ranges. Such changes in the emission intensity of the Bi^{3+} centers result in an increase in luminescence efficiency of Yb^{3+} ions in the range of 936-1030 nm. Thus, the mechanism of the energy transfer in $Lu_{3-x}Y_x$ Al_5O_{12}:Yb,Bi garnets is connected with *down-conversion* of one quantum of the Bi^{3+} luminescence, caused by the $^1S_0\rightarrow{}^3P_0$ transitions in the UV range, to three quanta of the Yb^{3+} luminescence, related to the $^2F_{7/2}\rightarrow{}^2F_{5/2}$ transitions, in the NIR range. However, increase in the luminescence intensity of Yb^{3+} ions in the various NIR bands takes place unevenly**.** The highest efficiency of the $Bi^{3+}\rightarrow Yb^{3+}$ energy transfer in solid solution of $Lu_{3-x}Y_xAl_5O_{12}$:Yb,Bi garnet at various Y content x is realized in the $Y_3Al_5O_{12}$:Yb,Bi SCFs. For this garnet, the coefficient of efficiency E_{eff}, as a ratio of the luminescence intensity of Bi^{3+} ions in the UV range to the Yb^{3+} ion emission intensity in the VIS range, reaches the highest value of 6.2. For the increase of E_{eff} value, the influence of Ga doping of $Y_3Al_5O_{12}$:Yb,Bi SCF is considered as well.

The analysis of the optical properties of SCFs of $Lu_{3-x}Y_xAl_5O_{12}$:Yb,Bi and Y_3Al_{5-x} Ga_xO_{12}:Yb,Bi garnets with different x values indicates that such materials can be considered as perspective light converters in solar panels.

*Acknowledgments***.** This work was supported by the Polish NCN 2017/25/B/ST8/02932 project.

1. Wei Xian-Tao, Zhao Jiang-Bo, Chen Yong-Hu, e. a. *Chinese Physics B*, **19** (2010) 077805.
2. X. Y. Huang and Q. Y. Zhanga, *Journal of Applied Physics*, **107** (2010) 063505.
3. Ya. Zhydachevskii, M. Baran, e. a. *Materials Chemistry and Physics,* **143** (2014) 622.

S5 Defects at surfaces and interfaces

Defects, defect mitigation and doping in highly fluorescent colloidal nanoplatelets

Iwan Moreels *

Department of Chemistry, Ghent University, Krijgslaan 281 – S3, Gent, Belgium
**iwan.moreels@ugent.be*

Colloidal semiconductor nanocrystals are small, crystalline building blocks that can be used for a wide range of photonic devices, from light-emitting diodes and lasers, to phosphors for displays, radiation detectors and life science.[1] They are synthesized by chemical methods, and can be prepared with diverse material compositions, sizes and shapes.[1] Due to a typical 2-10 nm diameter, they possess a large surface-to-volume ratio. Hence, to obtain high-quality nanocrystals with narrow band-edge emission, surface states needs to be meticulously controlled to avoid nonradiative recombination or long-lived, broadband deep trap emission.[2]

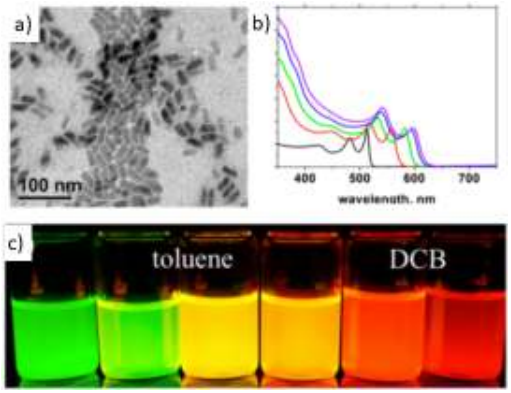

Fig. 2. *a) Transmission electron microscope image of CdSe/ZnS NPLs. b) Series of absorption spectra of CdSe/ZnS NPLs with different ZnS shell thickness. c) Corresponding fluorescence image.*

This becomes even more important when colloidal nanocrystals are grown as thin, atomically flat 2D nanoplatelets (NPLs).[3] In this talk, I will discuss how a new generation of colloidal bright band-edge emitters can be obtained with state-of-the-art, size-controlled CdSe NPLs. The extended lateral sizes lead to enhanced emission rates compared to spherical quantum dots. Despite large top and bottom surfaces, passivation of the lateral edges of the CdSe core is key to suppress surface trapping. By growing a ZnS shell (**Fig. 1**),[4] we can improve their optical stability and obtain color-tunable NPLs with quantum efficiencies around 60% and 10-20 ns fluorescence lifetimes. We have also developed protocols to dope CdSe NPLs, with silver ions via post-synthesis cation exchange. At the expense of a longer emission lifetime, these NPLs become excellent emitters when a large Stokes shift is required to suppress self-absorption. Our results demonstrate the versatility of CdSe NPLs, and demonstrate that we have substantial freedom to design their opto-electronic properties to target various photonic applications.

To demonstrate the latter, initial experiments have revealed that CdSe NPLs form excellent phosphors for solution-processed scintillators.[5] The high-energy excitation leads to biexcitons in NPL solids that exhibit a sub-ns lifetime. Further increasing the emission rate by an order of magnitude, this attests to their potential for ultrafast radiation detection.

[1] J.Q. Grim, L. Manna, I. Moreels, *Chem. Soc. Rev.* **44** (2015) 5897.
[2] P. Kambhampati, T. Mack, L. Jethi, *ACS Photonics* **4** (2017) 412.
[3] G.H.V. Bertrand, A. Polovitsyn, S. Christodoulou, A.H. Khan, I. Moreels, *Chem. Commun.* **52** (2016) 11975.
[4] A. Polovitsyn, Z. Dang, J. L. Movilla, B. Martín-García, A.H. Khan, G.H.V. Bertrand, R. Brescia, I. Moreels, *Chem. Mater.* **29** (2017) 5671.
[5] R.M. Turtos, S. Gundacker, A. Polovitsyn, S. Christodoulou, M. Salomoni, E. Auffray, I. Moreels, P. Lecoq, J.Q. Grim, *J. Instrum.* **11** (2016) P10015.

The role of defects in the stabilization of Eu^{2+} in dielectrics

Przemysław Dereń [1]*, Dagmara Stefańska [1], Grzegorz Banach [2], Bartosz Brzostowski [2], Piotr Wiśniewski [1]

[1]*Instytut Niskich Temperatur i Badań Strukturalnych PAN, ul. Okólna 2, Wrocław, Polska*
[2]*Uniwersytet Zielonogórski, Wydział Fizyki i Astronomii, ul. Prof. Z. Szafrana 4a, 65-516 Zielona Góra, Polska*
[*]*Corresponding author*

The search for a phosphor, which would exceed the Color Rendering Index and Color Temperature of the one commonly used in WLED's is still underway [1, 2]. Nowadays it turns out that instead of phosphors which exhibits narrow emission lines we need for our comfort and health broadband light sources, which will have an emission spectrum similar to the light emitted by the Sun.

Two dopants are considered: Ce^{3+} already applied in YAG, and Eu^{2+}. Both exhibit broad, allowed by the selection rules emission bands, and the latter dopant attracts currently a lot of attention. Therefore, all matrices with a sufficiently large energy gap in which Eu^{2+} ion levels can be located are widely studied. It should be remembered, however, that in nature there are no compounds with europium on the second oxidation stage. During the synthesis of phosphors, it is necessary to reduce the admixture of Eu^{3+} (usually introduced as oxide) to Eu^{2+}. Recently, many publications addressing the processes of reduction of europium in dielectric matrices were published, most of these works point to the role of defects in reducing europium [3, 4].

In this work, we will present a short review on the reduction and stabilization of europium on the second oxidation state in dielectrics. Next, detailed research results on melilite, i.e., solid solutions of åkermanite $Ca_2Mg(Si_2O_7)$ and gehlenite $Ca_2Al(AlSiO_7)$ doped with europium ions, will be presented. These are structures in which Eu^{2+} and Eu^{3+} coincide. By our research, it seems that matrix defects are necessary to obtain the reduction of Eu^{3+} to Eu^{2+}. We will compare different reduction methods and atmospheres. It will be shown as well, that Eu^{2+}/Eu^{3+} ratio depends on the chosen reduction method and the presence of co-admixtures.

[1] S.Ye, F. Xiao, Y.X. Pan, Y.Y. MaQ, Y.Zhang, *Mater. Sci. Eng. Rep*. **71** (2010), 1 – 34.
[2] Yang Zhang, Weitao Gong, Jingjie Yu, Zhiyuan Cheng and Guiling Ning, *RSC Adv*., **6** (2016), 30886-30894.
[3] Mingying Peng, Zhiwu Pei, Guangyan Hong and Qiang Su, *J. Mater. Chem*., **13** (2003), 1202-1205.
[4] Hongde Xie, Juan Lu, Ying Guan, Yanlin Huang, Donglei Wei, and Hyo Jin Seo, *Inorg. Chem*. **53** (2014) 827−834.

Study of defects in chemical vapor deposited diamond films

K. Paprocki and K. Fabisiak*

Institute of Physics, Kazimierz Wielki University, Powstańców Wielkopolskich 2, 85-090 Bydgoszcz, Poland

**Corresponding author: kfab@ukw.edu.pl*

Diamond due to its unique combination of physical properties as for instance, high electrical resistivity-high thermal conductivity, has been considered as a promising material for application in optics, electronics and thermal management.

In the case of application of CVD diamonds in electronics the key points is the control of their properties with accuracy and reproducibility. Since defects govern the electrical transport properties it is therefore important to obtain a detailed insight to the type of defects and their distribution created in diamond films during growth process. Although a great deal of efforts has been made to improve electrical properties of diamond films it is still far from to be sufficient. The data published by different group are sometimes very different, mainly due to using different gas sources and deposition system.

Defects causing colour in un-doped chemical vapour deposited (CVD) diamond can adversely affect the exceptional optical, electronic and dosimetric properties of the material. Several techniques were used to study these defects, namely Raman spectroscopy, thermoluminescence (TL) and cathodoluminescence (CL). From our studies, the defects causing colour in un-doped CVD diamond are clearly not the same as those in natural diamonds.

Previous electron microscope-CL studies, as those mentioned above, refer mainly either to measurements in plan view specimens of the diamond films or to analysis of defects and impurities of localized regions. However, SEM-CL studies of side view samples could provide information on the film structure and defect distribution along the growth axis. This is of interest for a more complete characterization of the films as well as in film growth problems. For this reason, CL investigation of the upper surface and of cross sections of CVD diamond films has been carried out in this work.

Effect of Magnetic Impurities on Monolayer Uniaxially Strained Graphene on TMD

Partha Goswami*

D.B. College, University of Delhi, Kalkaji, New Delhi-110019, India
**Corresponding author*

We calculate the electronic band dispersion of graphene monolayer on a two dimensional transition metal dichalcogenide substrate (GrTMD) , constituting a Van der Waals heterostructure (vdWH), around *K* and *K prime* points taking into account the interplay of the ferromagnetic impurities and the substrate induced interactions. The latter are (strongly enhanced) intrinsic spin-orbit interaction(SOI), the extrinsic Rashba spin-orbit interaction(RSOI), and the one related to the transfer of the electronic charge from graphene to substrate. We introduce uniform uniaxial strain and the exchange field (*M*) in the Hamiltonian [1,2] where the latter takes into account the deposition of magnetic impurities on the graphene surface. It is observed that whereas the strain field is responsible for the valley polarization, a Rashba coupling dependent pseudo Zeeman term, arising due to the interplay of substrate induced interactions and magnetic impurities, is found to bring about the spin degeneracy lifting and the gate voltage tunable spin-polarization. The latter turns out to be inversely proportional to the square root of the carrier concentration. Our graphical analysis with extremely low-lying states strongly suggests the following: The GrTMDs, such as graphene on WY_2, exhibit (direct)band gap narrowing/widening including the increase in spin-polarization at low temperature due to the increase in the exchange field (*M*) at the Dirac points. There is anti-crossing of non-parabolic bands with opposite spins, and the gap closing with same spins around Dirac point. A rather remarkable finding of ours is the latter. At the Dirac point *K*(*K prime*), for certain exchange field values $M = M_c$, the spin-split conduction and valence bands for GrTMD exhibit gap closing (Half-metal) for the spin-down (spin-up) valence band and the spin-down(spin-up)conduction band, while for the spin-up (spin-down) channel bands the gap remains finite; there is trivial band gap at $M < M_c$ and at $M > M_c$ the energy eigenvalues are inadmissible as they become complex. These findings are expected to pave the way towards possible engineering of graphene spin-filtering due to proximity of TMD.

[1] M. Gmitra, and J. Fabian, Phys. Rev. B **92** (2015) 155403.
[2] T. Frank, P. Hogl, M. Gmitra, D. Kochan, and J. Fabian, arXiv:1707.02124.

Structural, Electronic And Magnetic Properties Of Pure And Doped $FeNb_{11}O_{29}$

P. Galinetto [1,*], D. Spada [2], M.C. Mozzati [1], B. Albini [1], I. Quinzeni [2], D. Capsoni [2] and M. Bini [2]

[1]*Dept. of Physics, University of Pavia, via Bassi 6, 27100 Pavia Italy*
[2]*Dept. of Chemistry, University of Pavia, via Taramelli 16, 27100 Pavia Italy*
[*]*Corresponding author*

The electric vehicles industry asks continuously for more efficient and safe Lithium-ion batteries and in turn for improved anodes, key element of the power sources. In this frame researchers try unceasingly to find out materials with superior performances. Quite recently attention has been paid on a new anode material, $FeNb_{11}O_{29}$. Thanks to the redox couples Fe^{2+}/Fe^{3+}, Nb^{4+}/Nb^{5+} and Nb^{3+}/Nb^{4+} up to 23 electron can be transferred per formula unit so reaching the intriguing value of 400 mAh/g of theoretical capacity, also higher than that of graphite.

This promising functional property is accompanied in $FeNb_{11}O_{29}$ by other very intriguing basic properties related to a peculiar mixing of structural and electronic features. In $FeNb_{11}O_{29}$ the ReO_3-type octahedral-blocks sharing edges and corners can be arranged both in monoclinic and orthorhombic phases similar to those reported for the parent system $Nb_{12}O_{29}$, a rare example of niobium compounds with long-range magnetic order. In $FeNb_{11}O_{29}$ an active role in electronic and magnetic properties can be played by structural and electronic defects, related to the presence of oxygen vacancies and disorder in cations distribution on different crystalline sites. In this landscape the doping, very rarely explored in $FeNb_{11}O_{29}$, can be used to increase electronic conductivity, usually extremely low and limiting its rate capability.

In the present work we report on the experimental study of structural, electronic and magnetic properties of undoped and Mn/V doped $FeNb_{11}O_{29}$ (20% of Fe substitution) in both monoclinic and orthorhombic forms. The samples were synthesized by the conventional solid- state route at high temperature. X-ray powder diffraction helped to determine the success of doping and the main structural parameters of the phases by using the Rietveld structural refinement. SEM measurements allowed to study the morphological aspects. MicroRaman experiments gave evidence of the vibrational properties in different structural habits and allowed to check phase homogeneity and purity in comparison with XRD results. Electron paramagnetic resonance spectra, likely due to trivalent iron, allowed to obtain information about local environments around active species. Finally static magnetization has been measured for all the samples by SQUID technique.

The whole set of data allowed to fully characterize the effect of Mn and V doping on the structural, electronic and magnetic properties of pure $FeNb_{11}O_{29}$ and represents the base for the comprehension of the functional properties.

S6 Radiation effects, radiation induced defects, colour centers

Application of color centers in LiF crystals for fluorescent imaging of nuclear particles tracks

P. Bilski*, B. Marczewska, W. Gieszczyk, M. Kłosowski, M. Naruszewicz

Institute of Nuclear Physics, Polish Academy of Sciences (IFJ PAN), Radzikowskiego 152, 31-342 Kraków, Poland

Color centers in lithium fluoride crystals are a well-known phenomenon. Ionizing radiation creates F centers (anion vacancies trapping electrons), which tend to aggregate forming more complex defects. Among them of special interest are F_2 and F_3^+ color centers. F_2 center is composed of two anion vacancies with two bounded electrons, while F_3^+ of three vacancies with two electrons. Both these centers have overlapped absorption bands peaked around 440-450 nm, while the photoluminescence emission spectrum exhibits two peaks at about 670 nm (related to F_2) and about 520 nm (related to F_3^+).

Recently photoluminescence of of F_2/F_3^+ centers in LiF was successfully exploited for imaging of tracks of single nuclear particles [1, 2]. LiF single crystals were grown with the Czochralski and micro-pulling down methods at IFJ PAN. The crystalline samples were then irradiated with alpha particles, thermal and fast neutrons, protons and other radiation modalities. Microscopic observations were conducted using a wide-field fluorescent microscope equipped with a high-sensitive CCD camera. Excitation of the irradiated crystals with a blue light enabled visualization of nuclear particles tracks with the resolution below 0.5 μm. A very low focal depth of the used optical system, allowed also for scanning of the samples with depth into a crystal, in that way providing 3D images of particle tracks. The described method may be potentially used for dosimetry of ionizing radiation, in particular for neutron measurements.

Acknowledgements: This work was supported by the National Science Centre, Poland (Contract No. UMO-2015/17/B/ST8/02180).

[1] P. Bilski, B. Marczewska. *Nucl. Instr. Meth. B*, **392**, 2017, 41.
[2] P. Bilski, B. Marczewska, W. Gieszczyk, M. Kłosowski, T. Nowak, M. Naruszewicz. *Radiat. Prot. Dosim*. doi: 10.1093/rpd/ncx116.

Visible photoluminescence of colour centers in lithium fluoride detectors for low-energy proton beam Bragg curve imaging and dose mapping

Rosa Maria Montereali [1,*], Massimo Piccinini [1], Alessandro Ampollini [1], Luigi Picardi [1], Concetta Ronsivalle [1], Francesca Bonfigli [1], Enrico Nichelatti [2], Maria Aurora Vincenti [1]

[2]*ENEA C.R. Frascati, Fusion and Technologies for Nuclear Safety and Security, Via E. Fermi 45, 00044 Frascati (RM), Italy*
[1]*ENEA C.R. Casaccia, Fusion and Technologies for Nuclear Safety and Security, Via Anguillarese 301, 00123 Rome, Italy*
[*]*rosa.montereali@enea.it*

Point defects in lithium fluoride (LiF) are well known for application in tuneable lasers and dosimeters. The visible photoluminescence (PL) of radiation-induced, broad-band light-emitting colour centres (CCs) in LiF crystals and films has been proposed by our team for high spatial resolution X-ray imaging [1]; moreover, use of these LiF-based radiation detectors has been recently successfully extended to the advanced diagnostics of low-energy proton beams [1-3].

LiF crystals and thin films were irradiated with a proton beam of 7 MeV nominal energy in different geometries at a linear modular accelerator that is under development at ENEA C.R. Frascati for protontherapy applications. The ionisation induced by the protons in the LiF samples induced the stable formation of primary and aggregate CCs in the crystalline lattice. The F_2 and F_3^+ aggregate defects are optically active as they emit visible PL in the red and green spectral ranges, respectively, when optically pumped in the blue at wavelengths close to 450 nm. Under continuous wave pumping, the detectable PL intensity of these CCs has been found to be proportional to the dose over at least three orders of magnitude [2], so that bi-dimensional LiF solid-state dosimeters based on spectrally-integrated PL reading can be envisaged. With perpendicular exposure of LiF films to the proton beam, transversal dose mapping was obtained by acquiring the visible PL image of the irradiated spots in a fluorescence microscope equipped with blue-light sample illumination.

By changing the irradiation geometry, the visible fluorescence images, latently produced in LiF crystals that faced the beam with their thinner side, can be reasonably considered as photoluminescent fingerprints of the underlying Bragg curves [3]. Recent results and progress on Bragg curve imaging, dose mapping and detector linearity-range characterisation by using these two irradiation geometries are presented and discussed.

[1] R. M. Montereali, F. Bonfigli, M. Piccinini, E. Nichelatti, M. A. Vincenti, *J. Lumin*. **170** (2016) 761.
[2] M. Piccinini, F. Ambrosini, A. Ampollini, L. Picardi, C. Ronsivalle, F. Bonfigli, S. Libera, E. Nichelatti, M. A. Vincenti, and R. M. Montereali, *Appl. Phys. Lett.* **106** (2015) 261108.
[3] E. Nichelatti, M. Piccinini, A. Ampollini, L. Picardi, C. Ronsivalle, F. Bonfigli, M. A. Vincenti and R. M. Montereali, *Europhys. Lett*. **120** (2017) 56003.

Fast-Neutron-Induced and As-Grown Structural Defects in Mg-Al Spinel Crystals with Different Stoichiometry

Aleksandr Lushchik [1,*], Eduard Feldbach [1], Tiit Kärner [1], Nina Mironova-Ulmane [2], Anatoli I. Popov [2], Evgeni Shablonin [1], Evgeni Vasil'chenko [1] and Viktor Seeman [1]

[1]*Institute of Physics, University of Tartu, W. Ostwald Str. 1, 50411 Tartu, Estonia*
[2]*Institute of Solid State Physics, Latvia University, Kengaraga Str. 8, Riga, LV-1063, Latvia*

Insufficient resistance against prolonged irradiation is a serious limitation for the use of wide-gap materials in the environment of the future fusion reactors. Presently, the search for wide- gap materials with optical window capabilities and a high tolerance to neutron radiation in fusion devices is an urgent task in the research programs of the EUROfusion consortium. Mg- Al spinel exhibits high resistance against heavy irradiation, very little swelling and belongs to attractive candidates for window materials. It is generally accepted that a high radiation tolerance of $MgAl_2O_4$ is explained by the efficient recombination of interstitial-vacancy pairs formed during irradiation. Such self-healing process is stimulated by a huge concentration of "native" vacancies in the cation sublattice of a normal spinel and cation swapping between tetrahedral and octahedral sites. The swapping results in the formation of antisite defects (increase of inversion) – $Mg|_{Al}$ or $Al|_{Mg}$- i.e. Al^{3+} or Mg^{2+} in a "wrong" cation position.

The present study deals with structural defects induced by fast neutrons (energy >0.1 MeV, irradiation at $T < 90^oC$, fluence around 1e18 n/cm^2) in a stoichiometric $MgAl_2O_4$ ($1MgO{\cdot}1Al_2O_3$, i.e. 1:1, see also [1]) and a nonstoichiometric (1:2.5) spinel single crystals The damage was analyzed via induced optical absorption (IOA) at 1.4-9 eV and using an X-band EPR spectrometer ELEXSYS E500. The annealing of IOA or the EPR signal of paramagnetic centers was registered in a stepwise regime: the sample was heated in extra dry air to a certain T_i, kept there for 10 min and cooled down to 295 K, at which all spectra were measured. In addition, optical absorption in the region up to the fundamental edge and photoexcitation (5-10 eV) of different emissions were studied in virgin crystals at 6 and 295 K. Inversion degree of lattice was estimated by XRD method.

The analysis of the EPR signal angular dependencies at different microwave power after each preheating to T_i allowed to reveal a number of novel radiation defects. These defects possess positive shift of the *g*-factor and, therefore, are ascribed to the holes localized at regular O2- nearby negatively charged defects (e.g., Al and Mg vacancies or antisite defects) in 1:1 and 1:2.5 Mg-Al spinel samples. The pulse annealing of the EPR signal of these radiation centers was compared to that of IOA in the same crystals in order to determine correlation between intrinsic radiation defects and relevant IOA bands. The origin and microstructure of the revealed radiation defects in Mg-Al spinel is considered. After irreversible annealing of neutron-induced hole centers and an additional x-irradiation, some other EPR-active centers were detected in both Mg-Al spinel samples. These centers are formed via hole trapping at different as-grown complex defects and their reversible decay (measured again via EPR and IOA) is connected with the thermal release of holes. Taking into account the determined models of paramagnetic centers, the tentative scenario of the thermal annealing process of neutron-induced defects (hole-type and complementary electron F-type ones) is proposed.

[1] A. Lushchik, S. Dolgov, E. Feldbach, R. Pareja, A.I. Popov, E. Shablonin, and V. Seeman, *Nucl. Instrum. Meth. B* (2018) *http://dx.doi.org/10.1016/j.nimb.2017.10.018.*

Influence of inelastic stopping on critical amorphization parameters of indium arsenide implanted with heavy ions

E. Friedland*, E. Njoroge and C. Theron

Physics Department, University of Pretoria. Pretoria, South Africa

At ion energies with inelastic stopping powers less than a few keV/nm, radiation damage is the result of atomic displacements by elastic collisions only. However, it is well known that inelastic processes and non-linear effects due to defect interaction within collision cascades can significantly influence damage efficiencies. Such processes can cause defect annealing as well as a reduction of binding energy. Depending on which of these two mechanisms dominate, the critical amorphization parameters are either enhanced or reduced. Defect recovery processes are generally found to be the dominant mode in mono-elemental materials, while in compounds any one of them might be the dominating mechanism. The importance of these processes changes significantly along the ion's trajectory and becomes negligible at some distance beyond its projected range, where damage is mainly caused by slowly moving secondary recoils. In this region of homogeneous amorphization, the critical parameters become independent of the ion type and depend only on the intrinsic properties of the material [1].

To investigate the amorphization behaviour of indium arsenide, damage profiles were obtained for single crystalline wafers implanted at room temperature with heavy noble gas ions employing RBS/Channeling analysis. Fluences were chosen to place the amorphous- crystalline interface TAC at different depths in the range of $0.5 < RP < 2$, where RP is the projected ion range. Critical amorphization parameters and their dependence on electronic stopping were obtained by comparing these depths with TRIM simulations.

[1] E.Friedland, *Nucl. Instr. and Meth.* **B 391** (2017) 10-13

Radiation Induced Changes in the Luminescent Properties of Mn and Sm Doped $NaMgF_3$ for Non-destructive Radiation Dosimeter Readout

Joseph J. Schuyt [1,*], Grant V.M. Williams [1]

[1] *The MacDiarmid Institute for Advanced Materials and Nanotechnology, SCPS, Victoria University of Wellington, PO Box 600, Wellington 6140, New Zealand*
[*] *Corresponding author*

The development of novel dosimeter materials has been highly encouraged in recent years, with emphasis on devices suitable for dose verification in radiotherapy. Many studies have focused on using the phenomenon of optically stimulated luminescence (OSL) as a measurement technique [1,2]. OSL occurs in a material when exposure to ionizing radiation results in the trapping of charge and the consequent formation of metastable defects. Stimulation of the material with light of an appropriate energy then releases the stored charge, which may recombine where the light emission intensity is proportional to the concentration of trapped charge and therefore the radiation dose. OSL as a measurement technique is advantageous as it allows for fast all-optical readout with high sensitivity [1,2]. The main disadvantage of OSL is that it is necessarily destructive of the stored signal, as trapped charge is released from defects upon readout. More recently, focus has been placed on observing radiation induced changes in photoluminescence (PL) properties, particularly where radiation induces new PL centers within a material [2,3]. This can occur via the generation of luminescent color centers [3], defect-impurity complexes [2] and valence conversion of pre-existing luminescent centers [3]. In some cases, the PL changes can be probed without affecting the concentration or luminescence intensity of the induced centers [2,3]. Therefore, radiation induced changes in PL can provide non-destructive methods of measuring both real-time and cumulative radiation doses.

We present the results of studies on $NaMgF_3$ doped with Mn and Sm. $NaMgF_3$ is an approximately tissue equivalent compound making it suitable for medical applications. Optical absorption, PL and OSL measurements before and after x-ray irradiation show the presence of several defects in the materials. OSL is observed in both compounds, resulting in either Mn^{2+} emission or Sm^{3+} emission depending on the dopant and the OSL is shown to be proportional to total x-ray dose. In $NaMgF_3$(Mn) *F*-center-Mn complexes are observed after irradiation. The concentration increases with x-ray dose and can be probed non-destructively via PL. In $NaMgF_3$(Sm) valence conversion from Sm^{3+} to Sm^{2+} occurs during irradiation. The relative emission intensities of each valence are dependent on cumulative x-ray dose and can be non-destructively probed via PL even after OSL readout. We therefore show that doped $NaMgF_3$ has excellent potential for a versatile novel dosimeter material where both real time and cumulative dose measurements may be obtained using both OSL and PL techniques together.

[1] S. W. S. McKeever *et. al.*, *Rad. Prot. Dos.* **109** (2004) 269.
[2] J. J. Schuyt and G.V.M. Williams, *J. Appl. Phys.* **122** (2017) 063107.
[3] G. Okada, *Nucl. Instr. Meth. Phys. Res. B* (2018), https://doi.org/10.1016/j.nimb.2018.01.032

Scintillation and Optical Properties for Ce-doped $(Gd, La)_2Si_2O_7$ in Low Temperature

Shunsuke Kurosawa [1,2,*], Takahiko Horiai [3], Akihiro Yamaji [3], Rikito Murakami [3], Yasuhiro Shoji [3], Masao Yoshino [3], Yuji Ohashi [1], Yuui Yokota [1], Akira Yoshikawa [1,3], Akimasa Ohnishi [2] and Mamoru Kitaura [2]

[1]*New Industry Creation Hatchery Center, Tohoku University, 6-6-10 Aza-Aoba, Aramaki, Aoba-ku, Sendai, Japan.*
[2]*Faculty of Science, Yamagata University, 1-4-12 Kojirakawa-machi, Yamagata, Japan*
[3]*Institute of Material Research, Tohoku University, 2-1-1 Katahira, Aoba-ku, Sendai, Japan*
[*]*Corresponding author*

Recently, Ce:$(La, Gd)_2Si_2O_7$ (Ce:La-GPS) scintillator was reported the have a good energy resolution (FWHM) of around 5~6% at 662 keV, and its light output remained constant up to 150 °C (423K) [1,2]. Moreover, we evaluated the band gap energy (lower limit) for La-GPS as 7.13±0.03 eV [3], and this value was large one compared with many conventional oxide scintillators. Nevertheless, the light output of Ce:La-GPS was larger than that of the other scintillators commercially available, and "energy-transfer efficiency" from ionization process to emission process was found to be higher than other materials[3]. In order to reveal the emission, we measure thermo-luminescencespectra to evaluate the trap site for several Ce:La-GPS samples: $(Ce_x La_y, Gd_{1-x-y})_2Si_2O_7$, where $0.005 < x < 0.02$, $0.23 < y < 0.5$. Moreover, we also measure emission intensity of the Ce^{3+} emission band at low temperature excited by UV-VUV photons.

The samples, $(Ce_x La_y, Gd_{1-x-y})_2Si_2O_7$, were grown by the micro-pulling down method and Czochralski process. The emission intensities as a function of temperature were measured with a CCD camera at synchrotron facility (UVSOR) in Japan. In addition, decay time curves were measured with the pulse X-ray system including streak camera in our Lab.

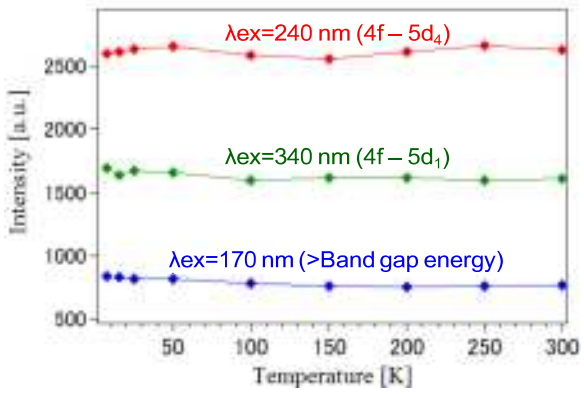

Fig. 1 emission intensity of $(Ce_{0.015}La_{0.235}Gd_{0.750})_2Si_2O_7$ as a function of temperature

Figure 1 show the temperature dependence of emission intensities for $(Ce_{0.015}La_{0.235}Gd_{0.750})_2Si_2O_7$ excited by 170, 240 and 340 nm corresponding to band-to-band, 4f-5d4 and 4f-5d1 excitation, respectively, and the intensities were not changed dramatically. TL spectra suggested a small number of the traps compared with other conventional scintillators such as Ce:$Gd_2Si_2O_5$. We show the detail of the results in this presentation.

[1] A. Suzuki, S. Kurosawa, and A. Yoshikawa et al., *Appl. Phys. Express* **5** (2012) 102601.
[2] S. Kurosawa, and A. Yoshikawa et al., *NIMA* **772** (2015) 72.
[3] S. Kurosawa, and A. Yoshikawa et al., *IEEE TNS*, accepted.

S7 Defects and material preparation technology

Defects in ultrawide-bandgap oxide semiconductor β-Ga_2O_3

Zbigniew Galazka [1,*]

[1] *Leibniz Institute for Crystal Growth (IKZ), Max-Born-Str. 2, 12489 Berlin, Germany*
[*] *Corresponding author*

β-Ga_2O_3 belongs to the group of ultrawide-bandgap (UWBG) semiconducting materials, which open a challenging area of research in semiconductor materials, physics, devices and applications. The bandgap of 4.85 eV and a large breakdown field of 8 MeV/cm brings β-Ga_2O_3 to the frontline of optoelectronic (solar-blind DUV photodetectors, light emitting diodes) and high power electronic (field effect transistors, Schottky barrier diodes) applications. Moreover, β-Ga_2O_3 is sensitive to detection of nuclear radiation (neutron and gamma radiation), as well as of different gaseous species at elevated temperatures enabling Ga_2O_3-based high temperature gas sensors. A great advantage of β-Ga_2O_3 is the availability of bulk crystals functioning as native substrates for device structures. Bulk crystals of large size and high structural quality were demonstrated by the Czochralski [1] and EFG [2] methods, while high quality homoepitaxial layers were demonstrated by a few epitaxial techniques, such as MOVPE [3] and MBE [4].

β-Ga_2O_3 is thermally unstable at high temperature, therefore the growth of bulk crystals from the melt leads to a structural and point defect formation that affect some of the electrical and optical properties. Epitaxial layers suffer from the defect formation even to larger extent than the bulk crystals. Identification of various types of defects in both bulk crystals and epitaxial layers is crucial to understand and control the optical and electrical properties of β-Ga_2O_3 dedicated for specific devices.

This report will focus on point (e.g. Fig. 1) and extended (e.g. Fig. 2) defects found in bulk crystals and epitaxial layers of β-Ga_2O_3, and on their impact on fundamental materials properties and device functionality.

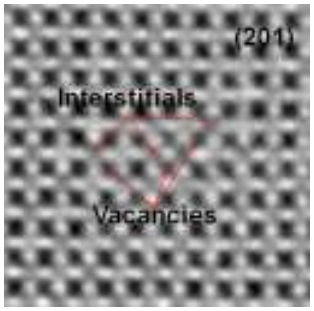

Fig. 1 Example of point defects in bulk β-Ga_2O_3 crystals [5].

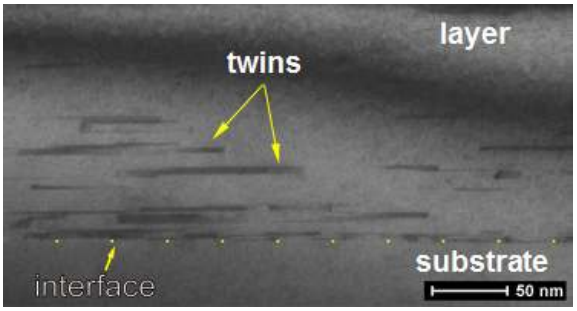

Fig. 2 Example of planar defects in epitaxial β-Ga_2O_3 layers (MOVPE) [6].

[1] Z. Galazka et al., ECS J. Solid State Sci. Technol. 6 (2017) Q3007-Q3011
[2] A. Kuramata et al., Jpn. J. Appl. Phys. 55 (2016) 1202A2
[3] M. Baldini et al., ECS J. Solid State Sci. Technol. 6 (2017) Q3040-Q3044
[4] K. Sasaki et al., Appl. Phys. Express 5 (2012) 035502
[5] Z. Galazka et al., Cryst. Res. Technol. 45 (2010) 1229-1236
[6] R. Schewski et al., J. Appl. Phys. 120 (2016) 225308

Defects in light conversion phosphors with a high fluorescence quantum yield for white light emitting diodes and solar cells

Ievgen Levchuk [1,2,3], Liudmyla M. Chepyga [1,2,3], Adrian Valenas [2], Leon Beickert [2], Andres Osvet [1,2], Nicholas Khaidukov [5], Rik Van Deun [6], Christoph J. Brabec [1,2], Yuriy Zorenko [4], Miroslaw Batentschuk [2,*]

[1]*Energie Campus Nürnberg (EnCN), Fürther Str. 250, 90429 Nürnberg, Germany*
[2]*Institute of Materials for Electronics and Energy Technology (i-MEET), Friedrich-Alexander Universität Erlangen-Nürnberg, Martensstraße 7, 91058 Erlangen, Germany*
[3]*Erlangen Graduate School in Advanced Optical Technologies (SAOT), Friedrich-Alexander Universität Erlangen-Nürnberg, Paul-Gordan-Str. 6, 91052 Erlangen, Germany*
[4]*Institute of Physics, Kazimierz Wielki University in Bydgoszcz, 85090 Bydgoszcz, Poland*
[5]*Kurnakov Institute of General and Inorganic Chemistry, RAS, 119991 Moscow, Russia*
[6]*Luminescent Lanthanide Lab, Ghent University, 9000 Gent, Belgium*
**miroslaw.batentschuk@fau.de*

Light conversion phosphors have gained in importance in the last decade first of all due to their extensive using in the novel generation of light sources – in white light emitting diodes (WLEDs). The WLEDs open wide and unique possibilities for energy-saving lighting with a spectrum similar to the sun light. These devices work on the principle of the conversion of blue light emitted by a (AlGaIn)N -based LED by luminescence converters. Phosphors already used for this purpose usually are powders of cerium doped yttrium-aluminium garnet $Y_3Al_5O_{12}$:Ce (YAG:Ce) or $Tb_3Al_5O_{12}$:Ce (TAG:Ce) embedded in polymers. However, several research teams are optimizing parameters like the emission spectrum which can improve the color rendering index or/and the color correlated temperature of WLEDs, and the thermal stability up to 150 °C.
One alternative phosphor is $Ca_3Sc_2Si_3O_{12}:Ce^{3+}$ (CSS:Ce) silicate garnet. This phosphor shows a similar to YAG:Ce emission spectrum, but has a higher thermal stability. Three different kinds of the O^{2-} polyhedra for cations in the garnet structure open the possibility of "colour engineering" of the emission spectrum by substitution of the lattice ions or by introducing impurities serving as activators or charge compensating ions. Furthermore, controlling the anti-site defects also helps to modify the spectra. These substitution possibilities and their influence on the emission spectrum and especially on the quantum yield of $Ca_3Sc_2Si_3O_{12}:Ce^{3+}$ and $Ca_3Sc_2Si_3O_{12}:Ce^{3+}$, Eu^{2+}/Eu^{3+} micro- and nanocrystals are topics of this talk.
The problem of high quantum yield is also crucial in another field of using light conversion phosphors, namely in improvement of the energy yield of solar cells by adaptation of the sunlight spectrum to the sensitivity spectrum of commercial solar cells. In this case, conversion from UV to visible light with zero re-absorption of the emission is necessary. The materials which are most suitable for these purposes are semiconductor phosphor dots, i.e. quantum dots doped with luminescent ions. Colloidally stable and highly luminescent semiconductor $Zn_xCd_{1-x}S$:Mn/ZnS core–shell nanocrystals (NCs) with a quantum yield (QY) of more than 70 % were developed and tested as a very prospective materials for this purposes. The nature of defects as well as dissipation mechanisms, which do not allow reaching higher QY of Mn^{2+} emission in $Zn_xCd_{1-x}S$:Mn/ZnS, are discussed in this talk.

The work was performed in the frame of ERANET-RUS Plus NANOLUX 2014 (ID #286) project and the project 1006-11 "Intelligenz im Solarglas", Bavarian Research Foundation.

Influence of Mg^{2+} and Si^{4+} substitution on the emission properties of $Y_3Al_5O_{12}$: Ce luminescence converter for white light emitting diodes

Liudmyla M. Chepyga [1,2,3,*], Maximilian Dierner [1], Andres Osvet [1], Christoph J. Brabec [2], Yuriy Zorenko [4], Miroslaw Batentschuk [2]

[1]Energie Campus Nürnberg (EnCN), Fürther Str. 250, 90429 Nürnberg, Germany
[2]Institute of Materials for Electronics and Energy Technology (i-MEET), Friedrich-Alexander Universität Erlangen-Nürnberg, Martensstraße 7, 91058 Erlangen, Germany
[3]Erlangen Graduate School in Advanced Optical Technologies (SAOT), Friedrich-Alexander Universität Erlangen-Nürnberg, Paul-Gordan-Str. 6, 91052 Erlangen, Germany
[4]Institute of Physics of Kazimierz Wielki University in Bydgoszcz, ul. Powstańcow Wielkopolskich 2, 85-064 Bydgoszcz, Poland
**liudmyla.chepyga@fau.de*

Yttrium aluminum garnet $Y_3Al_5O_{12}$ (YAG) crystallizes in a cubic crystal structure and generates large crystal-field strengths at 8-fold O^{2-} coordinated polyedra. Therefore, Ce^{3+}-doped garnet-type phosphors typically emit in green-yellow spectral region. A further red shift of the Ce^{3+} emission spectrum in YAG can be achieved by increased covalence, for instance, by substitution of Al^{3+} by Mg^{2+}–Si^{4+} pair on the octahedral and tetrahedral sites, respectively [1]. Recently, we have observed such red shift and Ce^{3+} multicenter formation in the single crystalline films of solid solution of $Y_3Mg_xSi_xAl_{5-2x}O_{12}$ garnet at x=0-0.5, grown by liquid phase epitaxy method [2]. Jiang et al. [3] reported also on progressive red shift from 528 to 552 nm in $Y_3Al_{5-2x}Mg_xGe_xO_{12}$:Ce with increasing of Mg^{2+}–Ge^{4+} ions concentration above x=0.5. In terms of interest towards new solid-state phosphors for white light emitting diodes (LEDs), highly luminescent phosphors with adjustable color range are necessary.

We report on the investigation of the influence of substitution of Al^{3+} ions by Mg^{2+} and Si^{4+} doping on luminescence properties of $Y_3Al_5O_{12}$:Ce^{3+} (YAG:Ce) micro- (MC) and nanopowder (NP) phosphors. The MP and NP phosphors were synthesized: 1) by conventional high temperature solid state synthesis (SSS) using CaF_2 as a flux; 2) by fatty acid-assisted co-precipitation technique (CPS) where SiO_2 nanoparticles served as a silicon source, respectively. In the MP SSS samples it was experimentally observed that the use of amount of flux affects the luminescent properties. Herein, a strategy involving the use of different amount of flux (3, 5, 10, 15 wt. %), concentration of Ce^{3+} (3, 5, 7, 10 mol %) ions and substitution of Al^{3+} ions by Mg^{2+} – Si^{4+} in YAG:Ce^{3+}, i.e. $Y_3Al_{(5-2x)}Mg_xSi_xO_{12}$:$Ce^{3+}$ with x = 0; 0,25; 0,5; 1; 2 has been developed to achieve high photoluminescence intensity of the signal and high purity of the garnet phase.

Calcinations of the phosphors in reducing (N_2/H_2) atmosphere results in bright luminescence of Ce^{3+} ions of NP and MP phosphors with up to 55 and 58 % of quantum yield (PLQY), respectively. The red shift of the photoluminescence was observable in phosphors synthesized by both synthesis methods. Depending on the concentration of Mg^{2+} – Si^{4+} substitution the red shift was in the range from 533 to 603 nm. The $Y_3Al_4Mg_{0,5}Si_{0,5}O_{12}$:5% Ce composition, independent of the synthesis method, shows the highest QY and purity of the garnet phase, what is desirable for improving the efficiency of white LEDs.

The work was performed in the frame of Era-Net Rus-Plus NANOLUX 2014 (ID #286) project.

[1] A. Katelnikovas *at al.*, *J. Lumin.*, vol. **129**, no. 11, pp. 1356–1361, 2009.
[2] V. Gorbenko, T. Zorenko, A. Iskaliyeva, K. Paprocki, K. Fabisiak, S. Witkiewicz, S. Dolaciński, A. Fedorov, F. Schröppel, E. Levchuk, A. Osvet, M. Batentschuk, Ya. Zhydachevskyy, A. Suchocki, Yu. Zorenko, *Optical Materials,* 2018, submitted.
[3] L. Jiang *et al.*, *Mater. Res. Bull.*, vol. **98**, pp. 180–186, 2018.

Single crystalline films in investigation of the intrinsic and defect–related luminescence of garnet compounds

Yuriy Zorenko

Institute of Physics, Kazimierz Wielki University in Bydgoszcz, Powstańców Wielkopolskich 2, 85-090 Bydgoszcz, Poland

**corresponding author: zorenko@ukw.edu.pl*

The garnets $A_3B_5O_{12}$ compounds are related to the well-known optical materials which are widely used as laser media, scintillators, LED convertors, etc. From the usual point of view, the intrinsic luminescence of hosts and luminescence of dopants can be simply investigated in garnets, if we have one of the structural forms of these compounds (crystals, films, micro- and nanopowders and ceramics). But this conclusion is not always true.

Meanwhile, substantial differences in the methods and conditions of material preparation from the melt (crystals), melt-solution (films) or solid-state reactions (ceramics) result in the significant differences in their luminescent properties even for the same garnet compounds. Such differences are caused by the different types of intrinsic defects, their content and distributions over the main volume and surface of sample as well as by interaction of the defects with impurity centers. Sometimes, in the well-known compounds, such as $Y_3Al_5O_{12}$ and $Lu_3Al_5O_{12}$ garnets, the contribution of defect centers to the intrinsic luminescence of host or the emission of dopants is so significant, that it can completely mask the native luminescent properties of matrix or impurities.

The concentration of intrinsic defects can be strongly reduced in the garnets prepared by low-temperature methods using the solid state reaction (ceramics) or liquid phase epitaxy growth from the melting fluxes (films). At the same time, the single crystalline films can contain the components of flux which also may influence their properties. The luminescent properties inside the nano and -micro-powders of garnets usually differ from the properties of their surface and borders of grains with substantially larger content of defects.

Thus, only the detailed comparison of the luminescent properties of garnet compounds, prepared in the film, crystal and ceramic forms, gives the possibility to extract the fundamental luminescent properties of the hosts from the background of defect luminescence as well as to detect the "real picture" of the dopant luminescence in these oxides. Using for this purpose the traditional spectral methods and synchrotron radiation excitation with the energy in the range of fundamental absorption of these materials opens a unique possibility for correct comparison of the luminescent properties of garnets in the different crystalline forms.

The aim of presentation is to show the characteristic examples of comparison of the structure of intrinsic luminescent centers in films and crystals of undoped and rare-earth doped garnets using the traditional spectral methods and luminescent spectroscopy under excitation by synchrotron radiation in the range of fundamental absorption edge of these materials. Main attention is directed on the study of the fundamental optical properties of garnets such as intrinsic luminescence of hosts of these oxides caused by the luminescence of excitons and the luminescence of the different type defects (antisite defects and charged oxygen vacancies and their aggregates) in the mentioned compounds.

*Acknowledgments***.** This work was supported by Polish NCBR NANOLUX 2014 ID 286 and NCN 2017/25/B/ST8/02932 projects.

Synthesis and Characterization of pure and doped $BaAl_2O_4$ via a Modified Sol-Gel Route using PVA

Simone Santos Melo [1], Jéssica Carla da Cunha Carvalho [1], Adriano Borges Andrade [2], Giordano Frederico da Cunha Bispo [1], Zélia Soares Macedo [1] and Mário Ernesto G. Valerio [1,*]

[1]*Physics Department, Federal University of Sergipe, 49100-000, Sao Cristovao-SE, Brazil*
[2]*Materials Science and Engineering Department, Federal University of Sergipe, 49100-000, Sao Cristovao-SE, Brazil*

The aluminates have many practical applications, especially in equipment for production of artificial light, modern lighting, displays and optical communications fields, such as fluorescent lamps and plasma panels [1]. They are also used as scintillators, which are materials that can convert ionizing radiation into ultraviolet, visible or infrared light [2]. Currently the scintillators are used as primary sensors and radiation detection sensors, being applied in industrial inspection devices, dosimetry, high energy physics and several imaging devices in nuclear medicine [3,4]. Due to the increasing demand, it is necessary to improve this technology, such as improving the physical and chemical resistance of scintillators, as well as the conversion efficiency combined with lower production costs. The barium aluminate when doped with cerium and/or manganese ions may exhibit scintillation phenomenon. In order to evaluate the insertion behavior of these ions in barium aluminate, a study of this material was carried out through several techniques. Pure barium aluminate samples were prepared using a modified Sol-Gel route using PVA as complexing agent, varying the pH and temperature until the best synthesis condition was reached. DTA/TG measurements made in parallel to the sample synthesis were performed and, from the thermal events observed, possible synthesis temperatures were chosen. In order to confirm the formation of the right crystalline phase, powder X-ray diffraction (XRD) measurements were performed. Rietveld refinement technique was used to analyze the XRD patterns. After obtaining the best synthesis conditions, Ce and Mn doped samples were produced. XANES measurements around the Ce and Mn absorption edges proved that both Ce^{3+} and Ce^{4+} and Mn^{2+} and Mn^{3+} ions are present in the samples. XEOL (X-ray excited optical luminesncence) measurements around Ce and Mn edges showed that the XEOL emission spectra are due to the dopants and the XEOL excitation spectra when excited around the Ba L3 edge decrease as the photon energy inceased, while for the excitation around the dopant edges, did not show this behavior. A mechanism is proposed to explain the features of the XEOL emission of the Ce and Mn – doped $BaAl_2O_4$.

[1] Wiglusz, R. J.and Grzyb, T., *Optical Materials.* **36** (2013) 539-545;
[2] Knoll, G. F., *Phoenix Usa*. **3** (2010) 830;
[3] Blasse, G., Grabmaier, B. C., *Luminescent Materials*. (1994).
[4] Cherry, S.; Sorenson, J.; Phelps, M., *Saunders Elsevier*. **4** (2012).

Transparent ceramics based on rare earth ions-doped cubic tungstate/molybdate matrices: a challenge and prospect for new efficient optical materials?

M. Guzik [1,*], M. Bieza [1], E. Tomaszewicz [2], Y. Guyot [3], G. Boulon [3]

[1]*Faculty of Chemistry, University of Wrocław ul. F. Joliot-Curie 14, 50-383 Wrocław, Poland*
[2]*Department of Inorganic and Analytical Chemistry, West Pomeranian University of Technology, Al. Piastów 42,71-065 Szczecin, Poland*
[3]*Univ Lyon, Université Claude Bernard Lyon1, CNRS, Institut Lumière Matière, F-69622, Villeurbanne, France*
**goguzik@poczta.fm*

Surprisingly, today available rare earth (RE^{3+}) luminescent ions-doped cubic optical transparent ceramics used as laser sources or phosphors for lighting are limited to a very small number. The main objective of this project is to select carefully new RE^{3+} luminescent ions-doped tungstate/molybdate chemical compositions, fulfilling two conditions, cubic crystallographic system and size of the crystallites up to 100 nm, different of usual garnets, sesquioxides or fluorites, owing to their long longevity, low cost, and excellent chemical stability. The choice of RE^{3+} ions has been Nd^{3+} and Yb^{3+} for IR and visible lasers and Eu^{3+} for red phosphors. The host lattices, in which the substitution of optically un-active trivalent La^{3+} or Y^{3+} by RE^{3+} ions will take place have been preferred. For each composition, nano-powder materials are researched by various methods: Pechini, combustion, hydrothermal, methods and high-temperature solid state reaction [1-4].

The results on both synthesis and spectroscopic characterizations of Yb^{3+} , Nd^{3+} and Eu^{3+}-doped La_2MoWO_9 , $La_2Mo_2O_9$ and Y_6MoO_{12} compounds will be presented. Our attention will be now focused on both the crystal growth by using the micro-pulling down method (μ-PD) and the fast SPS (Spark Plasma Sintering) and the slower but efficient HIP (Hot Isostatic Pressing) techniques to show the feasibility of transparent ceramics. Important information on the spectroscopic properties will be obtained by using site selective and time resolved spectroscopy techniques on both nano-powders, single crystals and transparent ceramics.

Acknowledgements: We wish to thank the Minister of Science and Higher Education in Poland and in France for the Grant POLONIUM for scientific exchange between Institute Light Matter (ILM), UMR5306 CNRS-University Lyon1, University of Lyon, France and Faculty of Chemistry, University of Wrocław in Poland, as well as the National Science Center of Poland for the grant HARMONIA No UMO-2016/22/M/ST5/00546.

[1] M. Bieza, M. Guzik, E. Tomaszewicz, Y. Guyot, G. Boulon, *Opt. Mat*. **63** (2017) 3-12.
[2] M. Bieza, M. Guzik, E. Tomaszewicz, Y. Guyot, K. Lebbou, E. Zych, G. Boulon, *J. Phys. Chem. C*, 2017, **121** (24), 13290–13302.
[3] M. Bieza, M. Guzik, E. Tomaszewicz, Y. Guyot, K. Lebbou, G. Boulon, *J. Phys. Chem. C*, 2017, **121** (24), 13303–13313.
[4] M. Bieza, M. Guzik, E. Tomaszewicz, Y. Guyot, G. Boulon, *J. Europ. Cer. Soc*., 2018 accepted, doi.org/10.1016/j.jeurceramsoc.2018.02.007.

Defects and Transport in Perovskites with Protons, Oxygen Vacancies and Electron Holes

R. Merkle [1,*], R. Zohourian [1], G. Raimondi [1], and J. Maier [1]

[1]*Max Planck Institute for Solid State Research, Heisenbergstr. 1, Stuttgart, Germany*

The defect chemistry of mixed-conducting perovskites with oxygen vacancies ($V_O^{\bullet\bullet}$), protonic defects ($OH_O^{\bullet}$) and holes ($h^{\bullet}$) is interesting from a fundamental point of view, but also relevant for applications. Protonic ceramic fuel cells (PCFC) are based on proton conducting Ba(Ce, Zr, Y)O_{3-x} perovskites as electrolyte which exhibit a higher ionic conductivity at intermediate temperatures (300-600 °C) than the typical oxide ion conductors such as Y-doped ZrO_2 [1]. In order to make the whole surface of the porous cathode active for the oxygen reduction reaction to water, a certain proton conductivity is required also in the cathode material which is typically a mixed conducting perovskite. These perovskites incorporate protons either by hydration (dissociative water uptake, filling of oxygen vacancies)

$$H_2O + V_O^{\bullet\bullet} + O_O^x \rightarrow 2OH_O^{\bullet}$$

which is a pure acid-base reaction, or hydrogen uptake from H_2O at expense of holes

$$H_2O + 2O_O^x + 2h^{\bullet} \rightarrow 2OH_O^{\bullet} + \frac{1}{2}O_2$$

which is a redox reaction. The relative contribution from these two reactions depends on the concentration ratio of oxygen vacancies and holes [2].

Thermogravimetric measurements show that the proton uptake is much smaller for (Ba,Sr,La)(Fe,Co,Zn,Y)$O_{3-\delta}$ perovskites employed as cathode materials in PCFC compared to Ba(Ce,Zr,Y)O_{3-x} perovskites which are used as electrolyte materials [3,4]. The basicity of the oxide ions which depends on the cation composition is identified as a key parameter for proton uptake. The maximum proton concentration of 10% at 250 °C was found for $(Ba_{0.95}La_{0.05})(Fe_{0.8}Zn_{0.2})O_{3-\delta}$ [5]. The proton concentration of Ba-rich cathode materials is expected to allow for an extension of the reactive zone beyond the three-phase boundary. Quantitative analysis of oxygen stoichiometry and proton uptake shows a significant hole-hole and hole-proton interaction which is related to a partial delocalization of holes from the transition metal to the oxide ions [5]. These interactions are key to understand the differences in the proton uptake of cathode versus electrolyte materials.

[1] K. D. Kreuer, *Ann. Rev. Mater. Res*. **33** (2003) 333.
[2] D. Poetzsch, R. Merkle, and J. Maier, *Adv. Funct. Mater*. **25** (2015) 1542.
[3] D. Poetzsch, R. Merkle, and J. Maier, *Farad. Discuss.* **182** (2015) 129.
[4] R. Zohourian, R. Merkle, and J. Maier, *Solid State Ionics* **299** (2017) 64.
[5] R. Zohourian, R. Merkle, and J. Maier, *in preparation*.

The charge transport characterization of thin diamonds layer by impedance method

Szymon Łoś [1], Kazimierz Paprocki [2], Kazimierz Fabisiak [2], Mirosław Szybowicz [3]

[1]*Institute of Molecular Physics, Polish Academy of Sciences, Smoluchowskiego 17, 61-179, Poznań, Poland*

[2]*Institute of Physics, Kazimierz Wielki University, Powstańców Wielkopolskich 2, 85-090 Bydgoszcz, Poland*

[3]*Faculty of Technical Physics, Poznan University of Technology, M. Sklodowskiej-Curie 5, 60-965 Poznań, Poland*

The impedance spectroscopy investigation of charges transport mechanism in thin diamonds layer grown by HF CVD (Hot Filament Chemical Vapor Deposition) method are reported. The measurements were performed in both, wide temperature and bias voltage range as well. The diamond crystal is considered as a wide band gap semiconductor but the CVD diamond polycrystalline films always contains some amount of sp^2 hybridized amorphous carbon phase which can has a main contribution in current conveyance. In disordered matter the variable range hopping mechanism can play a crucial role. However obtained results reveal that simultaneously holes and electrons are involved in current flowing. Their mutual interaction can lead to the Ohm's law breaking and have the influence on charge localization phenomenon. At low temperature there is observed a sudden change on the surface resistivity caused by helium atoms sorption on slowly moving holes states.

Impact of defects, strain, and magnetic field on electronic states in graphene and heterogeneous charge transfer kinetics

Paweł Szroeder [1,*], Igor Yu. Sagalianov [2], Taras M. Radchenko [3], Valentyn A. Tatarenko [3], Yuriy I. Prylutskyy [4]

[1]*Institute of Physics, Kazimierz Wielki University, Powstańców Wielkopolskich 2, 85-090 Bydgoszcz, Poland*
[2]*Dept. of General Physics, Taras Shevchenko National University of Kyiv, 64 Volodymyrska Street, 03022 Kyiv, Ukraine*
[3]*Dept. of Metallic State Theory, G. V. Kurdyumov Institute for Metal Physics, N.A.S. of Ukraine, 36 Academician Vernadsky Boulevard, 03142 Kyiv, Ukraine*
[4]*Dept. of Biophysics, Educational and Scientific Center "Institute of Biology and Medicine", Taras Shevchenko National University of Kyiv, 64 Volodymyrska Street, 03022 Kyiv, Ukraine*
[*]*Corresponding author*

Magnetoelectronic properties and charge transfer kinetics through graphene/ionic solution interface is strongly linked to graphene electronic density of states (DOS), which is very sensitive to different sources of disorder and external field effects. Among known and currently in use different ways for inducing goal-directed effects in electronic and transport properties of graphene, the application of external mechanical [1] and magnetic [2] fields are extremely useful for addressing its fundamental properties as it provides an external and adjustable parameter which drastically modifies graphene's electronic band structure. Thus, stress in combination with point or line defects and external (perpendicular) magnetic field is a natural route for tuning graphene properties towards fabrication of effective graphene based electrochemical transducers. We study numerically a role of the uniaxial tensile strains and disordered defects in their impact on DOS in graphene exposed to an external magnetic field. Observed non-equidistant Landau levels (LLs) in the energy spectrum of a defectless graphene undergo the displacement towards the non-shiftable zero-energy Landau level (LL), thus they get contraction as the uniaxial tension is applied independently on the stretching direction. The presence of both point and extended defects reduces LLs peaks, broadens, smears and can even suppress the LLs depending on a degree of disorders, their strength and especially effective ranges. The splitting of zero-energy LL is observable in case of the short-range disorder. Increase or decrease of the localized electronic states in graphene is sensitive to direction of the uniaxial strain: mutually perpendicular axes of elongation result to inverse effects that can be attributed to enhancement or reduction of DOS during the stretching along armchair or zigzag directions, respectively. Mutual action of perpendicular magnetic field and uniaxial stress along the zigzag direction in graphene makes a band gap in its energy spectrum more pronounced and even wider as compared with the case of zigzag strain effect only. We show that the enhancement/reduction of graphene DOS impacts the kinetics of heterogeneous charge transfer for the ferrocyanide/ferricyanide redox couple and can be used for tuning electrocatalytic activity towards other chemical species in ionic solutions.

[1] C. Si, Z. Sun, F. Liu, Strain engineering of graphene: a review, *Nanoscale* **8** (2016) 3207.
[2] M. Orlita, W. Escoffier, P. Plochocka, B. Raquet, U. Zeitler, Graphene in high magnetic fields, *C. R. Physique*, **14** (2013) 78.

Hole trap process and highly sensitive optical thermometry, host-sensitized and IVCT interfered in Pr^{3+}-doped $Na_2La_2Ti_3O_{10}$ micro-crystals with layered perovskite structure

Y.J. Wang [1,*], Y. Zhydachevskyy [1], V. Tsiumra [1], Liang H.B. [2], A. Suchocki [1,3]

[1]*Institute of Physics, Polish Academy of Sciences, Al. Lotnikow 32/46, 02-668, Warsaw, Poland*
[2]*MOE Key Laboratory of Bioinorganic and Synthetic Chemistry, KLGHEI of Environment and Energy Chemistry, School of Chemistry, Sun Yat-sen University, Guangzhou 510275, China*
[3]*Institute of Physics, Kazimierz Wielki University, Weyssenhoffa 11, 85-072, Bydgoszcz, Poland*

The layered perovskite oxide (LPO) compounds have been received considerable attention as functional materials that serve two-dimensional microspaces. In this work, we demonstrated a high-sensitivity optical thermometric material based on the diverse thermal quenching behaviors in the Ruddlesden-Popper type perovskite $Na_2La_{1.995}Pr_{0.005}Ti_3O_{10}$ (NLTO) miro-crystals, which provide a perspective approach to design self-referencing optical temperature sensing materials with superior temperature sensitivity. The fluorescence intensities ratio (FIR) of Pr^{3+} $^3P_0$ and $^1D_2$ multiplets, host excited and IVCT state interfered, reveals outstanding temperature sensing performance with the maximum relative sensitivity as high as 2.43% K^{-1} at 425 K. In the mean time, it is found that $^3P_1$ and $^3P_0$ levels of Pr^{3+} can be adopted as thermally coupled energy levels (TCEL) for thermal sensing with relatively high sensitivity in the low-temperature range from 150 to 275 K. Furthermore, the experimental results indicate that, in Pr^{3+}-doped NLTO, Pr^{3+} ions work as hole trap and recombination sites for efficient excitation energy transfer from host to Pr^{3+} ions [1]. The decay kinetics and high-pressure luminescence studies were also performed to confirm our interpretation of experimental results and the model proposed for the system. This work can be expected to lead to the development of novel photofunctional materials.

Acknowledgements: This work was partially supported by the grant No. UMO-2017/25/N/ST5/02285 of Polish National Research Center.

[1] A. Kudo and T. Sakata. *Chem. Mater.* **9** (1997) 664.

S9–S10 Luminescence spectroscopy of excitons, impurities, and defects, including using of synchrotron radiation

Distribution of dopants in crystals/ceramics/glasses/glass-ceramics analyzed by the conjugation of TEM, EDX, XPS and optical spectroscopic tools

G. Boulon [1,*], Y. Guyot [1], M. Guzik [2], T. Epicier [3], L. Esposito [4], W. Strek [5], A. Yoshikawa [6], Hu L. [7], Chen W. [7]

[1]*Institute Light Matter (ILM), UMR5306 CNRS-UCBLyon1, University of Lyon, 69622 Villeurbanne, France*
[2]*Faculty of Chemistry, University of Wroclaw, PL-50-383, Wroclaw, Poland*
[3]*MATEIS, UMR 5510 CNRS-INSA-Lyon, University of Lyon, 69621 Villeurbanne, France*
[4]*National Research Council, Institute of Science and Technology for Ceramic, 48018 Faenza, Italy*
[5]*Institute of Low Temperature and Structure Research, PAS, Wroclaw, Poland*
[6]*Institute for Materials Research, Tohoku University, Sendai 980-8577, Japan*
[7]*Key Laboratory of Materials for High Power Laser, Shanghai Institute of Optics and Fine Mechanics, Chinese Academy of Sciences, Shanghai 201800, PR China*
**Corresponding author : georges.boulon@univ-lyon1.fr*

There is a strong need of knowledge of the real distribution of dopants in crystals/ceramics/-glasses/glass-ceramics which play an important role in the behavior of their optical properties.

The localization of rare earth and transition metal dopants in different types of crystals, ceramics, glasses, glass- ceramics will be illustrated from recent cooperations in which we used the conjugation of the TEM, EDX, XPS and optical spectroscopy independent techniques. The following materials have been analyzed for relevant phenomena of dopants like selective segregation in grain boundaries of ceramics, radiative and non-radiative sites, pairs, different oxidation states and the increasing of their average distances:

- Ce^{3+}-doped $Y_3Al_5O_{12}$ transparent phosphor ceramics [1],
- Yb^{3+}-doped $Y_3Al_5O_{12}$ and Y_2O_3 transparent laser ceramics [2, 3],
- Yb^{3+}-doped $Y_3Al_5O_{12}$ optical nano-ceramics [4],
- Yb^{3+}-Er^{3+}-Co^{2+}-doped glass-ceramics composed of $MgAl_2O_4$ spinel nano-crystals of 10-20 nm size embedded in SiO_2 glass as saturable absorber [5],
- Yb^{3+}/Nd^{3+} spectroscopy of C_{3i} and C_2 site symmetries in laser ceramic/crystal Lu_2O_3 [6],
- Yb^{3+}-doped laser silica glass prepared by sol-gel method. How to play on the distribution of Yb^{3+} ions with the Al^{3+} and P^{5+} contents [7].

[1] W. Zhao, S. Anghel, C. Mancini, D. Amans, G. Boulon, T. Epicier, Y. Shi, X.Q. Feng, Y.B. Pan, V. Chani, A. Yoshikawa, *Opt Mat.* **33** (2011) 684–687.
[2] T. Epicier, G. Boulon, W. Zhao, M.Guzik, B. Jiang, A.Ikesue, L. Esposito, *J. Mater. Chem.* **22** (2012) 18221–18229.
[3] L. Esposito, M. Serantoni, A. Piancastelli, T. Epicier, D. Alderighi, A. Pirri, G. Toci, M. Vannini, S. Anghel, G. Boulon, *J. of the Europ. Cer. Soc.*, **32** (2012) 2273 – 2281.
[4] G. Boulon, Y. Guyot, M. Guzik, T. Epicier, P. Gluchowski, D. Hreniak, W. Strek, *J. Phys. Chem. C* **118** (28) (2014) 15474–15486.
[5] G.Boulon, Y. Guyot, G.Alombert-Goget, M. Guzik, T. Epicier, N. Blanchard, Chen L., Hu L.., Chen W., *J. of Mater. Chem. C*, **2** (2014) 9385–9397.
[6] Y. Guyot, M. Guzik, G. Alombert-Goget, J. Pejchal, A. Yoshikawa, A. Ito, T. Goto, G. Boulon, *J. of Luminescence,* **170** (2016) 513-519.
[7] S.Wang, F. Lou, C. Yu, Q. Zhou, M. Wang, S. Feng, D. Chen, Hu L.., Chen W., M. Guzik, G. Boulon, *J. Mater. Chem. C,* **2** (2014) 4406-4414.

A new model to explain anomalous emission from CaF_2:Yb and other systems

Zoila Barandiarán* and Luis Seijo

Departamento de Química, Instituto Universitario de Ciencia de Materiales Nicolás Cabrera, and Condensed Matter Physics Center (IFIMAC), Universidad Autónoma de Madrid, Spain
**Corresponding author*

Upon excitation in the lowest $4f^{14} \rightarrow 4f^{13}5d$ band of $CaF_2:Yb^{2+}$, in the UV, the expected Stokesshifted *d-f* emission is not observed. Rather, a much lower emission is detected at low temperature in the blue-green, with a very large bandwidth. This is the well-known and longknown *anomalous* emission (AE) of Yb^{2+} in CaF_2 [1].

For over 30 years it has been believed that the emitting state is an impurity-trapped exciton (ITE): a hole localized in the Yb^{2+} dopant and a bound electron presumably residing on the closest Na^+ neighbors [2]. However, ab initio calculations performed to confirm the ITE hypothesis failed to do it; instead, they suggested that the AE can be identified as an intervalence charge transfer (IVCT) luminescence [3].

X-ray and UV spectroscopy studies have shown evidences that CaF_2:Yb is not an ITE system but a very complex multivalent system whose AE is very difficult to understand: (i) The intensity of the AE is far from proportional to Yb^{2+} concentration [4]. (ii) X-ray excitation triggers the AE of Yb in CaF_2 but not in SrF_2 [5]. (iii) X-ray exposure kills the AE even though it can provoke a huge reduction of Yb^{3+} to Yb^{2+} [6]; the lost AE is never recovered unless the sample is heated well above room temperature.

I will address all of these aspects of the AE of Yb in fluorites from ab initio calculations which deal with electron transfer between dopant 2+/3+ valences, from the host to the dopant or from the charge compensators to the dopant. The combination of theoretical results with experimental data seems to be consistent and meaningful, but we still have interesting open questions. Furthermore, we are trying to address in similar ways a very challenging dopant for theory: Eu^{2+}/Eu^{3+}, whose anomalous emissions in BaF_2 are also well-known. The results that might be available for this important activator will be discussed as well.

[1] Feofilov P. P., *Opt. Spektrosk*. **1**, 992 (1956); A. A. Kaplyanskii and Feofilov P. P., *Opt. Spectrosc*. **13**, 129 (1962); E. G. Reut, *Opt. Spectrosc*. **40**, 55 (1976).
[2] D. S. McClure and C. Pédrini, *Phys. Rev. B* **32**, 8465 (1985); B. Moine, B. Courtois, and C. Pédrini, *J. Phys. France*, **50**, 2105 (1989).
[3] Z. Barandiarán and L. Seijo, *J. Chem. Phys.* **141,** (2014) 234704.
[4] C. MacKeen, F. Bridges, M. Kozina, A. Mehta, M. F. Reid, J.-P. R. Wells, and Z. Barandiarán, *J. Phys. Chem. Lett.* **8,** (2017) 3313.
[5] R. B. Hughes-Currie, K. V. Ivanovskikh, J.-P. R. Wells, M. F. Reid, R. A. Gordon, L. Seijo, and Z. Barandiarán, *J. Phys. Chem. Lett.* **8,** (2017) 1175.
[6] C. MacKeen, F. Bridges, L. Seijo, Z. Barandiarán, M. Kozina, A. Mehta, M. F. Reid, and J.-P. R. Wells, *J. Phys. Chem. C* **121,** (2017) , 28435.

Luminescence Zero-Phonon Lines of $3d^3$ Ions in Garnet Solid Solutions with Disorder in Different Cation Sublattices

Sergey Feofilov [1,*], Alexey Kulinkin [1], Vasily Khanin [2], Andries Meijerink [2] and Piotr Rodnyi [3]

[1]*Ioffe Institute, St. Petersburg, 194021, Russia*
[2]*Utrecht University, Utrecht, 3508 TC, The Netherlands*
[3]*Peter the Great St. Petersburg Polytechnic University, St. Petersburg, 195251, Russia*
[*]*Corresponding author*

The solid solution (mixed) insulating crystals and ceramics doped with rare-earth and transition metal ions attract significant attention in optical spectroscopy studies and are of interest from the point of view of potential applications as scintillators, phosphors, laser materials and spectral hole-burning media because they allow variation of the physical properties of the material by variation of the composition.

In [1,2] it was observed that (in contrast to most studied materials) the modification of zero-phonon R-lines (^2E–$^4A_2$) in the fluorescence spectra of Cr^{3+} impurity ions in the concentration series of $Lu_{3x}Y_{3-3x}Al_5O_{12}$ ($0<\boldsymbol{x}<1$) and $Tb_{3z}Y_{3-3z}Al_5O_{12}$ ($0<\boldsymbol{z}<1$) garnet crystals occurs in a discrete rather than a continuous fashion and is not accompanied by strong inhomogeneous broadening. The effect was ascribed to high C_{3i} symmetry of octahedral $Cr^{3+}{}_{Al}$ sites that allows only a limited number of non-equivalent Cr^{3+} centers in mixed environment of dodecahedral D_2 sites randomly occupied with ions of different size when the disorder is introduced into the Y/Lu/Tb sublattice.

The purpose of the current study is to trace the modification of the zero-phonon R-line spectrum of $3d^3$ ions in garnet solid solutions in a more complicated situation when the disorder is introduced into the two sublattices of tetrahedral and octahedral Al/Ga sites. We report the results of the fluorescence spectroscopy studies of Cr^{3+} and Mn^{4+} zero-phonon R-lines in $Y_3Al_{5-5y}Ga_{5y}O_{12}$ solid solution garnet ceramics.

It was observed experimentally that the modification of zero-phonon R-lines spectra of Cr^{3+} impurity ions in the concentration series of $Y_3Al_{5-5y}Ga_{5y}O_{12}$ ($0<\boldsymbol{y}<1$) solid solution ceramics occurs differently at high Al and high Ga content. The discrete Cr^{3+} R-line spectra, similar to those in [1,2], are observed at lower values of $\boldsymbol{y}$ whereas at high values of $\boldsymbol{y}$ the strong inhomogeneous broadening of the R-lines occurs and no discrete disorder response is visible. The effect may be explained by non-random distribution of Al and Ga ions in the tetrahedral sites sublattice, namely, the preferential occupation of tetrahedral sites with Ga ions. It may be concluded that fluorescence spectroscopy of probe $3d^3$ ions in solid solutions enables to detect the variations in the occupancy of different sublattices by different ions and to reveal their non-random distribution.

[1] S. Feofilov, A. Kulinkin, K. Ovanesyan, A. Petrosyan, C. Dujardin, *Phys. Chem. Chem. Phys.* **16** (2014) 22583.
[2] S. Feofilov P., A. B. Kulinkin, K. L. Ovanesyan, A. G. Petrosyan, *Solid State Commun.* **226** (2016) 39.

Exploring widespread hypotheses of luminescence with multiconfigurational ab initio calculations

Luis Seijo [1,*] and Zoila Barandiarán [1]

[1]*Departamento de Química, Instituto Universitario de Ciencia de Materiales Nicolás Cabrera, and Condensed Matter Physics Center (IFIMAC), Universidad Autónoma de Madrid, Spain*
**Corresponding author*

Excited states of luminescent materials can be studied with ab initio quantum chemical methods that use multiconfigurational wave functions and embedded clusters. The results are reliable when appropriate clusters and state-of-the-art embedding techniques, relativistic Hamiltonians (up to spin-orbit coupling), and multiconfigurational expansions that consider static and dynamic electron correlation, can be combined. Although this is not always possible for very complex problems, the range of complexity at reach is steadily increasing and many interesting problems of luminescence can be handled these days [1].

Here we show the results of multiconfigurational ab initio calculations aimed at exploring some well known hypotheses that are used to explain several luminescence phenomena.

1) In the phosphor $CaTiO_3:Pr^{3+}$, quenching of the greenish-blue emission (from $^3P_0$) in favor of the red one (from $^1D_2$) was assumed to be due to Pr-to-Ti metal-to-metal charge transfer states (MMCT). [2]. Attempts to support this hypothesis with multiconfigurational ab initio calculations failed to do it; however, they provided a new interpretation where LMCT states are involved and direct host-to-dopant energy transfer (released by electron−hole recombination following the interband excitation and structural reorganization) selectively populates the $^1D_2$ red luminescent state of Pr^{3+} and bypasses the $^3P_0$ greenish-blue emitter [3].
2) A very broad band centered at around 20000 cm^{-1} in the diffuse reflection spectrum of $SrTiO_3:CeAlO_3$(0.5%) is considered an archetype of MMCT absorption (Ce-to-Ti) in lanthanide compounds [4]. However, a multiconfigurational ab initio calculation on the embedded $(CeTiO_{15})^{23-}$ cluster could not support this interpretation. Other hypotheses involving perturbed LMCT transitions are being explored at this moment in our lab.
3) Two hypotheses are used to interpret the anomalous NIR luminescence in $KZnF_3:Mn^{2+}$ at high concentrations: Mn-Mn exchange interactions [5] and a strongly perturbed Mn^{2+} center [6]. We explore both of them with multiconfigurational ab initio calculations on the embedded $(Mn_2F_{11})^{7-}$ cluster.

[1] L. Seijo and Z. Barandiarán, in *Handbook on the Physics and Chemistry of Rare Earths*, Vol. **50**, 2016, pp. 65-89.
[2] E. Pinel, P. Boutinaud, and R. Mahiou*, J. Alloys Compd. **380** (2004) 225.*
[3] Z. Barandiarán, M. Bettinelli, and L. Seijo, *J. Phys. Chem. Lett.* **8** (2017) 3095.
[4] G. Blasse and G. J. Dirksen, *J. Solid State Chem.* **37** (1981) 390.
[5] E. Song, S. Ding, M. Wu, et al., *Adv. Optical Mater.* **2** (2014) 670.
[6] T. Arai and S. Adachi, *J. Appl. Phys.* **109** (2011) 103506.

Cooperative Luminescence of Yb Pairs in $Li_6Y(BO_3)_3$ Single Crystals

Krisztián Lengyel [1,*], Éva Tichy-Rács [1], Vitali Nagirnyi [2], Kõu Timpmann [2], Sebastian Vielhauer [2], Ivo Romet [2], László Kovács [1], Gábor Corradi [1], Rytis Butkus [3], Mikas Vengris [3], Rimantas Grigonis [3], Valdas Sirutkaitis [3], Ilmo Sildos [2], Valter Kiisk [2], Laurits Puust [2]

[1] *Wigner Research Centre for Physics, Hungarian Academy of Sciences, Konkoly-Thege út 29-33, H-1121 Budapest, Hungary*
[2] *Institute of Physics, University of Tartu, W. Ostwald str. 1, 50411 Tartu, Estonia*
[3] *Laser Research Center, Vilnius University, Sauletekio al 10, LT-10222, Vilnius, Lithuania*
[*] *Corresponding author*

$Li_6Y(BO_3)_3$ (LYB) may form solid solutions with homologous lithium rare earth (RE) borates. Therefore, LYB single crystals may accommodate large concentrations of RE dopants like Yb^{3+}. Their structure contains edge-sharing REO_8 polyhedra forming chains along the *c* axis allowing for relatively close RE^{3+} neighbors with a distance of about 3.85 Å. This geometry supports the emergence of cooperative luminescence (CL) where two excited neighboring RE^{3+} ions relax at the same time, emitting a single photon.

In this work, the results of spectroscopic study of the CL of Yb^{3+} pairs in LYB single crystals will be presented. The CL was successfully generated in the temperature range of 6-300 K in LYB crystal doped with 5 or 20 % Yb using a continuous laser excitation at the wavelength of 972.3 nm (Fig. 1a). The laser power dependence of the CL intensity was found to be quadratic at room temperature but nearly linear at 6 K. Measurements of the CL decay kinetics, and the comparison of the samples with different Yb concentration were performed using a tunable femtosecond laser system (Topas). CL was found to decay nearly twice faster than single ion luminescence and showed further slight shortening with growing Yb concentration (Fig. 1b). A possible explanation for the power and temperature dependence of the CL spectra based on the energy transfer process in the Yb chains will be also presented.

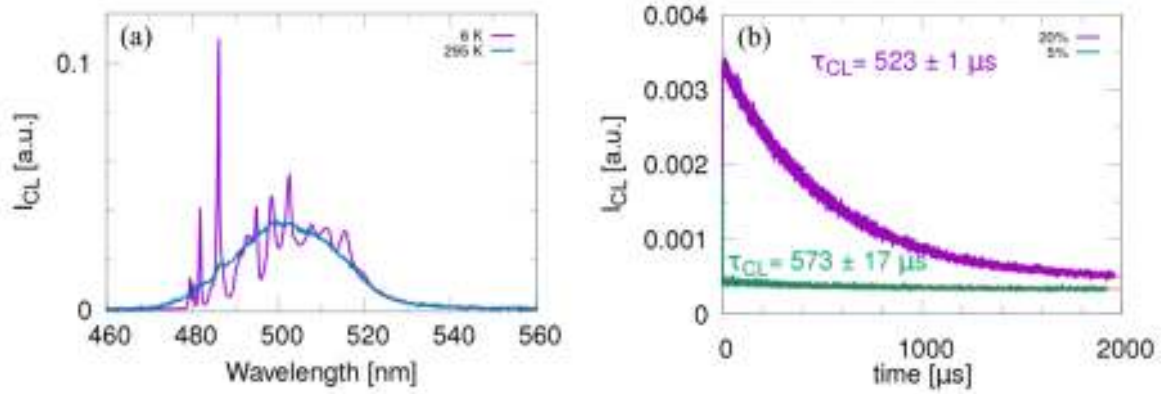

Fig. 1 CL spectra of the 20 mol% Yb doped LYB crystal measured at 6 K and 295 K (a). Evolution of the CL in the 5 and 20 mol% Yb doped LYB crystals following a 40 ps laser pulse excitation (b).

Relaxation of Intrinsic and Extrinsic Excitations in Nano- to Micro-Size Alumina

Marco Kirm [1,*]

[1] *Institute of Physics, University of Tartu, W. Ostwald str. 1, 50411 Tartu, Estonia*
[*] *Corresponding author*

Alumina (Al_2O_3) is a technological material widely used in the form of ceramics or single crystals. The most common structural phase of alumina is an α-phase, whose electronic excitations have been thoroughly studied (see [1] and references therein). However, there has been increasing interest towards transition alumina [2] which are metastable polymorphs (δ, θ, γ etc.) having different crystal structures, often in a nano-size scale. In comparison with a thermodynamically stable α-phase, the changes of electronic properties in transition alumina have been expected, but have received much less attention [3]. Our research team has been investigating electronic properties of alumina in various forms from single crystals, ceramics to nanopowders by means of time-resolved luminescence spectroscopy using vacuum ultraviolet synchrotron radiation and electron-beam excitation. The studied crystalline alumina nanopowders (crystallite size by XRD, d=80-180 and d < 10 nm for the α- and γ-phase, respectively) were prepared by combustion synthesis [4], oxidation of high purity aluminum (d=7-300 nm various phases) [3,5] and ceramics (micrometer grain size) using the spark plasma sintering method [6]. Thermochemical treatment of transition alumina samples resulted in changes of their phase composition and crystallite size. Also impurity ions (e.g., Cr^{3+}) could be used as local probes, which revealed peculiarities of relaxation processes and influence of dimensionality effects. Such extensive experimental data allow to discuss the role of intrinsic and extrinsic electronic excitations in relaxation processes in transitions alumina and to compare those with mechanisms known for a well-studied α-phase. The peculiarities of electronic structure and relaxation dynamics related to particle size will also be discussed.

The onset of intrinsic absorption energies for a mixture of δ- and θ-Al_2O_3 at 7.5 eV and γ-Al_2O_3 at 7 eV were determined. Analogously to α-Al_2O_3, where the existence of self-trapped excitons with radiative decay at 7.6 and 3.77 eV in ns time scale has been established [1], there are indications to triplet self-trapped excitons with emission at 4.6 eV in nano-size transition alumina [3,4]. Along with intrinsic excitations, the presence of F, F^+ and F_s^+ defect states was established. The experimental investigations have shown that the O^{2-} - Cr^{3+} charge transfer transition peaked at 7.0 eV exhibits a 0.2 eV red shift with decreasing crystallite size. Surprisingly, in comparison to the Al_2O_3 single crystals, α-phase nanopowders and alumina ceramics demonstrated a blue shift of the same value towards the higher energies. The origin of such effects observed in the excitation spectra of various intrinsic and extrinsic emissions will be discussed.

[1] M. Kirm, G. Zimmerer, E. Feldbach, *et al., Phys. Rev. B* **60** (1999) 502.
[2] I. Levin, D. Brandon, *J. Am. Ceram. Soc.* **81** (1998) 1995.
[3] L. Museur, M. Bouslama, M. Amamra, A. Kanaev, *Phys. Stat. Sol. RRL* **7** (2013) 1026.
[4] M. Oja, E. Feldbach, A. Kotlov, H. Mändar, *et al., Radiat. Meas.* **56** (2013) 411.
[5] M. Oja, E. Tõldsepp, E. Feldbach, *et al., Radiat. Meas.* **90** (2016) 75.
[6] E. Tõldsepp, F. Schoenstein, M. Amamra, *et al., Ceramics Int.* **42** (2016) 11709.

Relaxation of Electron Excitations in CeF_3 Nanocrystals

Anatoliy Voloshinovskii [1,*], Hryhoriy Stryhanyuk [2], Taras Demkiv [1], Vitaliy Vistovskyy [1], Aleksei Kotlov [3], Piotr Rodnyi [4], Alexander Gektin [5]

[1]*Ivan Franko National University of Lviv, 8 Kyryla i Mefodiya St., 79005, Lviv, Ukraine*
[2]*Helmholtz Centre for Environment Research, 15 Permoserstr, 04318 Leipzig, Germany*
[3]*Photon Science at DESY, Notkestrasse 85, 22607 Hamburg, Germany*
[4]*Saint-Petersburg State Polytechnical University, 29, Polytekhnicheskaya, 195251, Russia*
[5]*Institute for Scintillation Materials, 60 Nauky Ave, 61072, Kharkiv, Ukraine*

Attention to CeF_3 single crystals was attracted as to prospective materials for use in high-energy physics experiments. This material continues to attract the attention of scientists in view of the prospects for the use of nanoscale objects as nanoscillators for radiotherapy, fluorescent labels for bioimaging, etc. [1]. These applications require the elucidation of the luminescent mechanisms under the spatial confinement. The spatial confinement obligates to take into account the influence of the relations between the migration lengths of charge carriers in the process of electron-electronic scattering, electron-phonon interaction and the size of nanoparticles on the luminescent parameters.

The manifestation of size effects in luminescence is investigated in CeF_3 nanoparticles obtained by the precipitation from water-alcohol solutions. As-synthesized nanoparticles according to X-ray diffraction data have size of ~6 nm. The nanoparticles with larger sizes were obtained during annealing at 200, 400, 600 ^oC in an inert atmosphere. Measurement of luminescent-kinetic parameters was performed using synchrotron radiation on the SUPERLUMI station at DESY, Hamburg.

Nanoparticles of 6 nm size reveal only a wide luminescence band with a maximum at ~ 360 nm under both the optical and the X-ray excitation. This band can be attributed to the luminescence of perturbed cerium centers accordingly to the structure of the excitation spectrum and the luminescence time parameters. With increase of nanoparticle size, the intensity of perturbed cerium luminescence decreases, while the luminescence of regular cerium centers appears and increases. In the range of 4f-5d transitions (4.8-7.0 eV) the position of luminescence excitation maxima for nanoparticles correlates with dips in the excitation spectra of CeF_3 single crystal. Thus in the nanoparticles there is no distortion of the excitation spectra due to non-radiation losses on surface defects. This is due to the fact that the attenuation length of exciting light is comparable with the nanoparticle size.

Features of the cerium luminescence excitation spectra for energies $h\nu > 2\ E_{4f\text{-}5d}$ and $h\nu > 2E_g$ are discussed in terms of the electronic excitations multiplication based on the energy model proposed in [2]. When the size of the nanoparticles is reduced from 40 nm to 6 nm, the intensity of the photon multiplication bands decreases faster than the intensity of the bands corresponding to 4f-5d transitions. This fact could confirm the identification of the observed bands at $h\nu > 2\ E_{4f\text{-}5d}$ and $h\nu > 2E_g$ with the processes of photon multiplication involving band charge carriers that escape the nanoparticles.

[1] A-L. Kulin, Processus de relaxation d'energie dans les nanoscintillateurs. Thesis de l'Universite de Lion 2014
[2] R. Glukhov, A. Belsky, C. Pedrini, A.N. Vasil'ev, *J. of Alloys and Compounds*, **275** (1998) 488.

Quantum efficiency of the down-conversion process in some Bi^{3+}–Yb^{3+} or Ce^{3+}–Yb^{3+} co-doped oxide phosphors

V. Tsiumra [1], Ya. Zhydachevskyy [1,2,*], M. Baran [3], L. Lipińska [3], I.I. Syvorotka [4], A. Wierzbicka [1] and A. Suchocki [1,5]

[1] *Institute of Physics, Polish Academy of Sciences, Warsaw, Poland*
[2] *Lviv Polytechnic National University, Lviv, Ukraine*
[3] *Institute of Electronic Materials Technology, Warsaw, Poland*
[4] *Scientific Research Company "Carat", Lviv, Ukraine*
[5] *Institute of Physics, University of Bydgoszcz, Bydgoszcz, Poland*
[*] *Corresponding author:* zhydach@ifpan.edu.pl

Recently, a number of papers pointed out the application potential of Bi^{3+}–Yb^{3+} and Ce^{3+}–Yb^{3+} co-doped materials for solar spectrum modification by means of down-conversion and, consequently, for possible enhancement of the efficiency of silicon solar cells. Here, near-IR emission around 1 μm from Yb^{3+} ($^2F_{5/2}\rightarrow{}^2F_{7/2}$) is induced by excitation in UV-blue range of Bi^{3+} ($^1S_0\rightarrow{}^3P_1$) or Ce^{3+} ($4f\rightarrow5d$) ions.

Quantum efficiency of the down-converting materials is usually estimated from shortening of the luminescence decay of donor (Bi^{3+} or Ce^{3+}) ion, when the conversion ratio of 2.0 (*i.e.* an ideal quantum cutting mechanism) is postulated. However the real value of the energy transfer efficiency in such materials remains generally unknown. In other words, the question remains whether the energy transfer is cooperative (one-to-two) or non-cooperative (one-to-one energy transfer).

In this report, our previous [1,2] and recent results of direct measurements of external quantum yield (QY) for number of Bi^{3+}–Yb^{3+} and Ce^{3+}–Yb^{3+} codoped oxide phosphors are summarized. Among the studied phosphors are: $Y_4Al_2O_9$ (YAM):Bi,Yb; Gd_2O_3:Bi,Yb; YVO_4:Bi,Yb; $Y_3Al_5O_{12}$ (YAG):Bi,Yb; $Gd_3Ga_5O_{12}$ (GGG):Bi,Yb and YAG:Ce,Yb either in the form of powders or single-crystalline films. These measurements are combined with measurements of photoluminescence (PL), photoluminescence excitation (PLE), and photoluminescence decay kinetics.

Obtained results show that the conversion ratio is no more than 1.0 for YAM:Bi,Yb, Gd_2O_3:Bi,Yb, YVO_4:Bi,Yb and YAG:Ce,Yb, testifying an ordinary down-shifting mechanism in these materials. At the same time, for YAG:Bi,Yb and GGG:Bi,Yb the conversion ratio was found to be close to 2.0, suggesting the quantum cutting via cooperative energy transfer from one Bi^{3+} ion to two Yb^{3+} ions. Our results testify that the energy of donor (Bi^{3+} or Ce^{3+}) emission should exceed at least twice the excitation energy of acceptor (Yb^{3+}) ion for quantum cutting process to occur.

Acknowledgements: The work was supported by the Polish National Science Center (project 2015/17/B/ST5/01658) and by the EU within the European Regional Development Fund through the Innovative Economy grant (POIG.01.01.02.00-108/09).

[1] Ya. Zhydachevskyy, V. Tsiumra, M. Baran et al., *Ceram. Int.* **43** (2017) 10130.
[2] Ya. Zhydachevskyy, V. Tsiumra, M. Baran et al., *J. Lumin.* **196** (2018) 169.

Localized Excitons in Bi-Doped YVO_4

V. Tsiumra [1,2,*], T. Malyi [2], A. Zhyshkovych [2], Y. Chornodolskyy [2], V. Vistovskyy [2], A. Voloshinovskii [2], A. Zaichenko [3], Ya. Zhydachevskyy [1,3], A. Suchocki [1,4]

[1]*Institute of Physics, Polish Academy of Sciences, Al. Lotników 32/46, Warsaw 02-668, Poland*
[2]*Ivan Franko National University of Lviv, 8 Kyryla and Mefodiya, Lviv, Ukraine*
[3]*Lviv Polytechnic National University, 12 Bandera, Lviv 79646, Ukraine*
[4]*Institute of Physics, Kazimierz Wielki University, Weyssenhoffa 11, 85-072, Bydgoszcz, Poland*
[*]*Corresponding author:* tsiumra@ifpan.edu.pl

Yttrium orthovanadate doped by bismuth ions is a well-known matrix with a wide emission band with maximum at 560 nm. Despite the considerable interest to YVO_4:Bi and the large number of publications the nature of the YVO_4:Bi^{3+} emission remains unclear. Recent studies explaining the nature of the bismuth emission in the different matrices indicate the location of ^3P levels of bismuth ions in the conduction band of YVO_4, however a detailed model of bismuth ion emission in the YVO_4 has not yet been proposed.

In this study we propose an additional evidence of the exciton nature of the emission of YVO_4:Bi^{3+}. To confirm the conclusions of [1] about the localization of the ^3P energy levels of the Bi^{3+} ion in the conduction band, the luminescent parameters and decay time parameters of YVO_4 doped Bi^{3+} ions with different concentrations were studied. The temperature luminescence decay studies indicate an absence of the millisecond decay component which usually arises at low temperatures. This component appears in the case of intracenter emission of Bi^{3+} ion and is caused by the significant spin-orbital splitting between metastable and emission levels.

The temperature decay studies of the luminescence and the electron energy band structure calculations for YVO_4 doped with bismuth ions provide additional confirmation of the luminescence model as an exciton with hole on the Bi^{3+} and an electron localized on a metal cation of the matrix. The recombination of electron on V^{5+} with a hole causes the luminescence of localized exciton.

The features of rising and decay of the luminescence imply several mechanisms of localized exciton creation in YVO_4:Bi^{3+}. At the photon energy $h\nu > E_g$ and at $T < 100$K, the localized excitons are formed by the relaxation of the matrix exciton in the vicinity of Bi^{3+} center with subsequent localization of a hole near Bi^{3+} center, and the formation of a localized exciton as a Bi^{4+}-V^{4+} state. At $T > 100$ K, the migration of the electrons and holes with next localization on Bi^{3+} and V^{5+} ions is the dominant mechanism for the creation of localized excitons. Migration processes lead to a slower rising of the luminescence pulse.

Acknowledgements: The work was supported by the Ministry of Education and Science of Ukraine (grant for young scientists no. 0116U008071) and the Polish National Science Center (project 2015/17/B/ST5/01658).

[1] P. Boutinaud, *Inorg. Chem*. **52** (2013) 6028–6038.

Luminescent mechanism of RE^{3+}-doped BaY_2F_8 single crystals (RE= Tb, Er, Nd, Pr and Tm)

Adriano B. Andrade [1,2]*, Giordano F. da C. Bispo [1], Ana C. S. Mello [1,3], Zelia S. Macedo [1,2], Sonia L. Baldochi [4], and Mario E. G. Valerio [1,2]

[1]*Physics Department, Federal University of Sergipe, 49100-000, Sao Cristovao-SE, Brazil*
[2]*Materials Science and Engineering Department, Federal University of Sergipe, 49100-000, Sao Cristovao-SE, Brazil*
[3]*Petrobas, Transpetro 49037-440, Aracaju-SE, Brazil*
[4]*IPEN-CNEN, 11049, 05422-970, Sao Paulo-SP, Brazil*
**abandrade1@gmail.com*

Single crystalline Barium Yttrium Fluoride (BaY_2F_8 – BaYF) has been cited as a scintillator material due its efficient light emission output under ionizing radiation, when doped with rare earth ions [1]. The BaYF luminescence has been found to depend on the doping concentration [2] and lifetime [3]. However, there were only a few works that investigate the luminescent mechanism of this material focused on the defect properties responsible for the trapping centre and on the charge transfer mechanism from the BaYF matrix to the dopant. In this work, the luminescent mechanism of RE^{3+} - doped BaYF (RE=Er, Nd, Pr, Tb and Tm) was investigated. The fundamental absorption (band gap – Eg) of the BaYF was obtained by luminescence excitation measurements in the Vacuum Ultraviolet (VUV) range, at room temperature, showing that the Eg is around 10.5 eV. Additionally, the electronic transition from excited states of RE^{3+} ions and the exciton level were also identified. Shallow, deep and very deep charge trapping centres were investigated by thermally stimulated luminescence (TSL) between 10 to 673 K. This results were used in the determination of energy levels of defects associated to the host matrix and dopants. All samples showed phosphorescent emission, after exposition to ionizing irradiation. The decay curve was fitted to exponential decay models. The phosphorescent emission at room temperature was associated to the release of energy during detrapping process of trapped carrier charges located at shallow traps. Furthermore, colour centres induced by X-ray irradiation were present in all samples, and these radiation damages were investigated by optical absorption (OA) measurements. The absorption bands due to the colour centres were investigated as function of temperature. The OA bands decreased as the temperature increased above room temperature, following the behaviour of the TSL peaks. The role of the intrinsic and extrinsic defects in all these properties of RE^{3+}-doped BaYF was discussed and a mechanism that explains their luminescent is proposed.

[1] A. C. S. de Mello, A. B. Andrade, G. H. G. Nakamura, S. L. Baldochi and M. E. G. Valerio, *Opt. Mater.* **32** (2013) 1337.
[2] B. Di Bartolo and B. E. Bowlby, *J. lumin.***102 – 103** (2003) 481.
[3] J. Pejchal, M. Nikl, K. Fukuda, N. Kawaguchi, T. Yanagida, Y. Yokota, A. Yoshikawa and V. Babin, *Radiat. Meas.* **45** (2010) 265.

S11 Defects modeling and computational methods

Large scale first principles modelling of non-stoichiometric perovskites

E.A. Kotomin[*,1,2], M.M. Kuklja [3], Yu.A. Mastrikov [2], R. Merkle [1], J. Maier [1]

[1]*Max Planck Institute for Solid State Research, Stuttgart, Germany*
[2]*Institute for Solid State Physics, University of Latvia, Riga, Latvia*
[3]*Materials Science and Engineering Dept, University of Maryland, College Park, USA*
[*]*Corresponding author*

Two types of ABO_3-type perovskite solid solutions (BSCF: $Ba_{1-x}Sr_xCo_{1-y}Fe_yO_{3-\delta}$ and LSCF: $La_{1-x}Sr_xCo_{1-y}Fe_yO_{3-\delta}$), mixed ionic – electronic conductors, continue to attract attention because of a wide range of potential applications in modern technologies, e.g. gas separation membranes, solid oxide fuel cells (SOFC), etc [1,2]. The point defects, in particular oxygen vacancies and antisite defects, are decisive for the transport properties and affect the performance of perovskite materials in specific applications.

In this talk, we present the results of first principles large scale computer calculations of defective BSCF and LSCF, and discuss the thermodynamic stability of the cubic phase under different conditions [3,4]. We explored and analyzed in great detail the oxygen vacancy formation energies in the cubic and hexagonal phases of BSCF and demonstrated that a high concentration of vacancies (oxygen non-stoichiometry), in fact, stabilizes the cubic phase over the hexagonal phase. We also discuss peculiarities of the oxygen vacancy diffusion in BSCF and LSCF. We observed a considerable charge transfer between the migrating oxygen ion and the adjacent *B*-site cation in the transition state of diffusion, which is the main reason for the exceptionally low oxygen migration barrier in BSCF [5]. The smaller size mismatch between *A*- and *B*-site cations in LSCF results in twice higher vacancy formation energy and higher migration activation barrier, which give rise to a smaller oxygen vacancy concentration and thus a slower oxygen exchange reaction, as compared to BSCF. A considerable contribution of lattice vibrations to the Gibbs free energy of charged vacancy formation is demonstrated [6].

Based on the above-discussed results of first principles calculations of the defect formation and migration energies, as well as oxygen atom and molecule adsorption on perovskite surfaces, we calculated the kinetics of oxygen reduction reaction (ORR) at the surface as a function of adsorbed oxygen and surface vacancy concentrations [7]. This allowed us to determine *the rate-determining step* (which is important for improvement of fuel cell and permeation membrane performances) and suggest an interpretation of available experimental data. Special attention is paid to the role of polar surface termination on the ORR rate.

[1] M.M. Kuklja, E.A. Kotomin, R. Merkle, Yu.A. Mastrikov, J. Maier, *Phys. Chem. Chem. Phys.* **15** (2013) 5443 (a review article).
[2] E. Kotomin, R. Merkle, Yu. Mastrikov, M. Kuklja, J. Maier, Chapter 6 in a book: *Computational Approaches to Energy Materials* (J.Wiley, 2013).
[3] M. Kuklja, Yu. Mastrikov, B. Jansang, E. Kotomin, *J. Phys. Chem. C* **116** (2012) 18605
[4] D. Fuks, Yu. Mastrikov, E. Kotomin, J. Maier, J. Mater. Chem. A **1** (2013) 14320
[5] R. Merkle, Yu. Mastrikov, E. Kotomin, M. Kuklja, J. Maier, *JECS* **159** (2012) B 219
[6] T.S. Bjorheim, M. Arrigoni, D. Gryaznov, E.A. Kotomin, J. Maier, *Phys. Chem. Chem. Phys.* **17** (2015) 20765
[7] Yu.A. Mastrikov, R.Merkle, E.A.Kotomin, J.Maier, J.*Phys.Chem. C* **114** (2010) 3017.

Colloidal Clusters from Confined Self-assembly

Junwei Wang [1], Chrameh Mbah Fru [2], Thomas Przybilla [3], Erdmann Spiecker [3], Nicolas Vogel [1], and Michael Engel [2,*]

[1]*Institute of Particle Technology, Friedrich-Alexander University Erlangen-Nürnberg, 91058 Erlangen, Germany*
[2]*Institute for Multiscale Simulation, Friedrich-Alexander University Erlangen-Nürnberg, 91058 Erlangen, Germany*
[3]*Institute for Micro- and Nanostructure Research, Friedrich-Alexander University Erlangen-Nürnberg, 91058 Erlangen, Germany*
[*]*Corresponding author*

Spherical colloidal particles are promising building blocks for the hierarchical self-assembly of photonic materials. Complex structures have been achieved by varying composition, interaction, or shape of the constituent particles [1]. Another approach is to utilize interfacial effects from the introduction of confinement to achieve patterning on the micron-scale. Recently it has been shown that entropy favors icosahedral symmetry for colloids assembling in spherical confinement [2].
In this contribution, we investigate polystyrene colloids that aggregate within water-in-oil emulsion droplets and gradually densify upon water evaporation until crystallization sets in, resulting in densely packed colloidal clusters [3]. We utilize droplet-based microfluidics to synthesize near-monodisperse clusters of 100 to 10000 colloids. The clusters have a well-defined internal structure and correspond to a discrete series of multiply twinned crystals, as is confirmed by high-resolution electron microscopy and tomography. To explain the internal structure of the clusters, we propose a geometric model that is compared to computer simulations and allows extracting extremal principles and thermodynamic driving forces that govern the assembly process. We discuss the growth process of the clusters, analyze the presence of defects and the competition with other ordering mechanisms. Finally, we compare our results to the monodispersed occurrence of ultrasmall nanoparticles and atomic clusters.

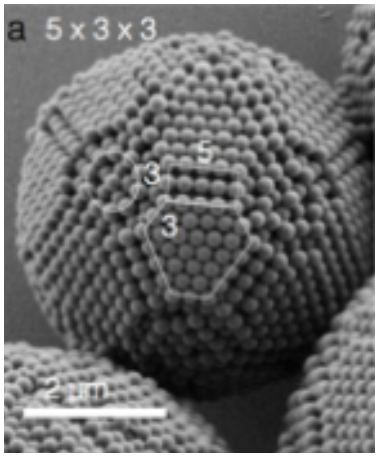

Colloidal cluster assembled in an emulsion droplet.

[1] M. A. Boles, M. Engel, and D.V. Talapin, *Chem. Rev.* **116** (2016) 11220.
[2] B. de Nijs, S. Dussi, F. Smallenburg, J.D. Meeldijk, D.J. Groenendijk, L. Filion, A. Imhof, A. van Blaaderen, and M. Dijkstra, *Nature Materials* **14** (2015) 56.
[3] N. Vogel, S. Utech, G. England, T. Shirman, K.R. Phillips, N. Koay, I. Burgess, M. Kolle, D. A. Weitz, andJ. Aizenberg, *Proc. Natl. Acad. Sci. USA* **112** (2015) 10845.

On grain-boundary fingerprint embodied in polycrystalline slowly evolving soft materials

Adam Gadomski [1], Natalia Kruszewska [1,*] and J. Miguel Rubí [2]

[1] *UTP University of Science & Technology, Physics Department, 85796, Bydgoszcz, Poland*
[2] *Universitat de Barcelona, Física Fonamental Department, 08028 Barcelona, Spain*
[*] *Corresponding author*

Optical properties of polycrystalline materials undergo substantial changes if size of their grains diminishes, an effect typically associated with imposing on the system certain control thermodynamic conditions, driving the system's basic constituents toward nanoscale [1-4]. Cuprate polycrystalline materials may develop their fractal type grain boundaries of appreciable dimensional characteristics [5], as can also do their more soft-material viz biomembraneous counterparts, both of them expressing their anomalous diffusion-relaxation properties [2,6]. A simple ideological example is given by means of a macroscopic system, composed of six egg-yolk "soft grains" poured over a plate's central round surface, the border of which is supposed to exert a balanced low-pressure effect on the system, Figure 1. The "soft grains" apparently form a quasi-equilibrium structure, with the grain-boundary junctions approaching 120^o as it can be expected for honeycomb structures [3,5]. (The hen-egg white is dispersed in between.)

Figure 1: A six egg-yolk "soft grain" configuration placed in a plate's round central spot; shadowed piece of the picture indicates two grain-boundary junctions approaching 120^o.

On the contrary, colloid type nanocrystals [3] emerge in nonequilibrium conditions, their grain boundaries are low-angle viz curvilinear and "fuzzy". Their corresponding diffusion- and freeenergy landscapes change distinctly when tuning them by the size effect as revealed by mesoscopic nonequilibrium thermodynamics [7], and described in terms of Smoluchowski approach [1,4,6].

[1] T. D. Edwards, Y. Yang, D. J. Beltran-Villegas and M. A. Bevan, *Sci. Rep.* **4** (2014) 6132.
[2] K. Hima Nagamanasa, S. Gokhale, R. Ganapathy, and A. K. Sood, *PNAS* **108** (2011) 11323.
[3] S. N. Gaponenko, *Optical Properties of Semiconductor Nanocrystals*. Cambridge University Press, Cambridge, 1998.
[4] N. Kruszewska, P. Weber, A. Gadomski, and K. Domino, *Acta Phys. Pol. B* **44** (2013) 1049.
[5] A. Gadomski, and N. Kruszewska, *Eur. Phys. J. B* **85** (2012) 416.
[6] A. Gadomski, *Phil. Mag. Lett.* **70** (1994) 335.
[7] A. Gadomski, and J. M. Rubí, *Chem. Phys*. **293** (2003) 169.

Shining a Light on Amorphous UO_3: A Computational and Experimental Approach to Understanding Amorphous Uranium Materials

Ashley E. Shields [1,*], **Andrew J. Miskowiec** [1], **Marie C. Kirkegaard** [1,2], **Michael W. Ambrogio** [1], **Roger J. Kapsimalis** [1], **and Anderson B.B.** [1,2]

[1]*Oak Ridge National Laboratory, 1 Bethel Valley Road, Oak Ridge, Tennessee, USA*
[2]*University of Tennessee, Knoxville, Tennessee USA*
[*]*Corresponding author*

Uranium oxide materials are important to the nuclear fuel cycle, but a complete description of these materials is not yet available because traditional analysis tools fail to easily characterize the structure of systems with low or no translational symmetry. The presence of multiple phases in samples further complicates matters. Even oxides of known stoichiometries, such as UO_3, are not yet fully characterized. X-ray amorphous UO_3 has been observed to form upon calcining the uranium peroxide mineral studtite, $[(UO_2)(O_2)(H_2O)_2](H_2O)_2$ [1–3]. During this process, amorphous-U_2O_7 (am-U_2O_7) was identified as a metastable intermediate state [1,2]. Using a suite of experimental techniques, we demonstrated that a sample of x-ray am-UO_3 is dominated by small crystallites of alpha-UO_3 with a nonstoichiometric uranium oxide impurity. Because of the formation of am-U_2O_7 phases during calcination, we predict this impurity may be metastable U_2O_7.

We used genetic algorithms for crystal structure prediction and density functional theory to search for possible configurations for U_2O_7. For the low energy structures identified through the genetic algorithm-based search process, we evaluated stability by calculating the phonon frequencies using density functional perturbation theory. In Fig. 1, we present a new stable U_2O_7 structure. This novel configuration contains peroxide units, which correspond to neutron scattering data on am-U_2O_7. We hope further information about x-ray amorphous and low-symmetry uranium materials may be discovered using this framework.

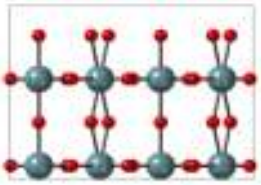

Fig. 1. A predicted U_2O_7 structure that has stable phonons and peroxide bonds. Uranium and oxygen ions are represented in gray and red, respectively.

[1] X. Guo, S. V. Ushakov, S. Labs, H. Curtius, D. Bosbach, A. Navrotsky, *Proc. Natl. Acad. Sci.* **111** (2014).
[2] S.O. Odoh, J. Shamblin, C.A. Colla, S. Hickam, H.L. Lobeck, R.A.K. Lopez, T. Olds, J.E.S. Szymanowski, G.E. Sigmon, J. Neuefeind, W.H. Casey, M. Lang, L. Gagliardi, P.C. Burns, *Inorg. Chem*. **55** (2016) 3541–3546.
[3] I.J. Schwerdt, A. Olsen, R. Lusk, S. Heffernan, M. Klosterman, B. Collins, S. Martinson, T. Kirkham, L.W. McDonald, *Talanta* **176** (2018) 284–292.

Modelling of Hyaluronic Acid in Solution: Parametrization of the Biopolymer Molecule in the Coarse-Grained Representation

Piotr Bełdowski [1], Jure Cerar [2], Jacek Siódmiak [1,*], Matija Tomšič [2], Andrej Jamnik [2], Adam Gadomski [1]

[1]*Department of Physics, Institute of Mathematics and Physics, UTP University of Science and Technology in Bydgoszcz, Al. prof. S. Kaliskiego 7, 85-796 Bydgoszcz, Poland.*
[2]*Faculty of Chemistry and Chemical Technology, University of Ljubljana, Večna pot 113, SI-1000 Ljubljana, Slovenia.*
[*]*Corresponding author*

Hyaluronic acid (HA) (see Fig. 1) is a polymeric substance that is occurring naturally and plays a key role in many processes in human body. Its molecular properties like high flexibility, hydrophilicity and other physico-chemical properties are very important in this respect. Its length-dependent properties are widely abused in many diagnostic and therapeutic methods. The high hopes lay in cancer imaging and in drug delivery systems. In this case the fluorescent imaging agents are delivered by HA [1]. In this work we present a molecular dynamics study of the HA in the coarse-grained MARTINI force-field model representation [2]. Since the computational cost of the all-atom molecular dynamics simulations of polymeric systems is very high, such coarse-grain methods importantly facilitate the simulation studies of a turbid system. However, to parametrize the hyaluronic acid molecule in the coarse-grained representation properly, the all-atom GROMOS force field molecular dynamics simulations will also be performed to determine the values of the parameters of bonding interactions inside the hyaluronan chain [3]. The most stable coarse-grained representation of the molecule will be compared with the results of all-atom simulations in various solutions and possibly also with the experimental data obtained by different light scattering and rheological techniques. The resulting optimal coarse-grained parametrization will make possible investigations of the systems containing hyaluronan on larger length-scales (up to hundreds of nm) and on time-scales of up to microseconds. An information about generic amphiphile-water fluctuations' dynamics [4] remains to be deduced based on the performed study.

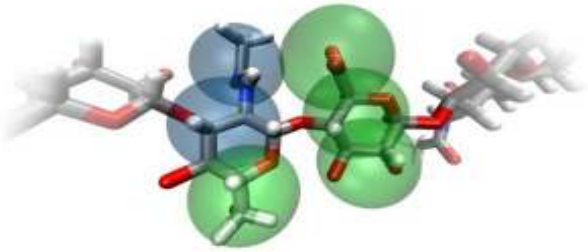

Fig. 1: The all-atom representation of the hyaluronic acid monomer and superimposed is the proposed coarse-grained Martini model (green spheres represent polar and blue spheres represent nonpolar parts of HA).

[1] Jae-Young Lee et al., *Biomaterials* ***85*** (2016) 218.
[2] S. J. Marrink et al., *J. Phys. Chem.* **111** (2007) 7812.
[3] W. R. P. Scott et al., *J. Phys. Chem.* **103** (1996) 3596.
[4] F. Bresme et al., *Phys. Rev. Let.* **101** (2008) 056102.

S12–S13 Scintillation, energy transfer and storage, carrier trapping phenomena

Rechargeable persistent phosphors for the first and third bio-imaging windows by electron traps redistribution

Setsuhisa Tanabe*, Xu J.

Graduate School of Human and Environmental Studies, Kyoto University, Sakyo-ku, Kyoto, Japan

Persistent luminescence (PersL) imaging without real-time external excitation has been regarded as the next generation of optical imaging technology without auto-fluorescence. However, in order to achieve improved imaging resolution and deep tissue penetration, developing new near-infrared (NIR) persistent phosphors with intense and long duration PersL over 1000 nm is still a challenging but urgent task in this field. Herein, by utilizing the persistent energy transfer from Cr^{3+} to Er^{3+}, we report a novel garnet persistent phosphor of $Y_3Al_2Ga_3O_{12}$ co-doped with Er^{3+} and Cr^{3+} (YAG*G*:Er-Cr), which exhibits intense deep-red and NIR PersL bands from Cr^{3+} and Er^{3+} ions matching well with the first (NIR-I, 650-950 nm) and third (NIR-III, 1500-1800 nm) biological windows as well as the sensitive regions of commercial Si and InGaAs detectors, respectively. The optical imaging through raw-pork tissues (thickness of 1 cm) indicates that the Er^{3+} emission can achieve higher spatial resolution than the Cr^{3+} emission due to the reduced light scattering at longer wavelengths. Furthermore, by making full use of two independent electron traps with different depths in YAG*G*: Er-Cr, the Cr^{3+}/ Er^{3+} PersL can even be recharged *in situ* by photostimulation with 660 nm LED thanks to the redistribution of trapped electrons from the deep trap to the shallow one. Our results serve as a guide in developing promising NIR (>1000 nm) persistent phosphors used for long-term optical imaging.

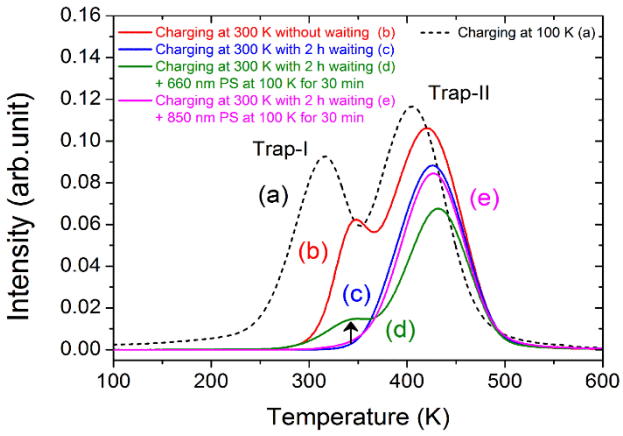

Fig.1. Thermoluminescence glow curves of YAG*G*: Cr-Er sample (a) after UV charging at 100K, (b) after UV charging at 300K, cooled down to 100K, (c) after UVcharging at 300K with 2h waiting, cooled down to 100K and photostimulation by (d) 660nm LED for 30min at 100K (e) 850nm LED for 30min at 100K.

[1] T. Maldiney, et al., *Nat. Mater.* **13** (2014) 418.
[2] Xu J., D. Murata, J. Ueda, S. Tanabe, *J. Mater. Chem. C* **4** (2016) 11096.
[3] Xu J., S. Tanabe, A. Sontakke, J. Ueda, *Appl. Phys. Lett.* **107** (2015) 081903.
[4] Y. Katayama, B. Viana, D. Gourier, Xu J., S. Tanabe, *Opt. Mater. Express* **6** (2016) 1405.

Double Doping for Energy Storage. The case of Lu_2O_3-Base Ceramics

E. Zych [1,*], D. Kulesza [1], P. Bolek [1], J. Zeler [1]

[1]*Faculty of Chemistry, University of Wroclaw 14 F. Joliot-Curie Street, 50-383 Wroclaw, Poland*

Lu_2O_3:Tb,M and Lu_2O_3:Pr,M (M=Ti, Zr, Hf, V, Nb, Ta) sintered ceramics were reported to store energy by means of excited charge carriers trapping [1-3]. In this presentation we shall summarize the present statues of understanding of the mechanism of carriers trapping and releasing by thermal or optical stimulation. Some surprising differences between Tb- and Pr-activated materials will be shown. Among others, in the latter only the Pr(C_2) site is active in thermoluminescence (TL) and optically stimulated luminescence (OSL), while Pr(C_{3i}) is not. In Lu_2O_3:Tb,M ceramics both Tb sites show TL and OSL.

Figure 1a presents the effect of co-doping with Hf for energy storage (=carriers trapping) efficacy by means of thermoluminescence efficiency variation. Figure 1b compares glow curves of three doubly-doped lutetia ceramics: Tb,Nb-, Tb,Hf- and Tb,Ti. The co-dopants appear to shape the traps depths. More effects of co-doping will be presented and discussed.

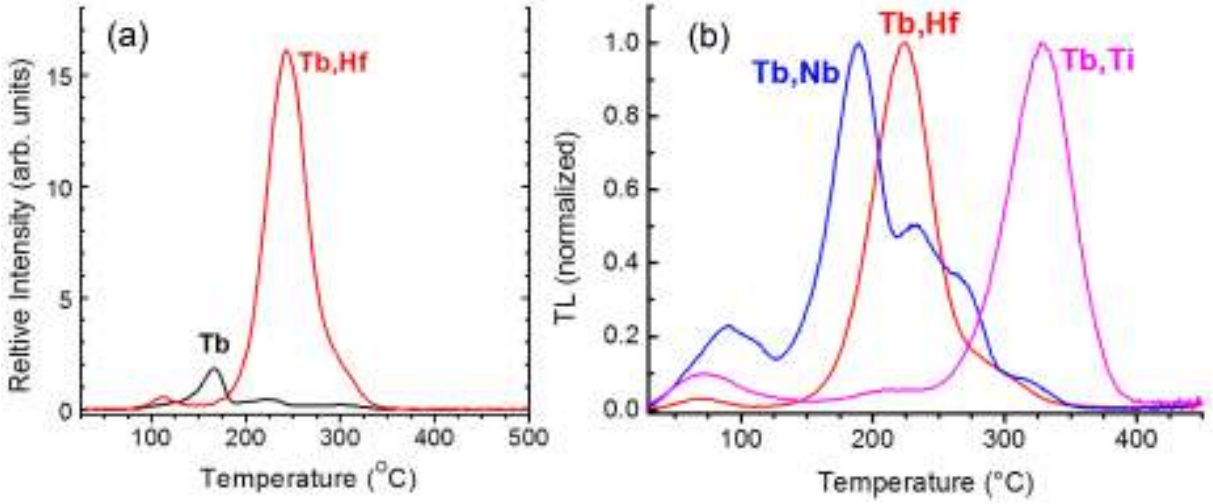

Fig. 1. TL glow cures of singly (Tb) and doubly (Tb,Hf) activated Lu_2O_3 ceramics (a), and Tb, Nb, Tb, Hf, Tb, Ti materials.

Support by the Polish National Science Centre (NCN) under the grant #UMO-2014/13/B/ST5/01535 is gratefully acknowledged.

[1] E. Zych, P. Bolek, D. Kulesza *J. Lumin*. **189** (2017) 153-158.
[2] P. Bolek, D. Kulesza, A. J. J. Bos, E. Zych, *J. Lumin.* **194** (2018) 641-648.
[3[D. Kulesza, P. Bolek, A. J. J. Bos, E. Zych, *Coord. Chem. Rev*. **325** (2016) 29-40.

Anion Vacancy as Killer Defect in $Cu_2ZnSnS(Se)_4$

Sunghyun Kim [1,*], Park J.-S. [1] and Aron Walsh [1,2]

[1]*Imperial College London, Department of Materials, Imperial College London, London SW7 2AZ, United Kingdom*
[2]*Department of Materials Science and Engineering, Yonsei University, Seoul 03722, Korea*
[*]*Corresponding author*

In photovoltaic materials, photogenerated carriers (electrons and holes) can be annihilated by recombination processes, limiting the performance of solar cell devices. Radiative and Auger recombinations are intrinsic properties of a material which are unavoidable. In solar cells with low carrier densities, trap-assisted non-radiative recombination process is a dominant mechanism described by Shockley-Read-Hall (SRH) statistics.

$Cu_2ZnSn(S,Se)_4$ (CZTS) has attracted much attention as a promising candidate in solar cell applications and a replacement of the commercial light absorber of $Cu(In,Ga)(S,Se)_2$ (CIGS), consisting of only earth-abundant elements. However, to realize the high efficiency of CZTS solar cells enough to support terawatt photovoltaic industry, a large open-circuit voltage (V_{OC}) deficit need to be overcome. Trap-assisted non-radiative recombination is the likely origin of the large V_{OC} deficit. We have performed first-principles calculations within the framework of density functional theory to search for efficient recombination center - killer defects - in CZTS.

In ionic semiconductors, anion vacancies commonly act as shallow electron donors or deep recombination centers. In CZTS, the anion vacancy is electrically benign without any donor levels in the band gap. We find that a neutral bipol1aronic state emerges due to the double reduction of Sn atom near the vacancy site. However, the sulfur vacancy can capture minority carriers (electrons) very efficiently with the aid of thermal and optical excitations. The excited anion vacancy can act as the killer non-radiative recombination center. We point out that trap-assisted non-radiative recombination does not necessarily accompany a charge transition level deep in the band gap of a semiconductor. [1]

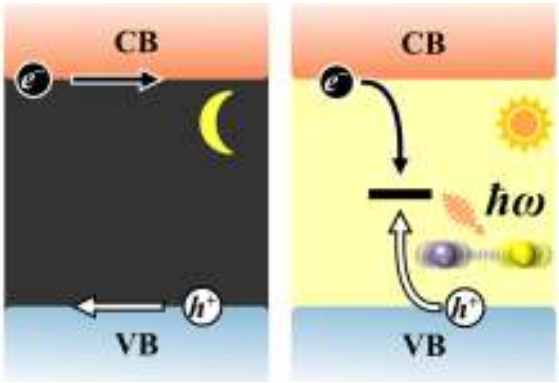

[1] S. Kim, Park J.-S., and A. Walsh, *ACS Energy Lett*. **3**, 496 (2018).

Structure, defects, non-stoichiometry and ion migration in bismuth germanate: experimental and computer modelling approaches

Zélia S. Macedo [1,*], Maria A. Gomes [1], Mário E.G. Valerio [1] and Robert A. Jackson [2]

[1]*Physics Department, Federal University of Sergipe, Campus Universitario, 49100-000, São Cristovão, SE, Brazil*
[2]*School of Physical and Geographical Sciences, Keele University, Keele, Staffordshire ST5 5BG, United Kingdom*
[*]*Corresponding author*

Bismuth germanate ($Bi_4Ge_3O_{12}$, BGO) has been the focus of several studies due to its scintillation properties. It has been employed as detector in scientific research and medicine. In this work, the experimental parameters to produce BGO powders, sintered ceramics and thin films by solid state synthesis, SHS (self-propagating high temperature synthesis) and Pechini's method were investigated. Structural, morphological, optical and electric properties were determined for the samples prepared. The produced samples yielded a blueish-white luminescence with a maximum emission peak at 500 nm corresponding to the $^3P_1 \rightarrow {}^1S_0$ electron transition of Bi^{3+}. The effects of non-stoichiometry in the $Bi_4Ge_3O_{12}$ phase were interpreted in terms of intrinsic defect disorder and in terms of the formation of small amounts of the $Bi_{12}GeO_{20}$ phase. The behaviour of the electric conductivity with frequency agrees with that predicted for conduction mechanisms over a random distribution of energy barriers in a disordered solid, with average activation energy of E_a = 1.41 eV as determined from Arrhenius plots. To enable an in deep understanding of BGO properties, computer modelling, including development of interatomic potentials, calculation of relative phase stabilities, calculation of formation energies of intrinsic and extrinsic defects, and activation energies for ion migration were also performed. A potential was fitted to reproduce the two main phases of the material, and used to explain their relative stability. Intrinsic defect formation energies were calculated and used to predict the expected form of defect disorder. In the $Bi_4Ge_3O_{12}$ phase the main intrinsic defect was found to be the Bi/Ge antisite, which in turn was used to explain why the $Bi_{12}GeO_{20}$ phase is formed in small quantities during the preparation process. Ion migration via the oxygen vacancy mechanism was found to have average activation energy of about 1.75 eV, with a distribution of activation energy values, corroborating the experimental results.

Afterglow decay curves modeled for mixed oxide garnets using TSL measurements

Ivan D. Venevtsev [1,*], Vasilii M. Khanin [2], Ivan I. Vrubel [3], Roman G. Polozkov [3], Piotr A. Rodnyi [1] and Cees Ronda [4]

[1]*Peter the Great St. Petersburg Polytechnic University, Polytechnicheskaya 29, 195251, St. Petersburg, Russia*
[2]*Utrecht University, Heidelberglaan 8, 3584 CS, Utrecht, Netherlands*
[3]*ITMO University, Kronverksky pr. 49, 197101, St. Petersburg, Russia*
[4]*Philips Research Eindhoven, High Tech Campus 4, 5656 AE, Eindhoven, Netherlands*
[*]*Corresponding author*

Cerium doped mixed oxide garnets are promising luminescent materials to use as LED phosphors or scintillators for radiation detectors. One of the main challenges for all applications is the appearance of slow tails of luminescence (also called afterglow [1]). It is known that the significant delay of light emission in luminescent materials appears due to temporary charge carrier trapping. This effect can be found useful in some applications (production of emergency signs and luminous paints using persistent phosphors) [2] while in other cases (medical imaging systems and radiation protection) the delayed scintillation response to ionizing radiation is undesired [3]. The understanding of the underlying mechanisms thus represents an important practical task.

The influence of the traps on charge carrier transport towards the luminescence centers is generally investigated with thermally stimulated luminescence (TSL) methods or measurements of isothermal decay for the afterglow. In this work a new method to analyze time-dependent afterglow of garnet scintillators using their TSL glow curves and the trap depth distribution model is described. The mathematical procedure requires a pre-calculated (with use of the classic models) frequency factor (s) and consists of two stages. The first step is the deconvolution of the function of the occupied trap density from the experimental TSL signal. The second step is the modeling of the time-dependent afterglow signal at given temperature using the reconstructed occupied trap density function via classical afterglow decay models. The objects under study are Ce doped mixed oxide garnet ceramics. Samples are either nominally pure or intentionally co-doped with metal ions known to be efficient electron traps [4] and for which a TSL peak in the range from 80 to 570 K could be assigned. With the use of TSL and afterglow experimental measurements followed by corresponding numerical modeling, the evidence for the distribution of thermal trap depth in the studied samples is demonstrated.

[1] S. W. S. McKeever, *Thermoluminescence of Solids*, Cambridge Solid State Science Series (Cambridge University Press, 1985).
[2] D. Poelman, N. Avci, and P. F. Smet, *Opt. Express* **17**, (2009) 358.
[3] C. W. E. van Eijk, *Physics in Medicine and Biology* **47**, (2002) R85.
[4] E. Milliken, L.C. Oliveira, G. Denis, and E. Yukihara, *Journal of Luminescence* **132**, (2012) 2495.

Paramagnetic Trapped-Electron and Trapped-Hole Centers in Oxide Scintillators

Valentin V. Laguta*, Maxym Buryi and Martin Nikl

Institute of Physics AS CR, Cukrovarnicka 10, 16253 Prague, Czech Republic
**Corresponding author*

Clarification of charge carriers trapping phenomena and nature of related lattice defects in insulating materials are important tasks of the solid state physics. These tasks are pressing especially for scintillating materials which are widely used as convertors transforming the energy of photons of ionizing radiation or high-energy particles into UV/visible light. Dielectric or semiconductor wide band-gap oxide materials of high degree of structural perfection are most suitable for such a purpose. They must accomplish fast and efficient transformation of energy of incoming photons/particles in a number of electron-hole pairs collected in the conduction and valence bands, respectively, and their radiative recombination at suitable luminescence centers. However, before the radiative recombination, the migrating electrons and holes (eventually created excitons) can be trapped at a lattice defect or even self-trapped leading potentially to marked decrease of the scintillation performance. Therefore, monitoring of electron/hole trapping states in a scintillator material and revealing the nature of corresponding lattice defects is of crucial importance to optimize the materials performance close to the intrinsic limits.

It is the aim of this report to present selected results of Electron Paramagnetic Resonance (EPR) study of various point defects which participate in the processes of charge carriers transfer and capture in the family of practically important complex oxide single crystal scintillators based on molybdates [1,2], aluminum perovskites [3] and garnets [4], and orthosilicates [5]. EPR allows not only the detection of impurity ion or lattice defect with unpaired spins but also the determination of their local structure and characteristics at atomistic level. Particular attention is paid to the most native defects inevitably present or created by radiation in oxide materials, such as self-trapped electron and hole states (small polarons), anion and cation vacancies, and antisite defects induced by structural disorder or natural nonstoichiometry of the material. Current understanding of the nature of charge trapping states and mechanisms of their creation in oxide scintillation materials will be discussed.

The support of the GA CR under project No. 17-09933S is gratefully acknowledged.

[1] D.A. Spassky, V. Nagirnyi, V.V. Mikhailin, et al., *Optical Mater*ials **35** (2013) 2465.
[2] M. Buryi, V. Laguta, M. Fasoli, et al., *J. Lumin*. **192** (2017) 767.
[3] V. V. Laguta, M. Nikl, A. Vedda, et al., *Phys. Rev. B* **80** (2009) 045114.
[4] M. Nikl, V. Babin, J. Pejchal, V.V. Laguta et al., *IEEE Trans. Nukl. Science* **63** (2016) 433.
[5] V.V. Laguta, M. Buryi, J. Rosa et al., *Phys. Rev. B* **90** (2014) 064104.

Energy Transfer to RE Ions in Scintillators with the Account for Excitation Density Effects

Andrey N. Vasil'ev [1,*] and Andrei N. Belsky [2]

[1]*Skobeltsyn Institute of Nuclear Physics, Lomonosov Moscow State University, Leninskie gory 1(2), Moscow 119991, Russia*
[2]*Institut Lumière Matiére, Université Lyon 1, 69622 Villeurbanne Cedex, France*
[*]*Corresponding author e-mail: anv@sinp.msu.ru*

We consider processes in wide-gap crystals following the absorption of a high-energy photon and relaxation cascade when electronic excitations have kinetic energy from zero to E_g. With the increase of kinetic energy of electronic excitations from zero to E_g new mechanisms of energy transfer to rare earth (RE) ions come into play. Strongly inhomogeneous spatial distribution of electronic excitations in scintillators is characterized by the values from 10^{12} to 10^{22} excitations per cubic cm. In crystals with high concentration of RE ions (from few percent up to 100%) the impact excitation and ionization of RE ions take place favorable for fast energy transfer from hot electronic excitations to RE ions. In regions with high concentration of excitations additional complex pathways of energy transfer could occur. An example is the Auger-like capture of a hole by RE ion in the presence of an electron in the vicinity. Both dipole-dipole and exchange types of interaction are discussed.

Classification of different processes of energy transfer from host electronic excitations to RE activators in scintillators is introduced and estimates of the rate of these processes are presented. Energy transfer transitions can result in the excitation, in the ionization of RE ions (in the latter case the release/capture of an electron or a hole is considered), or in the creation of charge transfer states.

The examples of energy transfer processes are based on Ce^{3+} and Gd^{3+} ions in different wide-band-gap hosts.

This research is carried out in the frame of Crystal Clear Collaboration and is supported by a European Union's Horizon 2020 research and innovation program under the Marie Skłodowska-Curie grant agreement No 644260 (INTELUM) and COST ACTION TD1401 (FAST).

Decay Mechanisms in YAG-Ce,Mg Fibers Excited by γ- and X-rays

A. Belsky [1,*], K. Lebbou [1], V. Kononets [2], O. Sidletskiy [2], A. Gektin [2], M. Lucchini [3], E. Auffray [3], D. Spassky [4], A.N. Vasil'ev [4]

[1]*Institute of Light and Matter, UMR5306 CNRS, Universite de Lyon 1, Villeurbanne Cedex, France*
[2]*Institute for Scintillation Materials, NAS of Ukraine, Kharkiv, Ukraine*
[3]*European Organization for Nuclear Research, Geneva 23, Switzerland*
[4]*Institute of Nuclear Physics, Moscow State University, Moscow, Russia*
**Corresponding author*

Success in development of new scintillators based on complex oxides demands deeper understanding of excitation mechanisms for cerium ions in these hosts, which takes into account different factors like inhomogeneous distribution of excitations in track region.

Samples YAG-Ce (150 ppm) with Mg co-doping were grown using Micro-pulling- down technique [1]. The samples were studied under pulsed X-ray excitation (repetition period 5 μs, anode voltage 30 kV), γ-rays (Cs 662 keV), or by direct excitation using monochromatized emission of Xe discharge.

Decay kinetics under X-ray excitation differs significantly from single exponential law. It is characterized by long hyperbolic tail $t^{-\alpha}$, $\alpha \approx 1.05$. The initial part of decay kinetics has short rise time (less than 1 ns) and is faster than for direct excitation (63 ns). The decay becomes faster with increase of Mg concentration. Slow component which dominates in YAG-Ce without Mg co-doping for t>500 ns practically vanishes for samples with 50 ppm co- doping. The latter samples under 340 nm excitation are characterized by the decrease of TSL in 10 times in comparison with samples without co-doping. The UV excitation spectra do not change essentially. This indicates that concentration of stable Ce^{4+} centers does not increase significantly in samples with 50 ppm of Mg in comparison with non-co-doped samples.

Decay kinetics under γ-rays also becomes faster with increase of Mg concentration. However, their profiles significantly differ from that observed under X-ray excitation. They are characterized by prominent rise component and slower decay initial part than under X- rays. Using simulation described in [2], this difference can be explained by the difference of the density distribution of excitations in the track region. The distribution under X-rays is shifted to higher densities which induces the acceleration of recombination and quenching.

The analysis of the decay curves under X-ray and γ excitation shows that most of excitation mechanisms involve the capture of an electron by Ce^{4+} ion, regardless of its nature (created during synthesis or created by ionization during excitation in the picosecond initial stages). The recombination kinetics is controlled by the distance between Ce^{4+} and electron and therefore depends on the density of excitations and mobility of electrons, which is controlled by the concentration and depth distribution of traps.

This research is carried out in the frame of Crystal Clear Collaboration and is supported by a European Union's Horizon 2020 research and innovation program under the Marie Skłodowska- Curie grant agreement No 644260 (INTELUM) and COST ACTION TD1401 (FAST).

[1] V. Kononets, et al. In *Engineering of Scintillation Materials and Radiation Technologies*, Springer Proceedings in Physics, v.**200**, Springer, 2017, p.114.
[2] A.N. Vasil'ev, ibid., p. 3.

Effect of Au codoping in BaBrCl:Eu scintillating single crystals

Federico Moretti [1,*], Peiyun Li [2], Sergii Gridin [2], K. Burak Ucer [2], Richard T. Williams [2], Tetiana Shalapska [1], Edith Bourret [1] and Gregory Bizarri [1]

[1]*Lawrence Berkeley National Laboratory, 1 Cyclotron road, Berkeley, (CA) USA*
[2]*Wake Forest University, Address2, Winston-Salem, (NC) USA*
[*]*Corresponding author*

The presence of defects in scintillators causes a series of adverse effects which limit, sometimes to a great extent, the scintillation properties of these materials. The competition between charge trapping and recombination is ultimately responsible for the degradation of the scintillator performances, with a reduction of light yield, the presence of long scintillation decays, afterglow, and luminescence sensitization. One of the strategies to limit the impact of defects is the introduction during material growth of aliovalent ions as codopants. For instance, the introduction of Sr and Ca in $LaBr_3$:Ce [1], or of Ca and Mg in Ce doped garnets and silicates [2], strongly improves the scintillation performance of these materials.

In this contribution we will discuss the influence of Au codoping on luminescence and scintillation properties of BaBrCl:Eu single crystals grown by the Bridgman-Stockbarger method. The study, performed by varying both Eu and Au concentration, reveals the highly effective role of gold in the improvement (up to threefold) of the scintillation light output of this material. Pulsed x-ray decays, and thermally/optically stimulated luminescence reveal a substantial reduction in delayed recombination and carrier storage at defect sites upon Au codoping, suggesting a reduction in defects impacting the scintillation process.

Picosecond absorption spectroscopy results suggest that these improvements are not exclusively related to a reduction in the concentration of defects, but also to a modification of the charge carrier recombination process, in particular for what concerns the formation and the lifetime of transient chlorine-related F centres. Transient absorption spectroscopy and optically detected EPR in the related system BaF_2 have established that the STE in BaF_2 is a transient F-centre/H-centre pair and includes the optical signature of a perturbed F-centre. In the case of Au codoped BaBrCl samples such F centres do not form after the initial fast UV excitation, in contrast to what occurs in the case of samples doped only with Eu or undoped ones. These results suggest that Au might have an active role in the disruption of the mechanisms leading to the formation of these temporary F centres and the associated H ones with possible repercussions on charge carrier migration and recombination on the luminescence centres.

Acknowledgements: This work was supported by the US Department of Energy/NNSA/DNN R&D and carried out at Lawrence Berkeley National Laboratory under contract No. AC02-05CH11231

[1] M.S. Alekhin et al., *Appl. Phys Lett.* 102 (2013) 161915
[2] M. Nikl, A. Yoshikawa, *Adv. Opt. Mater.* 3 (2015) 463.

Non-proportionality phenomenon in CsI:Tl scintillators – new observations

Z. Mianowska [1,*], M. Moszynski [1], A. Dziedzic [1], A. Gektin [2], S. Gridin [3], Lu X. [3], M. R. Mayhugh [4], S. Mianowski [1], P. Sibczynski [1], L. Swiderski [1], A. Syntfeld-Kazuch [1], T. Szczesniak [1], R.T. Williams [3], S. Vasyukov [2]

[1]*National Centre for Nuclear Research, A. Soltana 7, Otwock, Poland*
[2]*Institute for Scintillation Materials, 60 Nauki Ave., Kharkov, Ukraine*
[3]*Department of Physics, Wake Forest University, Winston Salem, NC,USA*
[4]*Faceted Development, LLC, 3641 Rawnsdale Road, Shaker Hts, OH, USA*
[*]*Corresponding author*

The scintillation process in CsI:Tl were investigated at the temperature from 303 K to 203 K. The crystals were excited by the gamma sources with the energies from 17 keV to 835 keV. Moszynski et al show that the light amount collected in the detector is conditioned by the integration time [1]. The maximally achievable peaking times with analogue techniques is close to 24 μs, what is not enough for whole CsI:Tl light collection. The authors decided to measure the CsI:Tl light pulses with the digital technique, where the integration time was prolonged up to 500 μs. This choice allows to register practically proportional characteristic of CsI:Tl, what is presented in fig. 1.

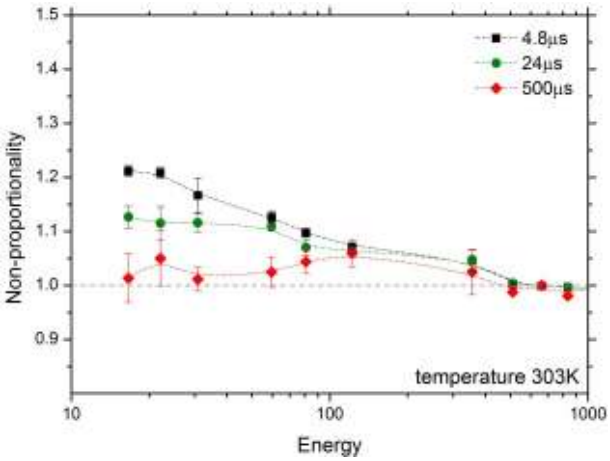

Figure 1. Non-proportionality of CsI:Tl at 303K calculated for different integration times.

We would like to underline by this work, that light pulse integration with different base times generates results discrepancy. The integration time must be carefully chosen during scintillation properties measurements, bothwith analogue and digital methods.

[1] M. Moszynski, A. Syntfeld-Kazuch, L. Swiderski, M. Grodzicka, J. Iwanowska, P. Sibczynski, T. Szczesniak, *Nucl. Instr. Meth. Phys. Res.*, **805** (2016) 25-35.

Effect of Ce and Mg Concentration Ratio on the Properties of $Gd_3Ga_3Al_2O_{12}$ Single Crystal Scintillators

K. Bartosiewicz [1,2,*], A. Yoshikawa [1,3,4], S. Kurosawa [1,3,5], A. Yamaji [1], M. Nikl [6]

[1]*Institute for Material Research, Tohoku University, 2-1-1 Katahira Aoba-ku, Sendai, Miyagi 980-8577, Japan*

[2]*Institute of Physics, Kazimierz Wielki University in Bydgoszcz, Powstańców Wielkopolskich 2, 85-090, Bydgoszcz, Poland*

[3]*New Industry Creation Hatchery Center, Tohoku University, 6-6-10 Aoba, Aramaki, Aoba-ku, Sendai, Miyagi, 980-8579, Japan*

[4]*C&A corporation, T-Biz, 6-6-40 Aoba, Aramaki, Aoba-ku, Sendai, Miyagi 980-8579, Japan*

[5]*Facility of Science, Yamagata University,1-4-12, Kojirakawa-machi, Yamagata 990-8560, Japan*

[6]*Institute of Physics, Academy of Sciences of the Czech Republic, Na Slovance 1999/2, Prague 8, 18221, Czech Republic*

[*]*Corresponding author: karol@imr.tohoku.ac.jp*

In gadolinium gallium aluminum garnets ($Gd_3Ga_3Al_2O_{12}$, GGAG), efficient luminescence is dependent on dopants to create a radiative transition within the forbidden band [1]. In medical imaging, Ce^{3+} is commonly used due to fast and bright 5d→4f transition with the emission wavelength that is suitable also for semiconductor photodetectors [2]. The Ce^{3+} activated GGAG is considered as a promising candidate for the next generation Positron Emission Tomography material due to its high light yield. Besides high density (~6.2 g/cm^3) and light yield value (~58,000 ph/MeV) this material suffers from the contribution of the undesired slow component in the scintillation response [3] and long rise time [4]. Recently, the codopants strategy has been used in order to mitigate the degraded scintillation properties that result from charge carrier traps and have been shown to improve light yield and decay times in some scintillators [5].

The motivation for this work comes from the positive impact of Mg^{2+} codoping on the GGAG:Ce scintillators. We study the influence of the concentration ratio of Mg^{2+} and Ce^{3+} in the GGAG crystals on the scintillation performance which is strongly dependent on the dopant and codopant content. The GGAG single crystals with a various dopant (Ce^{3+}) and codopant (Mg^{2+}) concentrations were grown from the melt by the micro-pulling-down method. They were characterized by optical absorption, photoluminescence excitation and emission and radioluminescence spectra. Scintillation properties of the crystals were studied by means of light yield and scintillation decay time measurements.

[1] M. Nikl, A. Yoshikawa, *Adv. Optical Mater*. **3** (2015) 463–481
[2] C. Ronda, *J. Solid State Sci. Technol*. **5** (2016) R3121-R3125
[3] K. Kamada et al. *Cryst. Growth Des*. **11** (2011) 4484–4490
[4] M. Lucchini et al. *Instr. Meth. Phys, Research A* **852**, (2017) 1-9
[5] C. Foster et al. *J. Cryst. Growth*, in press (10.1016/j.jcrysgro.2018.01.028)

Physics-Informed Machine Learning for Rapid Screening of Potential Inorganic Scintillator Chemistries

Ghanshyam Pilania [1,*], Kenneth J. Mcclellan [1], Christopher R. Stanek [1] and Blas P. Uberuaga [1]

[1]*Los Alamos National Laboratory, Los Alamos, NM 87545, USA*
**Corresponding author*

Applications of inorganic scintillators—activated with lanthanide dopants, such as Ce—are found in diverse fields. As a strict requirement to exhibit scintillation, the 4*f* ground state (with the electronic configuration of [Xe]$4f^{\{n\}}$ $5d^0$) and $5d^1$ lowest excited state (with the electronic configuration of [Xe]$4f^{\{n-1\}}5d^1$) levels induced by the activator must lie within the host bandgap. This talk will discuss a new machine learning (ML) based screening strategy that relies on a high throughput prediction of the lanthanide dopants' ground and excited state energy levels with respect to the host valance and conduction band edges for efficient chemical space explorations to discover novel inorganic scintillators [1]. Building upon well- known physics-based chemical trends for the host dependent electron binding energies within the 4*f* and $5d^1$ energy levels of lanthanide ions and available experimental data [2,3], the developed ML model can rapidly and reliably estimate the relative positions of the activator's energy levels relative to the valance and conduction band edges of any given host chemistry. Using a set of perovskite oxides and elpasolite halides as examples, it will be demonstrated that the developed approach is able to (*i*) capture systematic chemical trends across host chemistries and (*ii*) effectively screen promising compounds in a high-throughput manner. While a number of other application-specific performance requirements need to be considered for a viable scintillator, the present scheme can be a practically useful tool to systematically down-select the most promising candidate materials in a first line of screening for a subsequent in-depth investigation.

[1] G. Pilania, K. J. McClellan, C. R. Stanek, and B. P. Uberuaga, submitted to J. of Chem. Phys. (2018) under review.
[2] P. Dorenbos, Phys. Rev. B 85 (2012) 165107.
[3] P. Dorenbos, J. Lumin. 151 (2014) 224.

S14 Electronic excitations, excites state dynamics, radiative and non-radiative relaxations – 2

Determination of the location of impurity and defect states with respect to the bands by high pressure spectroscopy

S. Mahlik [1,*]

[1]*Institute of Experimental Physics, University of Gdansk, Wita Stwosza 57, 80-952 Gdańsk, Poland*
[*]*Author for correspondence: s.mahlik@ug.edu.p*

The location of the energy levels of divalent and trivalent lanthanide ions (Ln^{2+} and Ln^{3+}) relative to delocalized states (valence and conduction bands) of the lattice are crucial for luminescence materials performance. Location of the Ln^{2+} levels with respect to the valence band can be estimated from the energies of the charge transfer transition (CTT). CTT is considered as a transition of an electron from lattice ions to the Ln ion and corresponds to transition from the top of the valence band to the Ln^{2+} level. Location of the Ln^{3+} can be estimated from the energy of the ionization transition (IT). The IT is the opposite process to the CTT and corresponds to the transition of an electron from the Ln ion to the conduction band.

Several experimental techniques have been used to determine these energies like absorption, luminescence excitation or UV photoelectron emission, excited state absorption or photoluminescence. The unique technique that allows to determine the exact position of the localized states of Ln ions in the bandgap is high pressure spectroscopy. High hydrostatic pressure compress the Ln-lattice ions bound lengths. As the result the energies of localized states of Ln belonging to the $4f^n$ electronic configuration increases with pressure with respect to the conduction and valence band edges. Since pressure almost not influence the energies of the internal f-f transitions, pressure-induced crossing of the excited emitting states with the conduction band is observed and results the luminescence quenching. Then we can obtain directly the IT energy for given pressure and when pressure shift is known we can estimate the location of the ground state of Ln ions at ambient conditions. This method has been used to estimate the location of the ground states of Ln^{3+} and Ln^{2+} with respect to conduction and valence band in various luminescence materials.

Energy transfer and down- and up-conversion phenomena in $Gd_3(Al,Ga)_5O_{12}$ crystals containing Pr^{3+} and Yb^{3+} impurities.

J. Komar [1,*], R. Lisiecki [1], R. Kowalski [1], B. Macalik [1], P. Solarz [1], M. Głowacki [2], M. Berkowski [2], W. Ryba-Romanowski [1]

[1]*Institute of Low Temperature and Structure Research, Polish Academy of Sciences, Okólna 2, 50-422 Wrocław*

[2]*Institute of Physics, Polish Academy of Sciences, Lotników 32/46, 02-668 Warszawa*

[*]*Corresponding author*

Mixed garnet crystals with nominal stoichiometry $Gd_3Al_{2.5}Ga_{2.5}O_{12}$ undoped, single-doped with Pr^{3+} ions and double-doped with Pr^{3+} and Yb^{3+} ions were fabricated by the Czochralski technique and investigated employing methods of optical spectroscopy. Examination of optical spectra recorded at liquid helium temperature revealed that inherent disordered structure of the host determines large widths of inhomogeneously broadened lines amounting to 1.27 nm (12 cm^{-1}) FWHM for the 0-0 line of the $^2F_{7/2} - {}^2F_{5/2}$ transition of Yb^{3+} or 0.45 nm (19 cm^{-1}) for the $^3H_{4(1)} - {}^3P_0$ transition of Pr^{3+}. In addition, high resolution spectra revealed that Pr^{3+} ions are located in several non-equivalent sites in this host. Transition intensities and relaxation dynamics of the $^3P_0$ and $^1D_2$ luminescent levels of Pr^{3+} were determined employing the Judd-Ofelt treatment and the $Pr^{3+} \rightarrow Yb^{3+}$ energy transfer phenomena were determined analyzing the effect of Yb^{3+} concentration on luminescence decay curves of Pr^{3+} donor ions. It was found that the transfer of the $^3P_0$ excitation to the $^2F_{5/2}$ level of Yb^{3+} is significant. For a sample GAGG:0.45at% Pr^{3+},10%Yb^{3+} (the highest Yb^{3+} concentration studied) the transfer efficiency of 85% and the transfer rate of $3.04 \cdot 10^5$ s^{-1} were determined. Effect of Yb^{3+} concentration on infrared luminescence spectra related to transitions from the $^3P_0$, $^1D_2$ and $^1G_4$ levels of Pr^{3+} in 850 nm -1500 nm region was examined to identify mechanism responsible. It was concluded that a quantum cutting mechanism consisting of a two-step energy transfer from Pr^{3+} to Yb^{3+}, namely: (Pr^{3+}: $^3P_0 \rightarrow {}^1G_4$) and ($Yb^{3+}$: $^2F_{7/2} \rightarrow {}^2F_{5/2}$) (first step) and ($Pr^{3+}$: $^1G_4 \rightarrow {}^3H_4$) and ($Yb^{3+}$: $^2F_{7/2} \rightarrow {}^2F_{5/2}$) (second step) is involved in observed down-conversion phenomenon. Up-conversion of incident radiation at 970 nm into visible luminescence was observed for GAGG:Pr,Yb samples under CW excitation. Attempts to obtain up-converted emission when exciting with 6 ns pulses were not successful. However, an intense up-converted visible luminescence was observed upon excitation by femtosecond pulses of infrared light at different wavelengths between 1100 nm and 1500 nm. Mechanisms responsible for this phenomenon are discussed.

Acknowledgment: This work was supported by the National Science Centre, Poland under grant number DEC 2016/21/B/ST5/00890.

Eu^{3+} luminescent centers in RE=Y, Gd, Tb aluminum perovskites under high pressure

Lev-Ivan Bulyk [1], Andrzej Suchocki [1,2], V. Gorbenko [2], Yu. Zorenko [2]

[1]*Institute of Physics PAS, Lotników Av. 32/46, 02-668, Warsaw, Poland*
[2]*Institute of Physics, Kazimierz Wielki University, Pl. Weyssenhoffa 11, 85-072, Bydgoszcz, Poland*
[*]*Corresponding author – Lev-Ivan Bulyk – bulyk@ifpan.edu.pl*

In current work, the $YAlO_3$ $GdAlO_3$ and $TbAlO_3$ perovskites doped with trivalent europium were investigated. These materials in the form of the single crystalline film (SCF) are perspective as scintillating screens for microimaging applications. SCF samples were prepared by liquid phase epitaxy method from the melt solution based on the PbO-B_2O_3 flux onto YAP substrates. The structural quality of films was studied using X-ray diffraction.

In other recent investigations [1] it was shown, that in $RAlO_3$ perovskite compounds with different R=Y, Lu, Gd cations, Eu^{3+} tends to occupy various sites with various local symmetry. In order to better understand this phenomenon, high-pressure luminescence measurements were performed. So called asymmetry ratio for $^5D_0 \rightarrow {}^7F_2$ and $^5D_0 \rightarrow {}^7F_1$ transitions was calculated as $K = I(^5D_0 \rightarrow {}^7F_2)/I(^5D_0 \rightarrow {}^7F_1)$ for pressures up to 16 GPa. It was revealed, that for GdAP:Eu and TbAP:Eu perovskites, the K value have the tendency to change with increase of pressure but for YAP:Eu we not observed the changes of K values with pressure.

We have found that K-value at ambient pressure is in good agreement with [1]. In [1], luminescence originating from transitions $^5D_1 \rightarrow {}^7F_j$ was measured at room temperature. In our work luminescence associated with $^5D_2 \rightarrow {}^7F_j$ transitions are also clearly observed. For GdAP:Eu and TbAP:Eu all lines in luminescence spectra shift to the lower energies with increase of pressure. Only one $^5D_0 \rightarrow {}^7F_0$ line was detected in GdAP:Eu and TbAP:Eu SCFs. For this reason, we have concluded that Eu occupies only one site in these perovskites [2].

In the case of YAP:Eu, there are at least three lines, related to $^5D_0 \rightarrow {}^7F_0$ transitions. That means that Eu occupies multiple sites in this material [2]. Another difference is observed in luminescent properties of YAP:Eu, connected with shift to the higher energies of the lines originating from $^5D_0 \rightarrow {}^7F_2$ and $^5D_1 \rightarrow {}^7F_2$ transitions and shift to the lower energies of the lines related to $^5D_0 \rightarrow {}^7F_1$ and $^5D_1 \rightarrow {}^7F_1$ transitions, with increase of applied pressure. The nature of observed behavior is assigned to changes of local symmetry of different Eu^{3+} sites under pressure [3].

Acknowledgements: This work was performed in framework of the Polish National Science Center. project No. 2016/21/B/ST8/03200.

[1] V. Gorbenko et. al., *CrystEngComm,* **20** (2018) 937-945.
[2] Peter A. Tanner, *Chem. Soc. Rev.*, **42** (2013) 5090.
[3] A. Kaminska, R. Buczko, W. Paszkowicz, H. Przybylińska, E. Werner-Malento, A. Suchocki, M. Brik, A. Durygin, V. Drozd, S. Saxena, *Phys. Rev. B.* **84**, 075483 (2011)

Structural studies focused on $Ca_9R(VO_4)_7$ (R = La, Nd, Gd) whitlockites under elevated pressure

Damian Włodarczyk [1,*], Katarzyna M. Kosyl [1,*], Wojciech Paszkowicz [1], Jaroslaw Z. Domagala [1], Olga Ermakova [1], Roman Minikayev [1], Andrzej Suchocki [1,2], Alexei Shekhovtsov [3], Miron Kosyma [3], Catalin Popescu [4], Fancois Fauth [4]

[1]*Institute of Physics PAS, Lotnikow Av. 32/46, 02-668, Warsaw, Poland*
[2]*Institute of Physics, Kazimierz W. University, Weyssenhoffa 11, 85-072, Bydgoszcz, Poland*
[3]*Institute for Single Crystals, NAS of Ukraine, Nauky Av. 60, 61001, Kharkov, Ukraine*
[4]*CELLS-ALBA Synchrotron Light Facility, 08290 Cerdanyola, Bercelona, Spain*
[*]*Corresponding authors - Damian Wlodarczyk – wlodar@ifpan.edu.pl*
Katarzyna M. Kosyl – kosyl@ifpan.edu.pl

Whitlockites, named after famous mineralogist Herbert P. Whitlock (1868-1948), are minerals of idealized formula $Ca_9(MgFe)(PO_4)_6PO_3OH$. Synthetic or natural, these structures have nowadays extended formulas including multiple vanadates and several arsenates. All of them reported to crystallize in R3c space group. Some are even considered in applications for optoelectronics, nonlinear optics, and tunable light emitting laser diodes. Our $Ca_9R(VO_4)_7$ vanadate is mostly related to merrillite subgroup, reported to be a part of few existing meteorites. In this work, Czochralski-grown crystals with R=La, Nd, Gd were investigated using powder X-ray Diffraction, up to 9 GPa, in order to determine the equation of state parameters. Raman spectroscopy was performed further, in range up to 15÷21 GPa, to check for the presence of eventual phase transitions. The occurrence of compressibility anisotropy was observed in XRD pressure range, therefore the linear moduli tend to be larger by factor of 1,5÷1,6 in [001] direction than for [100]. Therefore, fitting of Birch-Murnaghan equation of state in diffraction data was performed to calculate bulk moduli and then, Grüneisen parameters. C(p) dependence tends to be linear in, earlier mentioned, XRD pressure range. Above that, Raman spectroscopy revealed the occurrence of partially-reversible phase transition, to amorphous state at pressures above 10÷11 GPa. This phenomena is mostly characterized by peak broadening and their rapid red-shift towards lower energies. Studied crystals also exhibit local modes which tend to quickly up-shift with increasing pressure (before amorphisation) – so called external modes. Furthermore, Raman spectra of $Ca_9Nd(VO_4)_7$ also display two, relatively strong bands at pressures between 5-7 GPa which have no recognition in powder XRD spectra. This could imply some changes in symmetry of the sample or possible activation of Nd centers inside the material.

[1] N. Guo et.al., *J. Mater. Chem*. **20** (2010) 9061.
[2] Ling Li et.al., *Opt. Mater. Express*. **4** (2014) 16.
[3] Y. J. Zhang, Z. Y. Mao, D. Wang J., and J. Zhao, *Mater. Res. Bull*. **67** (2015) 1.
[4] M. P. Demesh et.al., *Opt. Mater.* **60** (2016) 387.

S15 Nano-crystals, colloids and aggregates

NIR Fluorescence Concentration Self-Quenching and Quenching by OH^- Molecular Groups in Aqueous Colloids of Nd^{3+} Doped Nanocrystals Used for Bioimaging

Yu.V. Orlovskii [1,2*], A.V. Popov [1], E.O. Orlovskaya [1], I. Sildos [2], A.S. Vanetsev [1,2]

[1] *General Physics Institute RAS, 38 Vavilov street, Moscow, Russia*
[2] *Institute of Physics, University of Tartu, Ostwaldi 1, Tartu, Estonia*
[*] *yurii.orlovskii@yandex.ru*

The aqueous colloids of Nd^{3+}: LaF_3 nanocrystals (NCs) synthesized by "green" hydrothermal - microwave treatment (HTMW) have proven themselves as promising fluorescent agent for near IR fluorescent imaging in the first biological window of wavelengths (750 – 950 nm) [1], because of their lower fluorescence quenching and higher dispersibilty comparing to the NCs synthesized by traditional co-precipitation (CO) method. Two processes govern the fluorescence quenching in the NCs synthesized by water-based methods [2]: 1) Nd*-Nd selfquenching and 2) quenching by OH^- molecular groups positioned in their volume. The main issue considered in the talk is what are the main regularities and peculiarities of these processes in bulk crystals and NCs and are we able to control the fluorescence quenching by appropriate synthesis method or specific crystal matrix for Nd^{3+} doping?

At first, to select synthesis method we connected defects of the crystal structure of the nanoparticles (NPs) with the processes of the fluorescence quenching. These defects are 1) inhomogeneity of dopant distribution over La^{3+} sites in the volume of the synthesized NCs leading to formation of Nd^{3+} pairs and clusters possessing strong fluorescence self-quenching, and 2) the OH^- molecular groups positioned also in the volume of the NPs.

High inhomogeneity of Nd^{3+} distribution in the volume of NCs increases the self-quenching and manifests itself in the intensity and shape of the fluorescence spectra at liquid helium temperatures. The high concentration of OH^- groups in the volume of the NPs demonstrated by the "energy transfer probing" enhances the Nd - OH quenching and manifests itself in the shortening of the fluorescence kinetics and decreasing in the fluorescence quantum yield at room temperature. As a result we found that higher temperature of reaction mixture for HTMW synthesis method comparing to CO results in more homogeneous distribution of Nd^{3+} dopant over La^{3+} sites and lower concentration of OH^- acceptors in the volume of the NCs, which results to higher fluorescence brightness of the NCs in the water colloid.

Also, we set a simple criteria for crystal host selection for Nd^{3+} doping to synthesize NCs using as fluorescent agents in the first biological window of wavelengths. It is a ratio of JuddOfelt intensity parameters Ω_4/Ω_6, which must be as large as possible to reduce the fluorescence Nd*-Nd self-quenching and Nd*-OH^- quenching caused by vibrations of molecular groups positioned in the volume of NCs. Hypothesis is checked on the concentration series of highly dispersible aqueous colloidal solutions of the Nd^{3+}: LaF_3 and Nd^{3+}: KY_3F_{10} NCs synthesized by HTMW treatment with PVP as biocompatible surfactant. We found that due to higher the Ω_4/Ω_6 ratio in the Nd^{3+}: LaF_3 comparing to Nd^{3+}: KY_3F_{10} NCs the fluorescence quenching reduces and fluorescence brightness increases four times.

[1] U. Rocha, J. Hu, E. M. Rodríguez, A. S. Vanetsev, M. Rähn, V. Sammelselg, Yu. V. Orlovskii, J. García Solé, D. Jaque, D. H. Ortgies, *Small* **12** (2016) 5394.
[2] A. Vanetsev, K. Kaldvee, L. Puust, K. Keevend, A. Nefedova, S. Fedorenko, A. Baranchikov, I. Sildos, M.Rähn, V. Sammelselg, Y. Orlovskii, *ChemistrySelect* **2** (2017) 4874.

Radio-luminescence spectral features and fast emission in hafnium dioxide nanocrystals

I. Villa [1], A. Lauria [2], F. Moretti [3‡], M. Fasoli [1], C. Dujardin [3], M. Niederberger [2] and A. Vedda [1,*]

[1]Department of Materials Science, University of Milano-Bicocca, Via R. Cozzi 55, 20125 Milano, Italy.
[2]Laboratory for Multifunctional Materials, Department of Materials, ETH Zürich, Vladimir-Prelog-Weg 5, 8093 Zürich, Switzerland
[3]Institut Lumière Matière UMR5306 CNRS Université Claude Bernard Lyon 1, Bâtiment Kastler, 10 rue Ada Byron 69622 Villeurbanne CEDEX, France
[‡]Now at: Lawrence Berkeley National Laboratory, 1 Cyclotron road, Berkeley, CA 94720, USA
[*]Corresponding author

In this study we have investigated the optical response of hafnia nanocrystals prepared by non-acqueous sol-gel route following excitation with ionizing radiation, comparing the results with previous photoluminescence data [1, 2]. By performing a complete spectral analysis of the emissions, we have found the presence of as many as six bands in the visible and UV regions, whose relative intensities clearly depend upon nanocrystals radius that varies with the temperature of annealing treatments. The spectral analysis, coupled to the investigation of the temperature dependence of each emission intensity, has allowed us to propose distinct origins for all the RL emissions. In fact, the components lying in the visible-near UV region and displaying the same thermal quenching energy of about 0.08 eV have been related to intrinsic defects. On the other hand, two additional components peaking at 4.12 and at 4.69 eV with a similar thermal quenching energy of 0.23 eV have been associated to excitonic transitions. Moreover, scintillation measurements in the visible emission range have shown the presence of a fast decay in the nanosecond time scale for the case of the smallest nanocrystals annealed at 450 °C.
The present investigation concerning the relationship between material structure, morphology and optical properties provides a tool for the future engineering of hafnia-based nanostructures in different optical applications. Moreover, the measured scintillation properties disclose the potential application of hafnia nanocrystals as fast scintillators.

[1] A. Lauria, I. Villa, M. Fasoli, M. Niederberger and A. Vedda, *ACS Nano* **7** (2013) 7041.
[2] I. Villa, A. Vedda, M. Fasoli, R. Lorenzi, N. Kränzlin, F. Rechberger, G. Ilari, D. Primc, B. Hattendorf, F. J. Heiligtag, M. Niederberger and A. Lauria, *Chemistry of Materials* **28** (2016), 3245.

Optical Properties of Silicon Nanocrystals Synthesized by Reactive Pulsed Laser Deposition

T.S. Iwayama* and K. Ogihara

Department of Physics, Aichi University of Education, Kariya, Aichi, 448-8542 Japan
**Corresponding author*

After first reports on room temperature visible photoluminescence (PL) in the early 1990s [1], great interest in the optical properties of Si nanocrystals has grown over the last decade because of their potential applications toward Si-based integrated optoelectronic devices. Our group has focused on the formation of silicon nanocrystals, and developed the first examples of luminescent Si nanocrystals inside of SiO_2 using ion implantation [2]. Nowadays, it is well known that Si ion implantation into SiO_2 and subsequent high temperature annealing (more than 1000 ^oC) induce the formation of luminescent Si nanocrystals. The PL peaking in the near infrared or visible spectrum (between 1.4 eV and 1.8 eV) is evidently related to implanted Si nanocrystals formed by decomposition of the SiO_x phase and aggregation with high temperature annealing. The PL arising from implanted Si nanocrystals in SiO_2 has been attributed by some investigations to simple quantum confinement, while others have concluded that surface states present in the interfacial layer (including some types of defects) between the Si nanocrystals and the surrounding oxide matrix (localized surface states) play an important role in the emission process.

In this work, we report the optical properties of Si nanocrystals embedded in a SiO_2 synthesized by reactive pulsed laser deposition (PLD) in an oxygen atmosphere. Si sub-oxide (SiO_x, $0<x<2$) films were firstly deposited on Si wafers, by suing conventional PLD system with 2nd-harmonic YAG laser (532nm, 10Hz) under controlled low oxygen pressure. After deposition in the oxygen ambient, the produced SiO_x films were annealed using a conventional tube furnace (FA) for several hours at 1050 ^oC in N_2 atmosphere to induce the formation of Si nanocrystals, by decomposition of the SiO_x phase and aggregation. Some of the samples were irradiated with excimer-UV light (172 nm, 7.2 eV, Xe_2^*) for 2 hours with power density of 50 mW/cm^2 in vacuum or rapidly thermal annealed (RTA) at 1050 ^oC in N_2 atmosphere for 5 minutes with a rising rate of 50 ^oC/sec before FA. Conventional room temperature PL spectra were measured at various stages of the processing. A He-Cd laser (325 nm, 3.82 eV) was used as the excitation source and the luminescence was detected by a cooled photomultiplier tube, employing the photon counting technique.

We found that the luminescence intensity is strongly enhanced with UV irradiation and RTA. Based on our experimental results, we discuss the effects of excimer-UV lamp irradiation and RTA process on the formation of Si nanocrystals. In case for PLD produced samples, PL intensity increases with increasing oxygen gas pressure, and then decrease. We also found that the maximum intensity can be obtained with oxygen pressure around 0.6Pa. It is also noted that the peak energies of the PL are affected by ambient oxygen pressure. In some cases blue-shift, other cases red-shift. The formation process of luminescent Si nanocrystals with UV, RTA and FA treatments can be explained with bond-breaking (Si-Si and/or Si-O), defect generation, de-nucleation, defect-initiated nucleation and frozen of individual states.

[1] L.T.Canham, *Appl. Phys. Lett*. **57**, (1990) 1046.
[2] T.S.Iwayama, N.Kurumado, D.E.Hole, P.D.Townsend, *J. Appl. Phys*. **83** (1998), 6018.

Temperature-Sensitive Luminescence of $Y_2O_3:Nd^{3+}$ Nanocrystals Produced by an Eco-Friendly Route

Maria A. Gomes [1,*], Iure S. Carvalho [1], Antônio Carlos Brandão-Silva [1], Márcio A.R.C. Alencar [1] and Zélia S. Macedo [1]

[1] *Federal University of Sergipe, Marechal Rondon Avenue, São Cristóvão, Brazil*
**Corresponding author*

Lanthanide-doped inorganic nanocrystals have been shown great potential for temperature sensing in nanoscale mainly due to their high quantum yield, sharp excitation and emission spectra and large Stokes shift [1]. The use of neodymium as the dopant ions is particularly advantageous for biological applications, since its excitation and emission energies lie within the near-infrared, a spectral region in which the living tissues are highly transparent. In addition, yttrium oxide as host structure provides low nonradiative decays of the excited levels of the dopant ions. Despite these relevant properties, producing adequate nanoparticles for biological sensing, regards the size distribution of particles, efficiency of luminescence, thermal sensitivity and compatibility, remains as the main challenge. In this way, this work presents the structural, optical and thermal sensing properties of Y_2O_3:Nd nanocrystals which were synthesized using natural organic matter (NOM) from river water [2]. The advantages of this new route lie on its eco-friendly character, economic viability, low concentration of mineral impurities and similar composition of different NOM found around the world, which guarantees synthesis reproducibility. Y_2O_3:Nd samples with *bcc* structure were successfully produced with different dopant concentrations (0.5–3 mol%) and calcination temperatures, yielding crystallites in the size range of 12–25 nm. The emission spectra at room temperature of Y_2O_3:Nd (1 mol%) samples showed radiative transitions in the first and second Biological Windows, as observed in Fig.1. No significant change on line positions were found in comparison to bulk crystals, indicating the same Nd transitions, whereas increasing luminescence intensity is observed as the crystallite size rises. In the present stage of the work, the temperature sensitivity in the physiological temperature range (20–60 °C) of the thermally coupled and uncoupled Nd levels is been investigated.

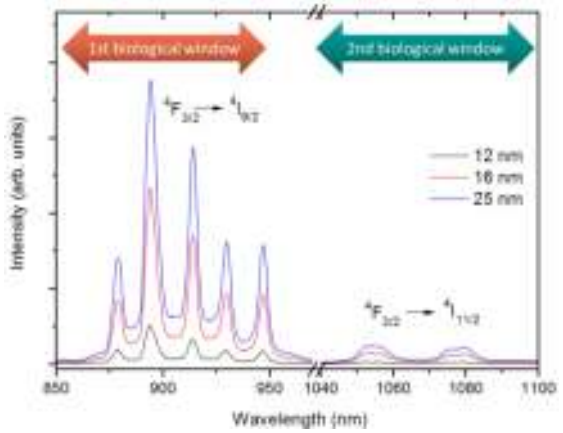

Fig.1: Room temperature emission spectra of Y_2O_3:Nd(1%) samples.

[1] E. Hemmer, A. Benayas, F. Légaré, and F. Vetrone, *Nanoscale Horiz.*, **1** (2016) 168.
[2] G.C. Cunha, L.P.C. Romão, and Z.S. Macedo, *Powder Technol.*, **254** (2014) 344.

Luminescence Impurity Quenching and Self-Quenching in Disordered Systems: From Bulk to Nanoparticles

Stanislav G. Fedorenko [1,*], Yurii V. Orlovskii [2,3]

[1] *Voevodsky Institute of Chemical Kinetics and Combustion, Siberian Branch of the Russian Academy of Sciences, Institutskaya 3, Novosibirsk, Russia*
[2] *A.M. Prokhorov General Physics Institute RAS, Vavilov street 38, Moscow, Russia*
[3] *Institute of Physics, University of Tartu, Ostwaldi 1, Tartu, Estonia*
[*] *fedorenk@kinetics.nsc.ru*

Being the important channel of the dissipation of electronic excitations, inductive resonance energy transfer through a system of impurity centers in disordered solid solutions leads to the appearance of luminescence concentration quenching [1]. This quenching is substantially accelerated by excitation migration in the system of donor centers that forces the delivery of energy to the sites of its death - acceptors on which excitations decay irreversibly. Commonly, acceptors are impurity centers with a short relaxation time which either are specifically introduced into the crystal with a certain concentration, or are present as uncontrolled impurities. In the systems with cross-relaxation the same centers can play the role of both donors and acceptors so the self-quenching processes are possible. Such a situation is realized in widely studied crystals and glasses activated by neodymium ions [2]. Investigation of concentration quenching kinetics makes it possible not only to determine the microparameters of the interaction and concentration of impurity centers, but also to obtain information about spatial structure of the system, which is especially important in studies of nano-objects.

We have developed the theory of luminescence decay for systems in which quenching and self-quenching processes can proceed simultaneously. The necessity of solving such a problem arises, in particular, in the investigation of water colloids of crystalline nanoparticles of fluorides doped with neodymium ions [3]. These colloids of synthesized Nd^{3+}: LaF_3 nanocrystals have established themselves as a promising fluorescent agent for near infrared fluorescence imaging in the first biological window (750 – 950 nm). The role of additional energy acceptors in these systems is playing by OH^- groups of water, whose molecules are always present in the system as an uncontrolled impurity. Calculations were carried out in the framework of self-consistent method of diagram summation proposed in [4, 5] to describe excitation migration and quenching processes in disordered system. The developed theory is used to describe the kinetics of luminescence decay in water colloids of Nd^{3+}: LaF_3 nanocrystals. Specific features of luminescence decay in nanocrystals are discussed.

The work was done under support of Russian Science Foundation grant #16-12-10077.

[1] A. I. Burshtein, *Usp. Fiz. Nauk* **143** (1984) 553, [*Sov. Phys. Usp.* **28** (1984) 579].
[2] S. G.Fedorenko, A.V. Popov, E. A. Vagapova, A. E. Baranchikov, Yu. V. Orlovskii, *J. Lumin.* **198** (2018) 138.
[3] A. Vanetsev, K. Kaldvee, L. Puust, K. Keevend, A. Nefedova, S. Fedorenko, A. Baranchikov, I. Sildos, M. Rähn, V. Sammelselg, Yu. Orlovskii, *Chem. Select* **2** (2017) 4874.
[4] C. R. Gochanour, H. C. Andersen, M. D. Fayer, *J. Chem. Phys.* **70** (1979) 4254.
[5] R. F. Loring, H. C. Andersen, M. D. Fayer, *J. Chem. Phys.* **76** (1982) 2015.

Enhancement of YAG:Ce, Yb photoluminescence by Ag nanoparticles

M. Kushlyk [1,2,*], V. Tsiumra [1], Ya. Zhydachevskyy [1,3], I.I. Syvorotka [4], V. Haiduchok [4], D. Sugak [3,4], A. Suchocki [1,5]

[1]*Institute of Physics, Polish Academy of Sciences, Al. Lotników 32/46 Warsaw 02-668, Poland*
[2]*Ivan Franko National University of Lviv, 107, Tarnavskoho str., Lviv 79017, Ukraine*
[3]*Lviv Polytechnic National University, 12 Bandera, Lviv 79646, Ukraine*
[4]*SRC „Carat", 202 Stryjska str., Lviv 79031, Ukraine*
[5]*Institute of Physics Kazimierz Wielki University, Weyssenhoffa 11, Bydgoszcz 85-072, Poland*
[*]*Corresponding author: kushlyk@ifpan.edu.pl*

Phosphors based on rare-earth ions are widely used to convert photons to wavelengths useful for a wide range of applications. Therefore the improvement of their emission efficiency remains a key challenge. In recent years, significant attention is paid to plasmonic effects of metal nanoparticles (NPs) formed in volume or on a surface of dielectrics.

In this work, the possibility to enhance luminescence efficiency of garnet phosphors based on YAG ($Y_3Al_5O_{12}$) is presented. Results of theoretical simulation and experimental characterization of silver NPs placed on a surface of single-crystalline YAG together with optical and luminescence properties of the studied phosphors combined with such plasmonic structures are shown. The effects of size and shape of Ag NPs controlled by preparation parameters (a magnetron-sputtering and subsequent annealing processes) on the optical and luminescence properties of the studied structures are discussed.

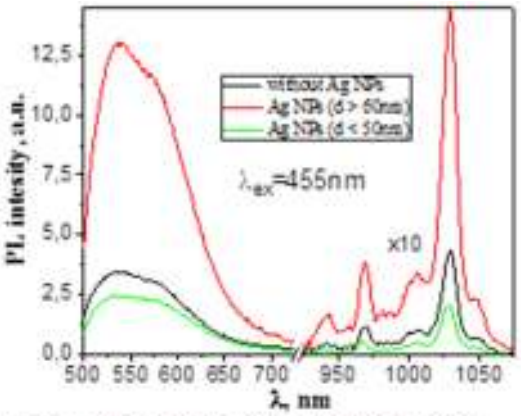

Fig.1. Enhancement (or quenching) of PL of YAG:Ce,Yb depending on size of Ag NPs.

A broad absorption band peaking in a region from 440 to 550 nm was observed due to dipole mode of surface plasmon resonance (SPR) of Ag NPs. This band corresponds to the 455 nm excitation band of Ce^{3+} ions in YAG. An enhancement of Ce^{3+} photoluminescence near 560 nm was observed for NPs bigger than 60 nm (Fig. 1). A corresponding enhancement of Yb^{3+} luminescence at 455 nm excitation (due to energy transfer from Ce^{3+} to Yb^{3+} ions) was also observed in this case. At the same time the samples with small NPs (d<50 nm) demonstrate quenching of the Ce^{3+} and Yb^{3+} luminescence. The enhancement of Ce^{3+} luminescence is mainly attributed to local field effects: the LSPR of Ag NPs causes an intensified electromagnetic field around the NPs, resulting in enhanced optical transitions of Ce^{3+} ions in the vicinity. The quenching effect in the presence of Ag NPs suggests an energy transfer from Ce3+ ions to Ag NPs. The competition between the plasmonic enhancement and the quenching effect is discussed for samples with different Ag plasmonics nanostructure.

Acknowledgements: The work was supported by the Polish National Science Center (project 2015/17/B/ST5/01658).

S16 Material preparation technology and technological applications

Development of luminescent materials for new thermoluminescence (TL) and optically stimulated luminescence (OSL) applications

Eduardo G. Yukihara [1,2,*], Timothy D. Gustafson [2], Elena D. Milliken [2,3], Luiz C. Oliveira [2,4], and Solmaz Bastani [2]

[1]*Department of Radiation Safety and Security, Paul Scherrer Institute, 5232 Villigen PSI, Switzerland*
[2]*Physics Department, Oklahoma State University, Stillwater, OK 74078, United States*
[3]*R&D Pigments, Ferro Corporation, 251 W. Wylie Ave, Washington, PA 15301, USA*
[4]*Departamento de Física, FFCLRP-Universidade de São Paulo, 14040-901 Ribeirão PretoSP, Brazil*
[*]*Corresponding author*

New applications of the thermoluminescence (TL) and optically stimulated luminescence (OSL) techniques in the areas of temperature sensing [1] and 2D dosimetry in radiotherapy [2] motivated the development of new materials with improved properties by 'material engineering', particularly using lanthanide doping. Such effort received renewed impetus by the advances in the understanding in the energy levels of lanthanides within the bandgap [3].

This presentation will provide an overview of these two new applications, with emphasis on material requirements. We will then present an overview of the investigations carried out by our group to develop new materials with tailored luminescence properties, and to understand the underlying luminescence mechanisms by systematic lanthanide doping. Examples include the TL mechanisms in $Y_3Al_5O_{12}$ (YAG) and the TL and OSL mechanisms in MgB_4O_7. Other materials of interest for particle temperature sensing (e.g. $Li_2B_4O_7$, and $CaSO_4$) will also be presented. Finally, some of the main challenges from both fundamental and applied points of view will be discussed.

[1] J.J. Talghader, M.L. Mah, E.G. Yukihara, A.C. Coleman, *Microsystems & Nanoengineering* **2** (2016) 16037.
[2] M.F. Ahmed, N. Shrestha, S. Ahmad, E. Schnell, M.S. Akselrod, E.G. Yukihara, *Radiat. Meas.* **106** (2017) 315.
[3] P. Dorenbos, J. Phys.: *Condens. Matter* **15** (2003) 8417.

Progress and challenges towards the development of a new optically stimulated luminescence (OSL) material based on MgB_4O_7

Timothy D. Gustafson [1,*] and Eduardo G. Yukihara [1,2]

[1]*Physics Department, Oklahoma State University, Stillwater, OK 74078, United States*
[2]*Department of Radiation Safety and Security, Paul Scherrer Institute, 5232 Villigen PSI, Switzerland*
[*]*Corresponding author*

The objective of this work is to present the advances towards the development of a new OSL material based on MgB_4O_7, which has high sensitivity to ionizing radiation, low effective atomic number (Z_{eff} = 8.4), and fast luminescence when doped with cerium (Ce^{3+} emission). The material was previously described by our group [1] and also identified by other researchers as a potential OSL dosimeter [2]. There are currently only two commercially available Optically Stimulated Luminescence (OSL) materials used in dosimetry: aluminum oxide (Al_2O_3:C) and beryllium oxide (BeO). They are highly sensitive to ionizing radiation and routinely used in personal, environmental, and medical dosimetry. Nevertheless, for some applications (e.g. dosimetry applications requiring low effective atomic number, 2D laser scanning readout requiring fast luminescence centers, applications requiring powder), materials with improved properties motivates the investigation and development of new materials.

MgB_4O_7 was synthesized by solution combustion synthesis (SCS) using $Mg(NO_3)_2$ (99.999%, Alfa-Aesar 10799), H_3BO_3 (99.99%, Alfa-Aesar 36771), urea (99.0-100.5%, Alfa-Aesar 36428), $LiNO_3$ (99%, Alfa-Aesar 13405), and $Ce(NO_3)_3$ (99.5%, Alfa-Aesar 11329), and subjected to annealing to improve the material's crystallinity. The synthesized materials were characterized by powder X-ray diffraction, radioluminescence (RL), thermoluminescence (TL), and OSL under both blue and green stimulation. Reusability data were collected for TL and OSL as well.

With the use of high purity reagents, a competing recombination center emitting at ~580 nm (possibly Mn^{2+}) has been eliminated, and as a result the Ce^{3+}emission at 338 nm and 358 nm has been increased by a factor of ~4.5 times, the TL and the OSL in the UV region (290 – 390 nm) have been increased about 4 - 4.5 times. TL sensitization has been reduced from ~48% to ~13%, but OSL sensitization increased from ~11% to 22% for green stimulation and from ~10% to ~13% for blue stimulation. Avenues for future improvements will be discussed as well.

Acknowledgements: this research was partially funded by the Oklahoma Center for the Advancement of Science and Technology, project number HR12-055.

[1] E.G. Yukihara, B.A. Doull, T. Gustafson, L.C. Oliveira, K. Kurt, E.D. Milliken, *J. Lumin.* **183** (2017) 525.
[2] L.F. Souza, A.M.B. Silva, P.L. Antonio, L.V.E. Caldas, S.O. Souza, F. d'Errico, D.N. Souza, *Radiat. Meas.* **106** (2017) 196.

Raman spectroscopic study of diamond foils synthesis

Marcin Gnyba [1,*]

[1]*Gdańsk University of Technology, Faculty of Electronics, Telecommunications and Informatics, 11/12 Narutowicza St., 80-233 Gdansk, Poland*
[*]*Corresponding author: mgnyba@eti.pg.edu.pl*

Diamond and boron-doped-diamond (BDD) foils are recently developed structures that can be used in production of e.g. highly sensitive sensors that use the flexible surface chemistry of nanocrystalline diamond capable of biological modification. The foil can be manufactured as thin film deposited on typical low adhesive substrate during the CVD process and subsequently removed from the substrate and transferred to the destination.
Synthesis and transfer of the diamond foils is a complex issue as it is necessary to deposit the film with moderated adhesion to the substrate and control the stress of the films which is consequence of mismatching between substrate and diamond film lattices. The stress of the growing layer significantly influences on the size and the shape of the diamond foil pieces available for the transfer. Also efficiency of the CVD process depends on numerous process parameters and other factors, e.g. type of substrate and its pretreatment, substrate temperature, microwave power, methane admixture and boron doping level. Thus, it is necessary to study deposition process including molecular composition of the films, its homogeneity, and stress distribution
Set of dedicated test samples enabled stress measurement and molecular composition investigation of diamond film deposition on different substrates (metal, fused silica, silicon). Moreover, influence of time of deposition on stress in the films, their molecular composition and thickness was studied. The range of tested growth time was from 15 to 120 minutes, producing film of a thickness up to 500 nm [1-3]. Before the vacuum process the substrates were washed and seeded by sonication in nanodiamond solution. Substrate temperature was kept at 500°C during the CVD process. Hydrogen, methane and diborane were used the process precursors, while total gas pressure inside the CVD chamber was set to 50 Torr.
Optical and Raman microscopy were used for the investigation. Analysis of the Raman bands assigned to diamond lattice (shift, intensity change) and other bands as well as their spatial distribution enabled study of molecular composition and its homogeneity, including quality of the lattice, content of diamond and non-diamond phase, stress distribution, content of defects and doping level as a function of the key CVD process parameters.

The author wish to acknowledge financial support from the National Centre for Research and Development under Grant Techmatstrateg No. 347324 and from the Faculty of ETI of the Gdansk University of Technology (the DS funds).

[1] R. Bogdanowicz, A. Fabiańska, L. Golunski, M. Sobaszek, M. Gnyba, J. Ryl, K. Darowicki, T. Ossowski, S. Janssens, and others, *Diam. Relat. Mater.* **39**, (2013), 82
[2] R. Bogdanowicz, M. Śmietana, M. Gnyba, and others, *Appl. Phys. A* **116**, (2014). 1927
[3] R. Bogdanowicz, M. Sobaszek, J. Ryl, M. Gnyba, M. Ficek, Ł. Gołuński, W.J. Bock, M. Śmietana, K. Darowicki, *Diam. Relat. Mater.* **55**, (2015), 52

Diamond as a transducer material for the production of biosensors

L. Mosińska*, K. Fabisiak, P. Popielarski

Institute of Physics, Kazimierz Wielki University, Powstańców Wielkopolskich 2, 85-090 Bydgoszcz, Poland

Bioelectronics is a field of research combining the latest achievements in biology and electronics. This new discipline of science is especially focused on the search for new types of sensors, biosensors with high sensitivity, selectivity and speed of response, and low price. Biosensors have a chance to play a key role in many fields of science, and above all in clinical trials.

The problem of durability of the biosensor is the material used as a transducer. Silicon is the most common, but hydrolysis processes leads to the loss of bioreceptors from its surface. Recently, the attention of researchers has been directed to a diamond whose physical properties exceed the possibilities of silicon. It seems, therefore, that it will be a perspective material for the construction of biosensors.

V. Poster session I

Concentration Self-Quenching of Luminescence in LaF_3: Nd^{3+} Crystals

Aleksandr V. Popov [1,*], Ekaterina A. Vagapova [1,2], Alexandr E. Baranchikov [3], Stanislav G. Fedorenko [4], and Yurii V. Orlovskii [1,2]

[1]*A.M. Prokhorov General Physics Institute RAS, Vavilov street 38, 119991, Moscow, Russia*
[2]*Institute of Physics, University of Tartu, W.Ostwaldi st.1, Tartu 50411, Estonia*
[3]*Kurnakov Institute of General and Inorganic Chemistry RAS, 31 Leninsky Pr., 119991 Moscow, Russia*
[4]*Voevodsky Institute of Chemical Kinetics and Combustion, Siberian Branch of the Russian Academy of Sciences, Institutskaya 3, Novosibirsk, Russia*
[*]*Corresponding author*

Resonance migration and cross-relaxation processes leading to concentration self-quenching of fluorescence have been studied experimentally and theoretically with Nd^{3+}: LaF_3 single crystal as an example. The specific feature of concentration self-quenching of luminescence is that there exists just one parameter $z = C_{DA}/C_{DD}$ (C_{DA} and C_{DD} are microparameters of a dipole-dipole interaction in cross-relaxations and resonance migration processes), which controls both the quenching mechanism (hopping or diffusion) and the kinetics decay character (migration-accelerated or non-stationary). If $z \ll 1$, self-quenching will be hopping and migration-accelerated.

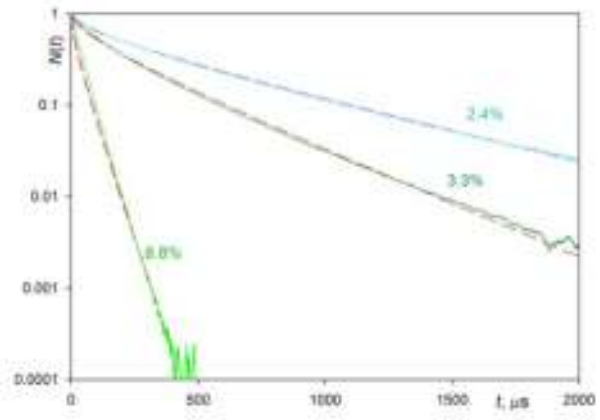

Figure. The impurity self-quenching kinetics depending on Nd^{3+} ion concentration in the Nd^{3+}: LaF_3 single crystal. Dashed lines correspond to theoretical calculations.

We have managed to consistently describe a full number of kinetic curves (Figure) of impurity self-quenching using one set of C_{DD} = 0.85 nm/ms^6 and C_{DA} = 0.13 nm/ms^6 (z = 0.15) and this agrees with the applicability range of the hopping theory of self-quenching (Eqs. [1]). We have obtained the estimate for critical concentration of donors at which the multistage kinetics of impurity self-quenching changes to single exponential ordered decay. Critical concentration depends on lattice constants of crystal and is an increasing function of the parameter z up to the boundary values of the existence of migration-accelerated stage. For the crystal Nd^{3+}:LaF_3, critical concentration of Nd^{3+} proved to be 12.8%.

The obtained results allow us to pass to the investigation of luminescence quenching problem in impurity crystal nanoparticles with RE ions where, along with self-quenching, the quenching on additional acceptors is observed (for example, OH^- groups, residing in the nanoparticles volume).

The research was supported by Russian Science Foundation (RSF) grant #16-12-10077.

[1] S. G. Fedorenko, A.V. Popov, E. A. Vagapova, A.E. Baranchikov, Yu.V. Orlovskii, *J. Lumin.* **198** (2018) 138.

Diffusion of 5p-holes in BaF_2 Nanoparticles

Maksym Chylii [1], Taras Malyi [1], Taras Demkiv [1], Vitaliy Vistovskyy [1,*], Piotr Rodnyi [2], Alexander Gektin [3], Andrey N. Vasil'ev [4], Anatoliy Voloshinovskii [1]

[1]*Ivan Franko National University of Lviv, 8 Kyryla i Mefodiya St., 79005, Lviv, Ukraine*
[2]*Saint-Petersburg State Polytechnical University, 29, Polytekhnicheskaya, 195251, Russian Federation*
[3]*Institute for Scintillation Materials, 60 Nauky Ave, 61072, Kharkiv, Ukraine*
[4]*Skobeltsyn Institute of Nuclear Physics, 119991 Moscow, Russian Federation*

Study of luminescent-kinetic parameters of nanoparticles allows not only to search for materials for various purposes, in particular, luminescent biolabels or nanoscintillators, but also to obtain a new knowledge about the peculiarities of the luminescence mechanisms. For example, the study of the recombination luminescence in nanoparticles of different sizes allows experimental estimation of the thermalization length of free charge carriers [1]. Analyzing the change of the exciton luminescence decay kinetics curve shape at decrease of nanoparticles size one can study the peculiarities of luminescence quenching caused by the interaction of the excitons with surface defects. Thus, in [2], an equation describing the shape of the luminescence decay kinetics curve for nanoparticles depending on the diffusion of excitations which non-radiatively relax on surface defects of nanoparticles is proposed. The use of this model for the luminescence of self-trapped excitons in SrF_2 allowed to estimate their diffusion length as ~ 15 nm. In this work the estimation of the diffusion length of core holes analyzing the decay kinetics of the core-valence luminescence (CVL) of BaF_2 nanoparticles of different sizes is undertaken. The BaF2 nanoparticles were synthesized by precipitation method with following temperature annealing. Samples of nanoparticles with different sizes in the range of 20 – 140 nm were obtained. The luminescence kinetic studies of BaF_2 nanocrystals were performed using synchrotron radiation at SUPERLUMI station (DESY, Hamburg).

The kinetic parameters of CVL of BaF_2 nanoparticles with different sizes were studied for a band peaked at 225 nm under excitation by the quanta with an energy of 18 eV at room temperature. At the transition from large (140 nm) to small (20 nm) nanoparticles, the decay kinetics of CVL reveals a certain shortening, which is accompanied with a decrease of intensity. Since the radiative transitions occur between a 5p-core hole and an electron from the entire continuum of the valence band, the quenching of the CVL is caused by the non-radiative relaxation of the core holes. Assuming that this non-radiation relaxation takes place on the surface of nanoparticles due to the diffusion of holes, the kinetics of the CVL has been analysed using the diffusion model proposed in [2]. From the decay curve shapes, the diffusion length of the core hole is estimated as 3 nm. This value is close to the estimates obtained by other authors – 7 nm for BaF_2 [3] and 1.5 nm for RbF-CsF system [4]. The small diffusion lengths of the core holes determine the weak sensitivity of the CVL intensity to the size confinement.

[1] V. Vistovskyy, Y. Chornodolskyy, A. Gloskovskii, et al., *Radiat. Meas*. **90**, (2016) 174.
[2] M. Chylii, T. Demkiv, V. Vistovskyy, et al., *J. Appl. Phys*. **123**, (2018) 034306.
[3] M.A. Terekhin, A.N. Vasil'ev, M. Kamada, et al., *Phys. Rev. B* **52**, (1995) 3117.
[4] M. Itoh, N. Ohno, and S. Hashimoto, *Phys. Rev. Lett*. **69** (1992) 1133.

Anomalous diffusion of small electron polarons in lithium niobate

Bazzan M.* and Vittadello L.

Università di Padova - Physics and Astronomy Dept., Via Marzolo 8, Padova, Italy
**Corresponding author*

Besides being a key material in photonic technology, lithium niobate ($LiNbO_3$, LN) is often taken as a paradigm for light induced charge transport phenomena in oxide crystals playing a major role in a number of applications [1]. This kind of phenomena was modelled in the past with the help of the phenomenological Kukhtarev- Vinetski equations [2] mutuated from semiconductor physics. Those equations are meaningful when charge carriers are normally diffusing particles, for which a mobility can be defined and obeys the Einstein relation: $\mu = eD/kT$.
However, it is nowadays clear that charge conduction in LN cannot be described in term of delocalized states like in semiconductors, but in terms of small polarons moving among regular and/or defective sites of the lattice by thermally activated hopping [3]. In standard conditions, LN crystals are of congruent composition and contain a high concentration of intrinsic defects, which bring a certain degree of disorder in the structure.
Under these circumstances, it is not clear whether standard diffusion laws apply to the polaron motion [4] and, as a consequence, what is the validity range of Kukhtarev's equations.
In this study, by a MonteCarlo simulation based on the Marcus-Holstein hopping model [5,6], we investigate the diffusion behavior of small electron polarons in LN. The diffusion process turns out to be more or less anomalous depending on the temperature and on the composition of the sample and on the time scale under which the process is observed.

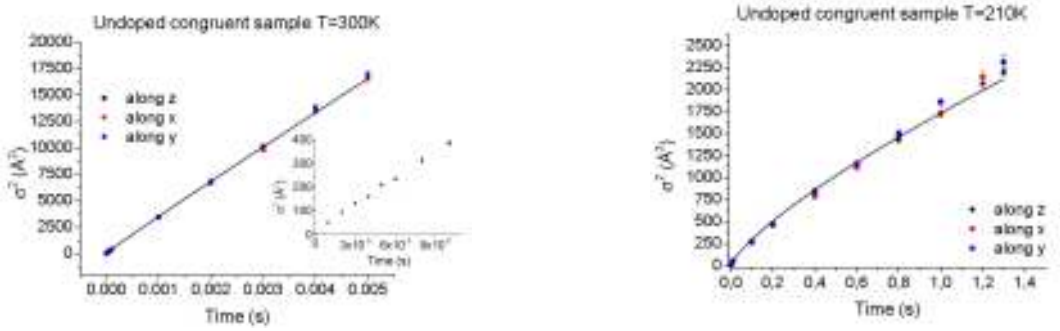

Figure 3: Second moment of the polaron distribution along x,y and z directions as a function of time. (Left) T = 300 K; the inset shows a zoom at short times. (Right) T = 210 K.

[1] Tatyana Volk and M. Wholecke, *Lithium Niobate* Springer-Verlag Berlin Heidelberg, 2009
[2] Kukhtarev, N. V.; Markov, V. B.; Odulov, S. G.; Soskin, M. S. & Vinetskii, V. L. *Ferroelectrics*, 1978, **22**, 949-960
[3] Schirmer, O. F., *Journal of Physics: Condensed Matter*, 2006, **18**, R667
[4] Metzler, R. and Klafter, *J. Physics Reports*, 2000, **339**, 1-77
[5] Marcus, R. A., *The Journal of Chemical Physics*, 1956, **24**, 966-978
[6] Holstein, T., *Annals of Physics*, 1959, **8**, 343 - 389

Dynamics of Changes in Optical Absorption in $Bi_{12}TiO_{20}$:Al Crystal Induced by Nanosecond Laser Pulses

V.G. Dyu *, T.D. Tokmashev, D.V. Sokolov, S.M. Shandarov

Tomsk State University of Control Systems and Radioelectronics (TUSUR University), 40 Lenin Avenue, Tomsk 634050, Russia

The appreciable light-induced changes in optical absorption (the photochromic effect) connected with a redistribution of the charge carriers over the defect centers with different photoionization cross-sections are observed in sillenite crystals [1–3]. We report on the experimental studies of the dynamics of changes in optical absorption at the wavelength of λ_p = 655 nm in the sample of aluminum-doped bismuth titanium oxide crystal ($Bi_{12}TiO_{20}$:Al) with thickness of 6.6 mm, which were caused by a laser pulse having the wavelength of λ_i = 526.5 nm, the duration of 10 ns and the repetition rate from 1 to 100 Hz.

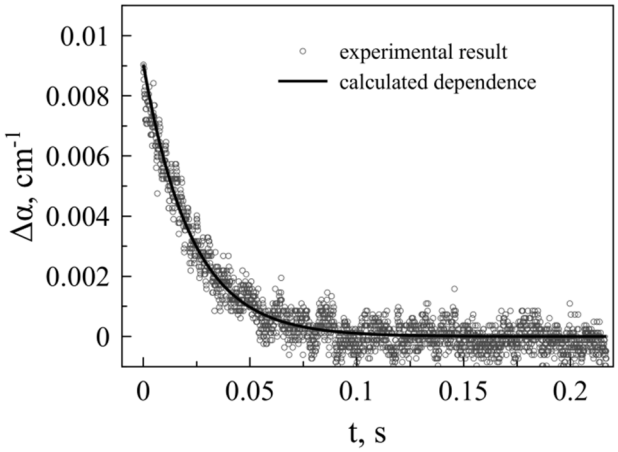

Figure 1: Time dependences of changes in the Lambert-Beer absorption coefficient at 655 nm induced in the $Bi_{12}TiO_{20}$:Al crystal by a single nanosecond pulse with the wavelength of 526.5 nm

We observed the changes in absorption for induced-light exposition in excess of 0.25 μJ/ cm^2. It was established that the increase in intensity of continuous probing beam with λ_p=655 nm from 0.5 to 2 mW/cm^2 leads to decrease in its inherent absorption. The maximum changes in the Lambert-Beer absorption coefficient are observed immediately after pulse illumination (see Fig. 1). The relaxation of these changes between the inductive pulses in the presence of probing beam with the intensity of 2 mW/cm^2 had been approximated by exponential function with relaxation time of 22 ms as it is shown by solid line on Fig. 1.

This work was supported by the State Assignment of the Ministry of Education and Science of Russian Federation (within the tasks No. 3.8898.2017/8.9 and 3.1110.2017/PCh) and the RFBR (grant No. 16-29-14046-ofi_m).

[1] K. Buse, *Appl.Phys. B*. Vol. **64** (1997) 273-291.
[2] Kobozev O.V., Shandarov S.M., Kamshilin A.A., Prokofiev V.V., *J. Opt. A: PureAppl. Opt*. Vol.**1** (1999) 442-447.
[3] A.L. Tolstik, A.Yu. Matusevich, M.G. Kisteneva, A.E. Mandel', N.I. Burimov, *Quantum Electron*. Vol. **37** (2007) 1027-1033.

Luminescence of Doped AlN Nanopowders for Marking of Biological Materials

Baiba Berzina*, Laima Trinkler and Valdis Korsaks

Institute of Solid State Physics, University of Latvia, 8 Kengaraga Str., Riga, Latvia
**Corresponding author:Baiba Berzina; baiber@latnet.lv*

Nanobiophysics is one of developing field in natural sciences, where knowledge in nanosciences is applied to biological materials allowing investigation of biological processes at the molecular level. The present research is devoted to the search of the appropriate nanomaterials, which could be used as luminescent markers for tracing of processes occurring in biomaterials. Doped AlN nanopowders (NP) were chosen as prospective candidates for realization of this task. This chose is based on the following considerations about material properties: *i)* possible low toxicity; *ii)* intensive and controllable luminescence within a convenient spectral region; *iii)* low cost of raw materials for nanostructure synthesis and accessible simple synthesis methods.

The aim of the present report is research of spectral properties of AlN doped with Tb and Mn in order to reveal their luminescence features. For this purpose doped AlN nanopowders: AlN:Tb and AlN:Mn with grain diameter of d ≈ 60 nm were used. Photoluminescence (PL) spectra and luminescence excitation (PLE) spectra were studied within a wide spectral region at room temperature (RT).

It was found that in both AlN nanopowder doped with Tb and Mn a strong luminescence with controllable intensity appears at 550 nm and ≈600 nm (Fig. 1), correspondingly, which can be excited with ultraviolet light using 263 nm laser. Besides, for luminescence of Tb ions so- called luminescence up-conversion also is known allowing use of light with lower energy for material excitation than that, which is necessary for Tb direct excitation.

In summary, we can conclude that luminescent AlN:Tb and AlN:Mn nanopowders are prospective materials for application as markers for biological materials.

This investigation is sponsored from the International Project Horizon -2020–MSCA–RISE- 2015; Proposal Nr. 690853; acronym – assymcurv.

High-frequency magnetic resonance study of non-Kramers Tb^{3+} ions in yttrium aluminum garnet crystals

R.A. Babunts [1], A.G. Badalyan [1], E.V. Edinach [1,*], A.S. Gurin [1], Yu.A. Uspenskaya [1], H.R. Asatryan [1], A.G. Petrosyan [2], N.G. Romanov [1], P.G. Baranov [1]

[1] *Ioffe Institute, St. Petersburg, 194021, Russia*
[2] *Institute for Physical Research, National Academy of Sciences of Armenia, Ashtarak-2, 0203, Armenia*

High-frequency (94 and 130 GHz) electron paramagnetic resonance (EPR), electron spin echo (ESE) and optically detected magnetic resonance (ODMR) of non-Kramers Tb^{3+} ions in yttrium aluminum garnet (YAG) crystals have been found and investigated in the temperature range 1.5 to 40 K.

In this study, we used an EPR-ODMR spectrometer developed at the Ioffe Institute. It is based on especially designed microwave bridges that provide high microwave power, extreme stability and sensitive super-heterodyne detection system. The spectrometer operates both in continuous wave (cw) and ESE modes. It allows measurements in a very broad range of magnetic fields (up to 7 T) and temperature (1.5 to 300 K) due to a closed circle magneto-optical cryostat. We investigated cerium and gadolinium co-doped $Y_3Al_5O_{12}$ crystals grown from the melt by vertical directed crystallization. Tb was found in these crystals as a contaminating impurity.

The cw EPR spectra of Tb^{3+} in YAG measured at 94 and 130 GHz at T = 5 K are shown in the figure together with the energy levels in magnetic field and EPR transitions. The electron configuration of the Tb^{3+} ion is $4f^8$ and the ground state of the free ion is $^7F_6$. The effective spin of the ground state is $S^*=1/2$, and the nuclear spin $I = 3/2$ arises from the 100% abundant Tb^{159} isotope. The observed spectra can be described using spin Hamiltonian $H=g_{||}\mu_B cos\theta S_z+\Delta_x S_x+\Delta_y S_y+AS_zI_z$ with the parameters: $g_{||} = 15.8$, $\Delta = (\Delta_x^2+\Delta_y^2)^{1/2} = =2.705$ cm^{-1}, and $A = 0.197$ cm^{-1}.

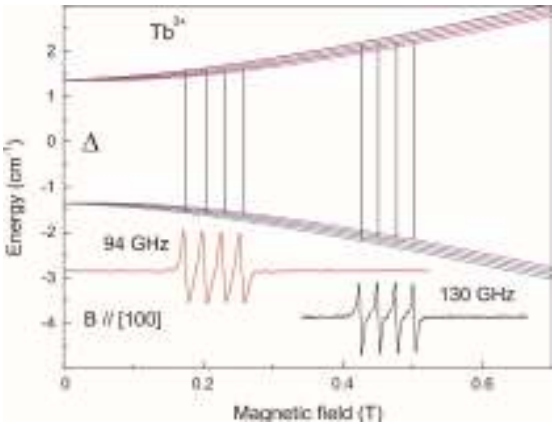

Recently ODMR of Gd^{3+} ions has been detected in YAG:Ce,Gd by monitoring the intensity of Ce luminescence that was excited by circularly polarized light [1]. Similarly, we have observed ODMR of Tb^{3+} but cross-relaxation effects that explained ODMR of Gd^{3+} seem not to work in the case of Tb^{3+}.

Weak signals of additional Tb^{3+} centers with slightly larger Δ were found. For one of them $\Delta = 3.1335$ cm^{-1} is very close to the energy of 94 GHz microwave quanta and strong ESE-detected EPR was observed near zero magnetic field.

This work has been supported by the Ministry of Education and Science of Russia under agreements #14.604.21.0200, RFMEFI60417X0200.

[1] D.O. Tolmachev, A.S. Gurin, Yu.A. Uspenskaya et al. *Phys. Rev.* B **95**, 224414 (2017).

OH^- Defects in Transition Metal Ion Doped Stoichiometric $LiNbO_3$

László Kovács*, Laura Kocsor, Éva Tichy-Rács, Krisztián Lengyel, László Bencs and Gábor Corradi

Institute for Solid State Physics and Optics, Wigner Research Centre for Physics, Hungarian Academy of Sciences, Konkoly-Thege Miklós út 29-33, 1121 Budapest, Hungary
**Corresponding author*

Transition metal dopants (Fe, Cr, Ti) play an important role in a number of applications utilizing e.g. the photorefractive and waveguiding properties of lithium niobate ($LiNbO_3$) crystals. The effect of transition metals on optical and related properties strongly depends on the site occupation of the dopants in the $LiNbO_3$ lattice; the incorporation of the dopants has accordingly been widely studied by various chemical and physical methods as well as theoretical modelling.

Infrared absorption spectroscopy of the stretching vibration of hydroxyl ions (OH^-), always present in *as grown* $LiNbO_3$, has proved to be an excellent probe of the defect structure of the crystal. As shown recently, both optical damage resistant (ODR: Mg^{2+}, Zn^{2+}, In^{3+}, Sc^{3+}, Hf^{4+}, Zr^{4+}, Sn^{4+}) and rare earth (RE: Nd^{3+}, Er^{3+}, Yb^{3+}) ions, occupying Nb sites above their photorefractive threshold concentrations, form complexes with a neighboring OH^- ion [1, 2].

In the present work transition metal ion (M: Fe^{3+}, Cr^{3+}, and/or Ti^{4+}) doped stoichiometric $LiNbO_3$ (SLN) crystals have been grown by the high temperature top seeded solution growth and Czochralski methods. In all cases the presence of an $M_{Nb}^{n+} - OH^-$ type complex has been found above the threshold concentration of each dopant. The observed vibrational frequencies of the hydroxyl ions and their polarization dependences agree well with our previous model established for the ODR and RE ions confirming its general validity.

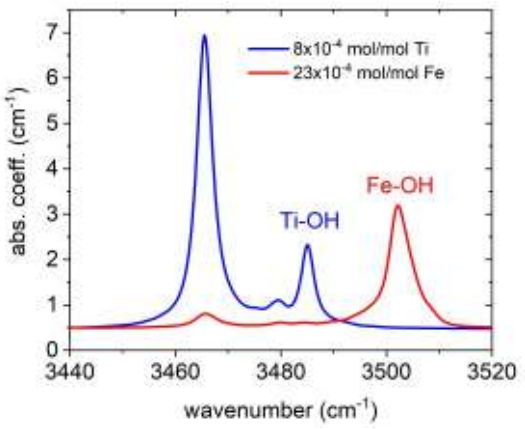

Fig. 1. OH^- spectra of Fe^{3+} and Ti^{4+} doped SLN

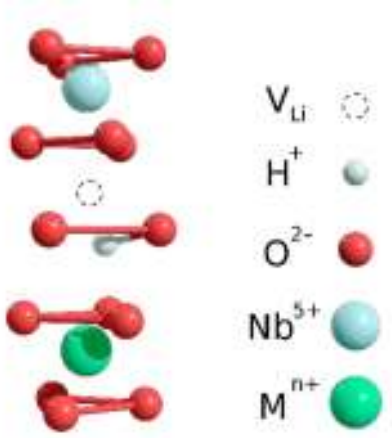

Fig. 2. The model of the $M_{Nb}^{n+} - OH^-$ type defect complex

[1] L. Kovács, Zs. Szaller, K. Lengyel, G. Corradi, *Optical Materials*, **37** (2014) 55-58.
[2] L. Kovács, L. Kocsor, Zs. Szaller, I. Hajdara, G. Dravecz, K. Lengyel, G. Corradi, *Crystals*, **7** (2017) 230/1-9.

Optical Spectroscopy of $Li_6Y(BO_3)_3$ Single Crystals Doped with Praseodymium

Éva Tichy-Rács [1,*], Ivo Romet [2], Krisztián Lengyel [1], László Kovács [1], Vitali Nagirnyi [2], Gábor Corradi [1], Laura Kocsor [1]

[1] *Institute for Solid State Physics and Optics, Wigner Research Centre for Physics, Hungarian Academy of Sciences, Konkoly-Thege út 29-33, 1121 Budapest, Hungary*
[2] *Institute of Physics, University of Tartu, W. Ostwaldi 1, 50411, Tartu, Estonia*
[*] *Corresponding author*

Lithium yttrium borate (LYB) crystal with monoclinic structure having the $P2_1/c$ space group is an excellent nonlinear optical material with wide UV transmittance range. Doped LYB crystals are also good candidates for lasers and for scintillation materials due to the flexibility of the host lattice and the easy incorporation of rare earth dopants at the yttrium sites. Praseodymium doped LYB single crystals have not been studied yet, only an isostructural $Li_6Lu(BO_3)_3$:Pr polycrystalline phosphor has been investigated [1].

In the present work the results of luminescence, Fourier transform infrared and UV/Vis absorption spectroscopic measurements on $Li_6Y(BO_3)_3$ single crystal doped with 10% praseodymium grown by the Czochralski method [2] will be presented.

Electronic transitions of the incorporated Pr^{3+} ions were successfully identified by absorption measurements in the 5000–25000 cm^{-1} wavenumber range and also by luminescence excitation spectra in the 2.3–3 eV range. The effect of crystal-field splitting due to the low symmetry of the crystal was investigated in detail by temperature and polarization dependent absorption and luminescence measurements.

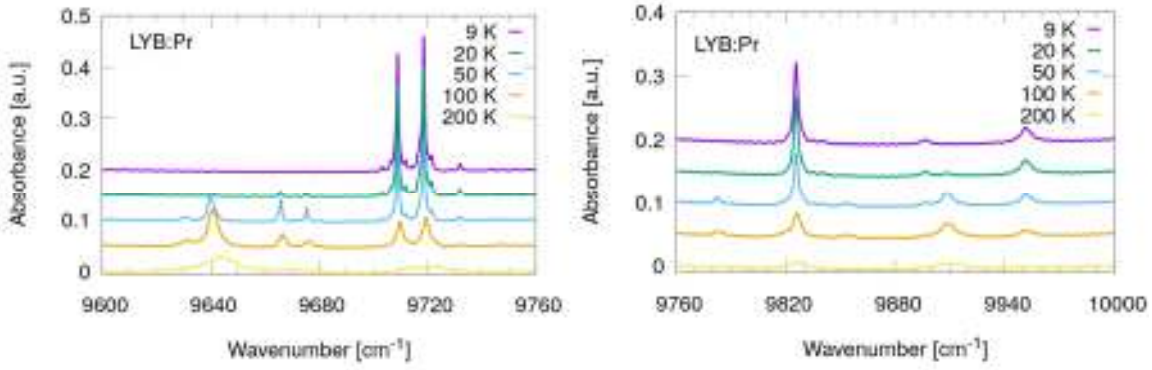

Fig. 1 Temperature dependence of the FTIR absorption spectrum of the Pr^{3+} ion's $^3H_4 \rightarrow {}^1G_4$ electronic transition in the monoclinic $Li_6Y(BO_3)_3$ crystal.

[1] U. Fawad, M. Oh, H. Park and H. J. Kim, S. Kim, *J. Korean Phys. Soc.*, **62**, (2013) 1102
[2] Á. Péter, K. Polgár, M. Tóth, *J. Cryst. Growth* **346** (2012) 69.

Time-resolved Analysis of the NV Centers' Fluorescence Dynamics

Maria Gieysztor [1,*], Mariusz Mrózek [2], Krystian Sycz [2], Andrzej Kruk [2], Wojciech Gawlik [2] and Piotr Kolenderski [1]

[1]*Institute of Physics, Faculty of Physics, Astronomy and Informatics, Nicolaus Copernicus University, Grudziądzka 5, 87-100 Toruń, Poland*
[2]I*nstitute of Physics, Faculty of Physics, Astronomy and Informatics, Jagiellonian University, Reymonta 4, 30-059 Kraków, Poland*
[*]*Corresponding author*

Nitrogen-vacancy (NV) center emerges as an important system exhibiting promising properties for applications in quantum technologies, including quantum information processing, quantum metrology as well as single photon sources. Research on these defects is held since 60's, but the underlying physics is still not fully understood.
In our work, we investigate the dynamics of NV centers excited by pulsed laser (140 fs, 80 MHz repetition rate) tuned over the 417-515 nm range. By means of time-resolved fluorescence measurements we are able to establish the fluorescence decay rate. The experimental setup is shown in Fig. 1. The sample is studied in a home-built confocal microscope. Photon detection is realized by single photon detection modules.

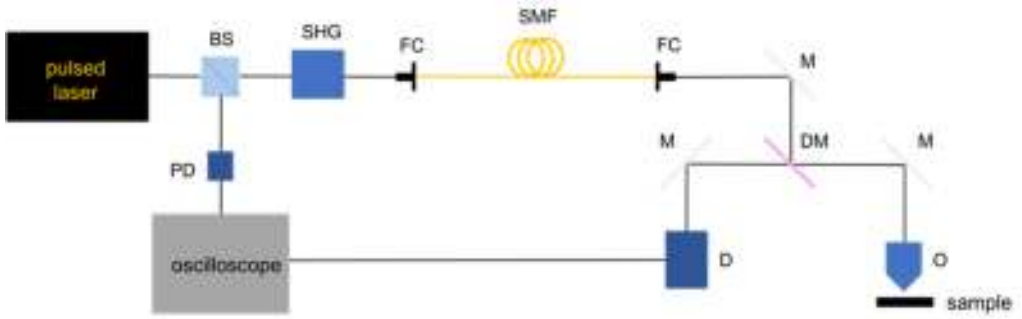

Fig. 1 Experimental setup. BS - beam splitter, SHG - second harmonic generation, FC - fiber coupler, SMF - single mode fiber, M - mirror, DM - dichroic mirror, PD - photodiode, D - detector, O - objective.

As a result, we obtain a histogram of the delay of the single photon detector (D) click with respect to the reference photodiode (PD) signal. To model NV centers' behaviour we use a double-exponential decay model, assuming fast non-radiative decay followed by a radiative one (time constants τ_C and τ_N). A very peculiar wavelength dependence of τ_C and τ_N is observed, as shown in Fig. 2.

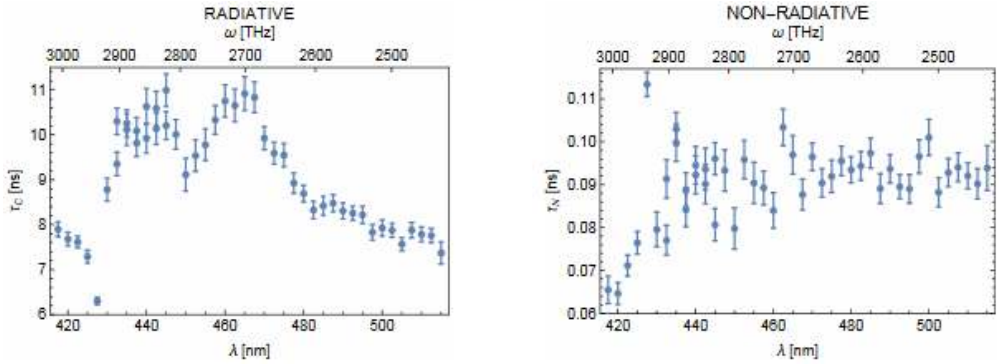

Fig. 2 Radiative and non-radiative decay rates as a function of λ/ω.

Proton uptake and mobility in (Ba,Sr,La)FeO_3 perovskites: DFT results

D. Gryaznov [1], M.F. Hödl [2], R. Merkle [2,*], E.A. Kotomin [1,2] and J. Maier [2]

[1]*Institute of Solid State Physics, University of Latvia, Kengaraga St.,Riga, Latvia.*
[2]*Max Planck Institute for Solid State Research, Heisenbergstr. 1, Stuttgart, Germany*

Protonic ceramic fuel cells (PCFC) based on proton conducting Ba(Ce,Zr,Y)O_{3-x} perovskite electrolytes require cathode materials which exhibit a mixed electronic and protonic conductivity. Protons (present as hydroxide ions on oxide sites $OH_O^\bullet$) can be incorporated either by hydration (dissociative water uptake, filling of oxygen vacancies $V_O^{\bullet\bullet}$)

$$H_2O + V_O^{\bullet\bullet} + O_O^x \rightarrow 2OH_O^\bullet \quad (1)$$

as it occurs also in the electrolyte materials [1], or hydrogen uptake from H_2O at expense of holes $h^\bullet$ in a redox reaction

$$H_2O + 2O_O^x + 2h^\bullet \rightarrow 2OH_O^\bullet + \frac{1}{2}O_2 \quad (2)$$

Thermogravimetry typically yields a significantly lower proton uptake for (Ba,Sr,La)(Fe,Co,Zn,Y)$O_{3-\delta}$ cathode materials compared to Ba(Ce,Zr,Y)O_{3-x} electrolytes [2-4]. These measurements also indicate that the basicity of the oxide ions is a key parameter for the proton uptake. By means of DFT+U and hybrid DFT calculations [5,6] we explore the enthalpy of the hydration reaction (1) for different (Ba,Sr,La)$FeO_{3-\delta}$ perovskites as a function of cation composition, Fe oxidation state and degree of hydration. In these calculations, the identification of the global energy minimum is challenging because of the large number of possible defect configurations (including hydrogen bonding of $OH_O^\bullet$ to neighboring oxide ions) in the supercell. As simplistic relations e.g. with the charge of the oxide ions do not suffice to rationalize the trends of proton uptake, correlations to other materials parameters have to be derived. Proton migration barriers are calculated and compared to those in Ba(Ce,Zr,Y)O_{3-x} electrolytes.

[1] K. D. Kreuer, *Ann. Rev. Mater. Res*. **33** (2003) 333.
[2] D. Poetzsch, R. Merkle, and J. Maier, *Farad. Discuss.* **182** (2015) 129.
[3] R. Zohourian, R. Merkle, and J. Maier, *Solid State Ionics* **299** (2017) 64.
[4] R. Zohourian, R. Merkle, G. Raimondi, and J. Maier, *submitted*.
[5] D. Gryaznov, R. Merkle, E. A. Kotomin, and J. Maier, *J. Mater. Chem. A* **4** (2016) 13093.
[6] M. F. Hödl, R. Merkle, E. A. Kotomin, and J. Maier, *in preparation*.

Photoluminescence of Single-Walled Carbon Nanotube Thin Films

A. Zawadzka [1], P. Płóciennik [1] and P. Szroeder [2,*]

[1]*Department of Automatic and Measurement Systems, Faculty of Physics, Astronomy and Informatics, Nicolaus Copernicus University, Grudziądzka 5, 87-100 Torun, Poland*
[2]*Institute of Physics, Kazimierz Wielki University, Powstańców Wielkopolskich 2, 85-090 Bydgoszcz, Poland*
[*]*Corresponding author*

A growing number of nanomaterials including carbon allotropes have been shown to possess remarkable optical properties [1-3]. Particularly, the carbon allotropes discovered in recent decades are the most representative products of nanotechnology: from carbon nanoparticles (graphite) or fullerenes to carbon nanotubes (CNTs) and then to graphene discovered most recently. Recent development of carbon nanotubes has opened up a whole new field of research opportunities in materials science, solid state physics and optics.

This work contains investigation results of the structural and optical properties of thin films containing single-walled carbon nanotubes (SWCNTs). To investigate the optical properties 0.25, 0.5 and 1 mg of SWCNTs were dispersed in low concentration aqueous SDS solution. These solutions were used to fabricate thin films. The films were successfully grown by spin-coating technique in ambient atmosphere on transparent and semiconductor substrates. Spectral properties of thin films were examined using Transmission and Photoluminescence techniques.

Photoluminescence spectra (PL) of the SWCNT thin film on silicon wafer recorded at 325K are shown in Fig.1. PL spectra were measured in the wavelength range from 350nm to 900nm. The highest intensity of the photoluminescence was observed for the thin films prepared from the solution containing 1mg SWCNTs (the highest concentration). PL intensities for other (lower) concentrations were significantly lower at the room temperature. Photoluminescence spectra showed asymmetrical shape regardless the concentration but for the higher concentration typical sharp maxima started to appear. Decay time of photoluminescence showed two exponential character with the values equal to <1ns and tens of nanoseconds.

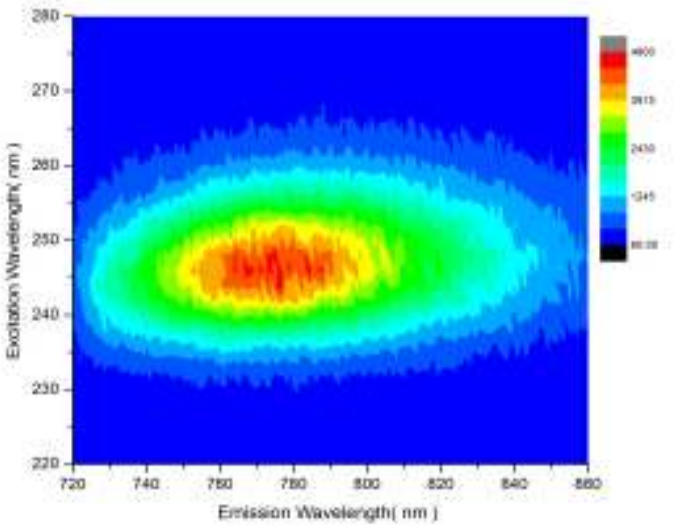

Fig.1. Photoluminescence spectra of thin film containing MWCNTs.

[1] H. Kataura, Y. Kumazawa, Y. Maniwa, I. Umezu, S. Suzuki, Y. Ohtsuka, Y. Achiba, *Synthetic Metals*, **103** (1999) 2555.
[2] G. Y. Guo, K. C. Chu, D.-S. Wang, C.-G. Duan, *Phys. Rev. B* **69** (2004) 205416.
[3] A. Zawadzka, P. Płóciennik, P. Szroeder, A. Korcala, B. Kulyk, B. Sahraoui, *IEEE ICTON* (2016) Electronic ISSN: **2161-2064**, DOI: 10.1109/ICTON.2016.7550394

Eu^{3+} multicenter formation and luminescent properties of $Ca_3Sc_2Si_3O_{12}$:Eu and $Ca_2YScMgSiO_{12}$:Eu single crystalline films

V. Gorbenko [1], T. Zorenko [1], K. Paprocki [1], A.M. Kaczmarek [2,*], R.Van Deun [2], Yu. Zorenko [1*]

[1] *Institute of Physics, Kazimierz Wielki University in Bydgoszcz, 85-090 Bydgoszcz, Poland*
[2] *L^3– Luminescent Lanthanide Lab, Department of Chemistry, Ghent University, Ghent, Belgium*
[*] *corresponding authors: anna.kaczmarek@ugent.be, zorenko@ukw.edu.pl*

Red emitting Eu^{3+} doped luminescent materials in the different crystalline forms are widely used in many types of light sources such as LED and plasma screens, fluorescent lamps and markers as well as the cathodoluminescent and scintillating screens. Nowadays, a new class of Ce^{3+} and Eu^{3+} doped garnet phosphors based on the $A_3B_2C_3O_{12}$ (A= Ca, R= Y, Lu; B= Mg, Sc, Al, Ga; C= Ga, Al, Si) silicate garnets is proposed for creation of high-power white LEDs and other optoelectronic applications.

In this work, we report of the first results on the growth and luminescent properties of the Eu^{3+} doped $Ca_3Sc_2Si_3O_{12}$ (CSSG) and $Ca_2YScMgSiO_{12}$ (CYMSSG) single crystalline films (SCFs) by the liquid phase epitaxy method from the melt-solution PbO-B_2O_3 flux onto $Gd_3Ga_{2.5}Al_{2.5}O_{12}$ and $Y_3Al_5O_{12}$ (YAG) substrates with a SCF/substrate misfit of 0.2 and 1.3%, respectively. The Eu_2O_3 content in the melt was 1mole %. The structural quality of the SCFs was investigated using X-ray diffraction. The optical and scintillation properties CSSG:Eu and CYMSSG:Eu SCFs were studied using the absorption, cathode- and photoluminescence (PL) spectra as well as the light yield and scintillation decay kinetics measurements under α–particles excitation in comparison with the reference YAG:Eu SCF counterpart.

The normalized PL spectra of the CSSG:Eu and CYMSSG:Eu SCFs (Fig.1) are caused by the $^5D_0 \rightarrow {}^7F_{1\text{-}4}$ transitions of Eu^{3+} ions but the relative intensity of the respective bands strongly depends on the garnet host. *No sign of the Eu^{2+} luminescence was found in the emission spectra of these SCFs*. The notable differences in the luminescent properties of CSSG:Eu and CYMSSG:Eu SCFs were found. The differences in the emission spectra of CSSG:Eu and CYMSSG:Eu SCFs are caused by *the Eu^{3+} multicenter formation* in the both garnets due to the different local surrounding of Eu^{3+} ions in the dodecahedral positions by the non-isovalent Sc^{3+}/Mg^{2+} and Si^{4+} cations in the octahedral and tetrahedral positions of garnet hosts, respectively. In CYMSSG:Eu garnet the Eu^{3+} multicenter formation is stimulated also by the localization of Eu^{3+} ions in the dodecahedral sites of both Ca^{3+} and Y^{3+} cations. The formation of different Eu^{3+} centers results in the various dominant Eu^{3+} emission transitions (Fig.1) and their luminescent decay kinetics under excitation at different wavelengths. Such phenomenon is also responsible for the different color coordinates of emission CSSG:Eu and CYMSSG:Eu SCFs under e-beam excitation.

The influence of high-temperature thermal treatment in the reduction H_2+N_2 atmosphere on the optical properties of CSSG:Eu and CYMSSG:Eu SCFs was investigated as well.

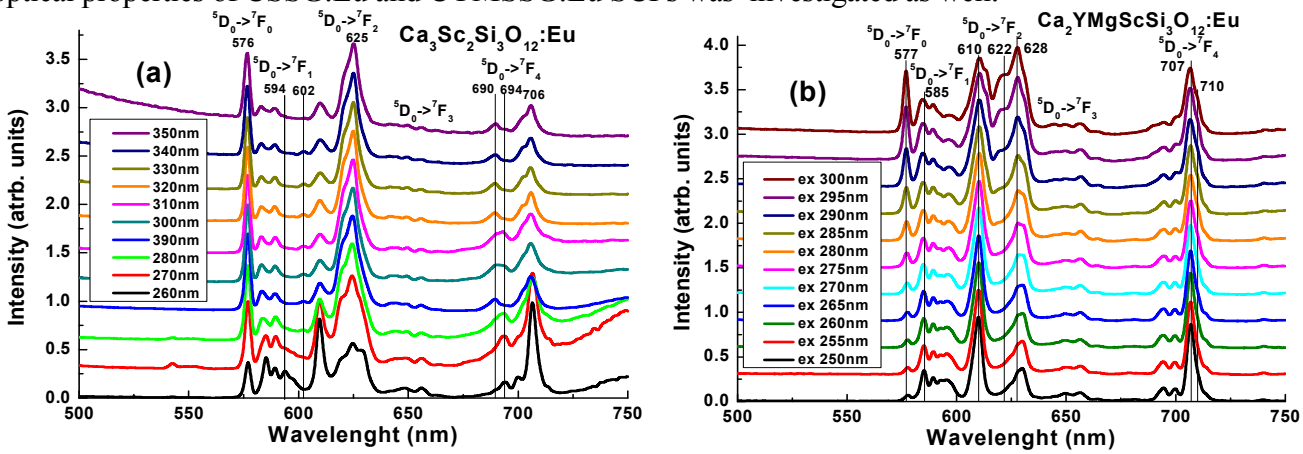

Fig.1 PL spectra of CSSG:Eu and CYMSSG:Eu SCFs at 10K under excitation with different wavelengthes.

Acknowledgments: This work was supported by the Era-Net NANOLUX 2014 #286 project.

Growth and luminescent properties of $Ca_3Sc_2Si_3O_{12}$:Pr and $Ca_2YScMgSiO_{12}$:Pr single crystalline films

V. Gorbenko [1], T. Zorenko [1,*], S. Witkiewicz [1], K. Paprocki [1], Yu. Zorenko [1]

[1] *Institute of Physics, Kazimierz Wielki University in Bydgoszcz, Powstańców Wielkopolskich 2, 85-090 Bydgoszcz, Poland*

[*] *corresponding author: tzorenko@ukw.edu.pl*

The development of luminescent materials based on the single crystalline films (SCFs) of garnet compounds has been stimulated by the possibility of their application as cathode-luminescent and scintillating screens, laser media and in the luminescent thermometry.

The first results on growth of the Pr^{3+} doped $Ca_3Sc_2Si_3O_{12}$ (CSSG) and $Ca_2YScMg\ SiO_{12}$ (CYMSSG) SCFs by the Liquid Phase Epitaxy (LPE) method from the melt-solution $PbO\text{-}B_2O_3$ flux onto $Gd_3Ga_{2.5}Al_{2.5}O_{12}$ (GAGG) and $Y_3Al_5O_{12}$ (YAG) substrates are reported in this work. The Pr_4O_7 concentration in the melt was changed in the 1-5% range. The structural quality of the SCFs was studied using X-ray diffraction. The SCF/substrate misfit was about of 1.3%. The optical and scintillation properties CSSG:Pr and CYMSSG:Pr SCFs were studied using the absorption, cathode- and photoluminescence spectra as well as the light yield (LY) and scintillation decay kinetics measurements under α–particles excitation in comparison with the properties of reference YAG:Pr and LuAG:Pr SCF counterparts (Fig.1).

The notable differences was found in the luminescent properties of CSSG:Pr and CYMSSG:Pr SCFs. The d-f transitions of Pr^{3+} ions in the UV range were observed in the emission spectra of CSSG:Pr whereas in the spectra of CYMSSG:Pr this luminescence is practically quenched. Such conclusion is confirmed by the study of the threshold of temperature quenching of Pr^{3+} emission decay kinetics in CYMSSG:Pr SCF. The emission bands in the 387-395 range in the spectra both SCFs are caused by the luminescence of F centers in the CSSG:Pr and CYMSSG:Pr hosts.

The f-f transitions of Pr^{3+} ions in the visible ranges dominate in the spectra of SCFs of both garnets (Fig.1). In Pr-Ce doped CSSG:Pr SCF the visible luminescence of both Ce^{3+} and Pr^{3+} ions is observed. Meanwhile, the differences in the emission spectra in the range of Pr^{3+} f-f transitions in CSSG:Pr and CYMSSG:Pr SCFs are caused by the ***Pr^{3+} multicenter formation*** on the last garnet due to the localization of Pr^{3+} ions in the dodecahedral sites of Ca^{3+} and Y^{3+} cations and different local surrounding of these positions by the non-isovalent Sc^{3+}/Mg^{2+} and Si^{4+} cations in the octahedral and tetrahedral positions of the garnet hosts, respectively.

The influence of high-temperature thermal treatment in the reduction H_2+N_2 atmosphere on the optical properties of CSSG:Pr and CYMSSG:Pr SCFs was investigated as well.

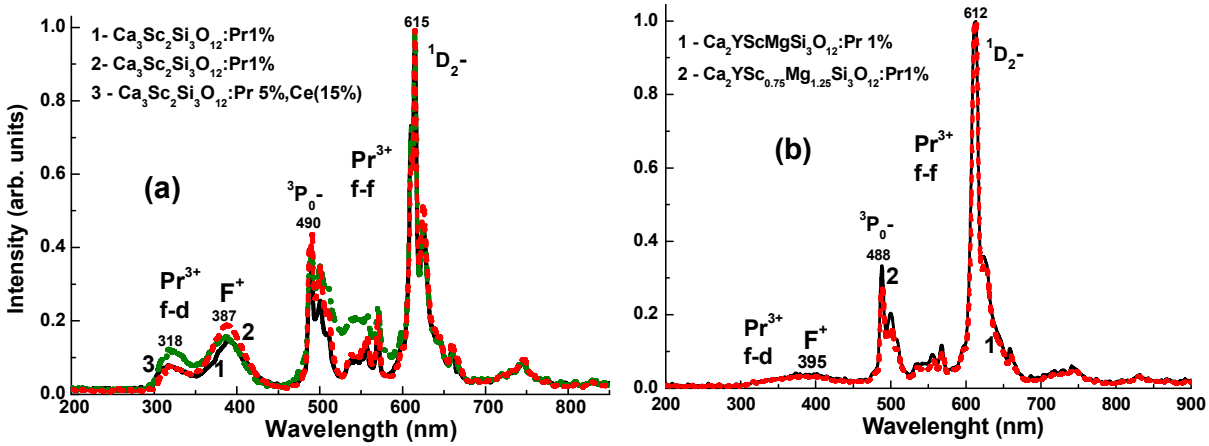

Fig.1 CL spectra of CSSG:Pr (1, 2) and CSSG:Pr,Ce (3) SCFs (a) and CYMSSG:Pr SCF at 300 K

*Acknowledgments***.** This work was supported by the Era-Net NANOLUX 2014 #286 project.

Luminescent properties of $Ca_3Sc_2Si_3O_{12}$:Mn and $Ca_2YScMgSiO_{12}$:Mn single crystalline films

V. Gorbenko [1], T. Zorenko [1], K. Paprocki [1], S. Witkiewicz-Łukaszek [1*], Yu. Zorenko [1]

[1]Institute of Physics, Kazimierz Wielki University in Bydgoszcz, 85-090 Bydgoszcz, Poland
[*]corresponding authors: s-witkiewicz@wp.pl

Rare-earth and transition metal doped $A_3B_2C_3O_{12}$ (A= Ca, R= Y, Lu; B= Mg, Sc, Al, Ga; C= Ga, Al, Si) silicate garnets are considered now as perspective matrixes for creation of phosphors for high-power white LEDs and other optoelectronic applications. In this work, we report the first results on the luminescent properties of the singly Mn^{2+} doped and doubly Mn^{2+} and Ce^{3+} doped $Ca_3Sc_2Si_3O_{12}$ (CSSG) and $Ca_2YScMgSiO_{12}$ (CYMSSG) single crystalline films (SCF) growth by the liquid phase epitaxy method from the melt-solution PbO-B_2O_3 flux onto $Gd_3Ga_{2.5}Al_{2.5}O_{12}$ and $Y_3Al_5O_{12}$ substrates with a SCF/substrate misfit of 0.2 and 1.3%, respectively. The content MnO_2 and CeO_2 activating oxide in the melt was 1 and 15 mole %. The structural quality of the SCFs was investigated using X-ray diffraction. The optical and scintillation properties of Mn^{2+} and Ce^{3+} doped CSSG:Mn and CYMSSG:Mn SCFs were studied using the absorption, cathode- and photoluminescence as well as the light yield and scintillation decay kinetics measurements under α–particles excitation in comparison with the reference YAG:Mn and TbAG:Mn SCF counterparts.

Mn ions can incorporate in the oxides in the different valence states (4+, 3+ and 2+) depending on the condition of their preparation. We have found that the Mn ions in CSSG and CYMSSG SCFs are incorporated mainly in the Mn^{2+} state and emit in the 587 nm and 575 nm bands, respectively. The weak luminescence of Mn^{3+} ions in the 685 nm band is observed also in the spectra of CYMSSG:Mn SCF (Fig. 3). Meanwhile, the notable differences were found in the luminescent properties of CSSG:Mn and CYMSSG:Mn SCFs. The luminescence of Mn^{2+} ions is dominate in the emission spectra of CYMSSG:Mn SCF (Fig.1a) whereas in the spectra of CSSG:Mn SCF (Fig.1b) this emission is very weak. In CSSG:Mn,Ce SCFs the luminescence of Mn^{2+} ions is practically quenched and the Ce^{3+} ion emission dominates (Fig.1a). Meanwhile, adding Y ions leads to significant increasing the Mn^{2+} luminescence in to $Ca_{2.5}Y_{0.5}Sc_{0.5}Mg_{0.5}Si_3O_{12}$ SCF (Fig.1a). Therefore, the Mn^{2+} ions have a tendency to be localized in the Y^{3+} sites of garnet host. The emission bands peaked in the 320-342 nm and 389-397 ranges in the spectra of both SCFs are caused by the luminescence of F^+ and F centers in the CSSG and CYMSSG hosts.

The influence of high-temperature thermal treatment in the air and reduction H_2+N_2 atmospheres on the optical properties of CSSG:Mn and CYMSSG:Mn SCFs was investigated as well.

Concluding, the double Ce^{3+} and Mn^{2+} doped CYMSSG:Mn garnet can be considered as useful material for the creation of film-substrate convectors of white LEDs. Singly Mn^{2+} doped CYMSSG garnet can be considered also as efficient luminescent material with emission in the orange-red range.

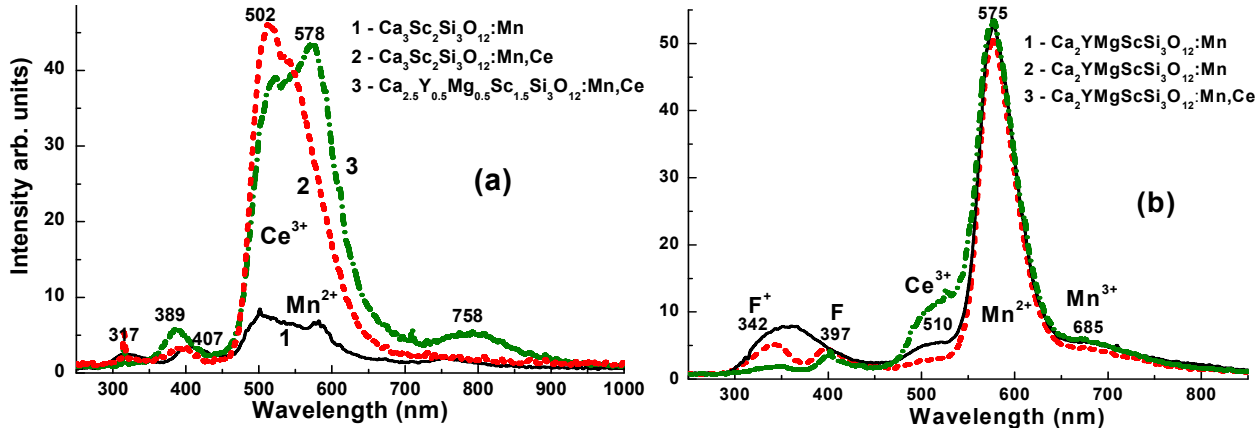

Fig.1 CL spectra of CSSG:Mn (1a), and CSSG:Mn,Ce (2a), $Ca_{2.5}Y_{2.5}Mg_{0.5}Sc_{1.5}Si_3O_{12}$:Mn,Ce (3) and CYMSSG:Mn (1b), CYMSSG:Mn (2b) and CYMSSG:Mn,Ce (3b) SCFs at RT.

Acknowledgments. This work was supported by Era-Net NANOLUX 2014 #286 project.

Lithiation Induced Structural Changes in Layered-Spinel Bulk and Nanoporous Li-Mn-O Electrode Materials

Beauty Shibiri*, Raesibe S. Ledwaba, and Phuti E. Ngoepe

Materials Modelling Centre, School of Physical and Mineral Sciences ,University of Limpopo, Private Bag x 1106, Sovenga, 0727, South Africa

Layered-spinel lithium manganese oxides (LMOs) have become the most desirable cathodes owing to their spontaneously great reversible capacity (302 mAh/g) and superior rate capability [1]. In this study, the simulated amorphization and recrystallization technique [2] has been employed to generate the Li-Mn-O nanoarchitectures. Lithiation of such nanoarchitectures was carried out, with a strategy similar to that used for lithiatingTiO_2 and MnO_2 binary systems [3, 4]. The effect of lithiation on structural integrity of the LMO electrode was investigated under the NVT and NST ensemble to facilitate investigation of structural properties associated with the charge/discharge processes of a lithium ion battery.

Simulations under the NVT ensemble yielded spontaneously crystallized Li-Mn-O composites nanoarchitectures with point defects and grain boundaries. The microstructures and XRD patterns showed formation of spinel and layered components co-existing in the nanostructures. Simulations carried out under the NST ensemble allowed for evaluation of diffusion induced volume changes. Analysis showed that the bulk structure expands when it contains 63% lithium content whilst the nanoporous materials experience no change in volume when containing the same amount of lithiums. When lithium content was increased above 75%, the bulk structure depicted expansion and the nanoporous structured contracted. This may be attributed to flexing of the nanoporous material into its pore/channel when experiencing diffusion induced stress.

[1] Deng Y. P., Fu F., Wu Z. G., Yin Z. W., Zhang T., Li J. T., Huang L. and Sun S.G. , *J. Mat.Chem. A,* vol. **4**, pp. 257-263, 2016.
[2] Sayle T.X.T., Maphanga R.R., Ngoepe P.E. and Sayle D.C., *J. Amer. Chem. Soc.,* vol. **131**, pp. 6162-6123, 2009.
[3] Matshaba M.G., Sayle D.C., Sayle T.X.T. and Ngoepe P.E., *J.Phys.Chem,* vol. **120**, pp. 2-3, 2016.
[4] Maphanga R.R., Sayle D.C., Sayle T.X.T. and Ngoepe P.E., *J.Phys.Chem,* vol. **13**, pp. 1308-1309, 2011.

Luminescent Properties of Undoped and Ce^{3+} Doped $Y_2O_3 – Al_2O_3$ Double System Crystals Prepared by Micro-Pulling Down Method

W. Gieszczyk [1,*], P. Bilski [1], M. Kłosowski [1], Yu. Zorenko [2], T. Zorenko [2], K. Paprocki [2], S. Witkiewicz [2]

[1]*Institute of Nuclear Physics Polish Academy of Sciences (IFJ PAN), Radzikowskiego 152, PL31342 Krakow, Poland*

[2]*Institute of Physics, Kazimierz Wielki University, Weyssenhoffa 11, PL85090 Bydgoszcz, Poland*

[*]*corresponding author: Wojciech.Gieszczyk@ifj.edu.pl*

Three very well-known phases occur in yttrium oxide – aluminum oxide double system. These are particularly garnet ($Y_3Al_5O_{12}$, YAG), perovskite ($YAlO_3$, YAP) and monoclinic ($Y_4Al_2O_9$, YAM) yttrium-aluminum phases. Among them, the perovskite phase single crystals (SC) are of increasing interest due to a large field of their potential applications. Polycrystalline materials based on YAP find a broad range of applications, mainly in optoelectronics. Because of a high reflectivity, a pure YAP can be used as a material optically transparent over a wavelength range from 200 to 1000 nm. Rare earths (RE) doped YAP crystals are considered as good candidates for laser media. Doped with alkali earth's ions and prepared in a reducing atmosphere, YAP crystals show a strong photoluminescence (PL) within a visible range after the exposure to UV radiation. Moreover, Cr doped YAP powders found an application as a new type of red ceramic dyes. The Ce^{3+} doped YAP and $Y_{1-x}Lu_xAP$ bulk crystals are well-known scintillation materials for positron emission tomography. RE doped single crystalline films based on YAP and LuAP think plates of these SCs can be also applied as scintillating screens for visualization of X-ray images with high spatial resolution.

In this work, the undoped and Ce^{3+} doped YAP crystals were grown by the micro-pulling down method at the IFJ PAN, Krakow. Starting materials were prepared by mixing the appropriate oxides in stoichiometric proportions. Mixed perovskite crystals $Y_{1-x}Lu_xAP$ obtained by partial or overall substitution of Y_2O_3 by Lu_2O_3 (x = 0–1) were also investigated. The crystals were grown at the constant growth rate of 0.25 mm/min in the inert gas atmosphere. The obtained crystals had around 3.5 mm diameter and up to several cm length.

Luminescent properties of the obtained crystals were studied by absorption, cathodo-, photo- and thermoluminescence methods (CL, PL and TL, respectively). The scintillation light yield and decay kinetics under excitation by alpha particles sources were also investigated. The TL spectra were measured after the samples irradiation with both beta and alpha particles. It was found that the obtained cerium doped crystals exhibit dominant PL emission bands with maxima at around 380 nm in the centers of crystals, and low-intensive satellite band peaked at 560 nm at the boundaries of crystals, corresponding to the perovskite and garnet phases, respectively. For Y-Lu substituted crystals only the emission band of garnet phase was observed. It tends to suggest that even a small substitution of Y^{3+} ions by Lu^{3+} ions causes a strong suppression of the 380 nm luminescence of the perovskite phase. These and the other obtained results will be discussed in details in the paper.

*Acknowledgements***.** This work is supported by Polish National Science Centre within OPUS 11 program (2017-2020), project No. 2016/21/B/ST8/03200

High-Resolution XRD Study on Selected Czochralski-Grown Rare-Earth Containing Borates and Gallates

A. Sulich [1,*], J.Z. Domagala [1], W. Paszkowicz [1], M. Berkowski [1], A. Shekhovtsov [2], and M. Kosmyna [2]

[1] *Institute of Physics PAS, Al. Lotników 32/46, PL-02-668 Warsaw, Poland*
[2] *Institute for Single Crystals, NASU, Nauki Ave. 60, 61001 Kharkov, Ukraine*
[*] *Corresponding author*

Multicomponent rare-earth containing oxides constitute extended important group of materials, investigated as potential components of optoelectronic devices [1-5]. In the present work, two families of such oxides, $Ca_3RE_2(BO_3)_4$ (RE = Y, Gd) and $La_3Ga_{5,5}Ta_{0,3}O_{14}$:RE (RE = 1% Er, 3% Er), are studied. All these crystals were grown by the Czochralski method.

The main aim of this research was a comprehension of the structural-perfection degree of each single crystal, being of importance for the material development. As an experimental method, a laboratory high-resolution X-ray diffraction with wavelength 1.5406 Å was applied. The values of rocking-curve FWHM's obtained through ω-scans and the character of diffraction patterns (2θ-ω scans) showed a generally good crystal quality and chemical homogeneity of the samples. The reciprocal space mapping provided a detailed information about the nature of defects of the crystal structure. Examples of crystals with a block structure with up to 1 deg misorientation and micromosaics are shown in Fig. 1a and 1b respectively.

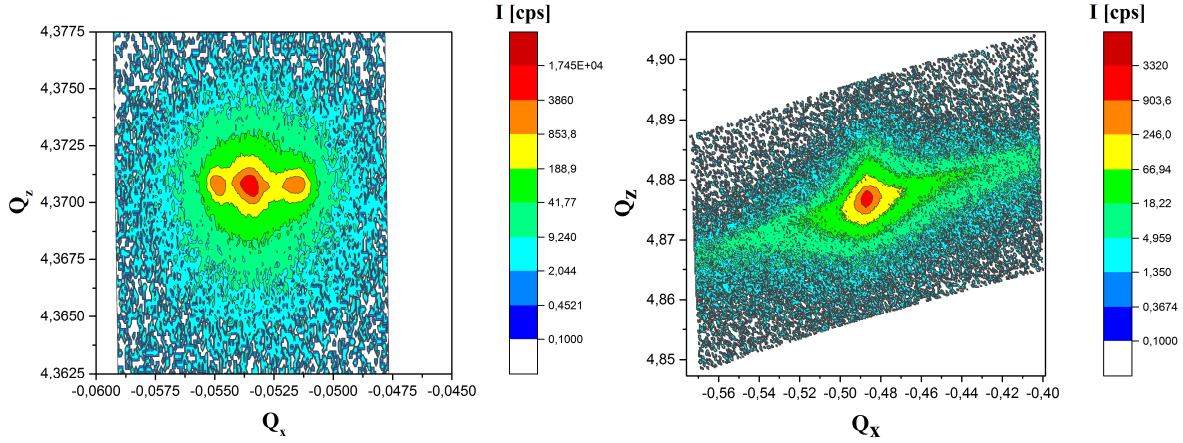

Fig. 1. Reciprocal space maps of (a) $Ca_3Gd_2(BO_3)_4$ + 2% Nd, 006 reflection, (b) $La_3Ga_{5,5}Ta_{0,3}O_{14}$ + 3% Er, 004 reflection.

[1] G. M. Kuz'micheva, E. A. Tyunina, E. N. Domoroshchina, V. B. Rybakov, and A. B. Dubovskii, *Inorg. Mater.* **41** (2005) 412.
[2] Z. B. Pan, H. J. Zhang, H. H. Yu, M. Xu, Y. Y. Zhang, S. Q. Sun, Y.J. Wang, Q. Wang, Z. Y. Wei, and Z. G. Zhang, *Appl. Phys.* **106**, (2012) 197.
[3] F. Yu, X. Duan, S. Zhang, Q. Lu, and X. Zhao, *Crystals* **4** (2014) 241.
[4] L. V. Gudzenko, M. B. Kosmyna, A. N. Shekhovtsov, W. Paszkowicz, A. Sulich, J. Z. Domagała, P. A. Popov, and S. A. Skrobov, *Crystals* **7** (2017) 88.
[5] T. N. Khamaganova, *Russ. Chem. Bull.* **66** (2017) 187.

Preparation of $LiNbO_3$ Nanocrystals and Rare Earth Diffused Layers for Quantum Optical Experiments

Laura Kocsor*, László Péter, Éva Tichy-Rács, Krisztián Lengyel, László Kovács, and Zsolt Kis

Institute for Solid State Physics and Optics, Wigner Research Centre for Physics, Hungarian Academy of Sciences, Konkoly-Thege Miklós út 29-33, 1121 Budapest, Hungary
**Corresponding author*

Rare earth-doped single crystals play an important role in coherent quantum optical experiments. Dopant ions could be useful in single photon sources, which require high level ion selectivity. Two main methods are generally used: doped nanocrystals and surface implantation on bulk crystals.
Nanocrystals are often prepared by ball-milling starting from single crystals. In the case of $LiNbO_3$ a grain size of about 20 nm can be reached by this method [1,2]. A number of methods are known for preparing surface-doped crystals, one of them is high-temperature diffusion. The most common approach is the heat treatment of samples having a thin rare earth metal film on their surface. Diffusion of rare earth ions from either oxides or molten salts containing rare earth ions have also been reported [3-5].
In the present work similar procedures have been used to prepare Yb-doped $LiNbO_3$ nanocrystals and surface-doped $LiNbO_3$. Nanocrystals have been prepared by ball-milling of doped single crystals using different types of vials with various parameters. The samples have been characterised by dynamic light scattering, X-ray diffraction and optical absorption spectroscopy measurements.
We also worked out a simple method to prepare diffused single crystals applying rare earth oxides and salts instead of metal films. In-diffusion was carried out by annealing at 1100°C for 1, 50 and 150 hours. The depth of the diffused layer was measured by Secondary Neutral Mass Spectrometry.

This research was supported by the National Research Development and Innovation Office of Hungary (Project No. 2017-1.2.1-NKP-2017-00001).

[1] S. Indris, D. Bork and P. Heitjans, *J. Mater. Synth. Process.* **8** (2000) 245.
[2] J. R. Schwesyg, H. A. Eggert, K. Buse, E. ĝliwińska, S. Khalil, M. Kaiser, K. Meerholz, *Appl. Phys B* **89** (2007) 15.
[3] I. Baumann, R. Brinkmann, M. Dinand, W. Sohler, L. Beckers, C. Buchal, M. Fleuster, H. Holzbrecher, H. Paulus, K. H. Müller, T. Gog, G. Materlik, O. Witte, H. Stolz, W. Von Der Osten, *Appl. Phys A* **64** (1997) 33.
[4] P. Nekvindová, J. Špirková-Hradilová, J. Schröfel, M. Slunečko, V. PeĜina, J. Vacík, *Proceedings of SPIE* **3858** (1999) 180.
[5] C. Sada, F. Caccavale, F. Segato, B. Allieri, L. E. Depero, *Opt. Mater.* **19** (2002) 23.

Synthesis and Characterization of Hydroxyapatite Nanoparticles Produced via Proteic Sol-Gel Method

Cruz B.M. [1], Janaína A. Peixoto [2], Giordano F. da C. Bispo [1], Zélia S. Macedo [1,2] and Mário E.G. Valerio [1,2,*]

[1]Physics Department, *Federal University of Sergipe, Av. Marechal Rondon, Jardim Rosa Elze, São Cristóvão, Brazil*
[2]*Material Science and Engineering Postgraduation Course*, *Federal University of Sergipe, Av. Marechal Rondon, Jardim Rosa Elze, São Cristóvão, Brazil*

The calcium phosphate ceramics are materials with large biomedical applications (orthopedic, healing bone defects, etc.). Furthermore the phosphates Hydroxyapatite (HAP), with chemical formula $Ca_{10}(PO_4)_6(OH)_2$ and hexagonal structure ($P6_{3/m}$ space group), presents strong similarities with the mineral constituents of the bones and human teeth. HAP has received a great attention due to excellent biocompatibility and osteointegration properties [1-3]. HAP has been synthesized by several methods that influenced the final morphological and structural characteristics of the material. This work has the purpose of investigating the efficiency of a new route, the proteic sol-gel route (PSGP), that employs green coconut water as the main solvent for the precursor salts, instead of conventional metal alkoxides. The influence of temperatures in thermal treatment (600° to 900°C) and the pH of the precursor solution were investigated. The reaction occurred through the mixture of a solution containing $Ca(NO_3)_2{\cdot}4H2O$ (tetrahydrate calcium nitrate) in the solution of $(NH_4)_2HPO_4$ (dibasic ammonium phosphate). The pH was controlled by addition of ammonium hydroxide. The characterization was made by X-Ray powder Diffraction (XRD), Fourier Transformed Infrared (FTIR) spectroscopy and Scanning Electron Microscopy (SEM). The results showed that the pH of the precursor solution and the temperature of the thermal treatment influenced the HAP formation. The apparent crystallite size and the crystallinity degree of the studied samples grew as the temperature increased. The FTIR spectrums confirmed the presence of the expected functional groups associated with the HAP characteristic vibrational modes. The SEM images showed that the HAP particle sizes are in the submicrometric to nanometric ranges and there is a variation of the format of the particles with different pH values of the samples. The mechanical resistance of ceramic bodies and the colorimetry of the samples produced under different conditions were also evaluated to verify possible dental and orthopedic applications.

Acknowledgments: The authors thanks to CNPq for the scholarship grant, FAPITEC and FINEP for the financial support and CMNano-UFS for the SEM analysis.

[1] T. C. Xuan, N. N Trung, and V. H. Pham, *Optik*. **126** (2015) 5019–5021.
[2] G. Gonzalez, C. Costa-Vera, L. J. Borrero, D. Soto, L. Lozada, J. I. Chango, J. C. Diaz, and L. Lascano, *J. of Lumi*. **195** (2018) 385-395.
[3] R. S. Pillai, M. Frasnelli, and V. M. Sglavo, *Ceram. Int.* **44** (2018) 1328-1333.

Persistent photoconductivity in ZnO thin films grown on Si substrate by spin coating method

P. Popielarski*, L. Mosińska, W. Bała, K. Paprocki, Y. Zorenko

Faculty of Mathematics, Physics and Technical Sciences, Kazimierz Wielki University, Powstańców Wielkopolskich 2, 85-090 Bydgoszcz, Poland.
fizyka@ukw.edu.pl, www.fizyka.ukw.edu.pl
**Corresponding author*

Photoluminescence (PL) and photoconductivity(PC) have been studied in ZnO thin films grown by a sipn-coating method on Si and glass substrates. Processes are obtained as a result of ultraviolet (UV) illumination in the air and in a vacuum, which appear as the inducedphotocurrents. Their dependence on UV intensity in the air is explained by a decrease in depth of photoinduced surface depletion caused by oxygen desorption induced by photogenerated holes.

VI. Poster session II

Permanent and irradiation-induced point defects in molybdenum rich $PbMoO_4$ and their participation in charge trapping processes

M. Buryi [1,*], V. Laguta [1], M. Fasoli [2], F. Moretti [2], M. Trubitsyn [3], M. Volnianskii [3], A. Vedda [2], M. Nikl [1]

[1]*Institute of Physics CAS in Prague, Cukrovarnicka 10/112, Prague, Czech Republic*
[2]*Department of Materials Science, University of Milano-Bicocca, Via Cozzi 55, 20125 Milan, Italy*
[3]*Oles' Honchar Dnipropetrovsk National University, prosp. Gagarina 72, Dnipro, 49010, Ukraine*

Scheelite type lead molybdate ($PbMoO_4$) is an eligible candidate for implementation as a detector in the neutrinoless double β decay due to the radioactive ^{100}Mo isotope naturally occurring in the material. It is worth mentioning that, for decades, PMO also found application in acousto-optics and optoelectronics. Point defects creating their own trap states in the bandgap affect significantly the physical properties of the crystal, the luminescence and scintillation, in particular. New ways to avoid or suppress negative consequences of the defects are the focus of an intense exploration. The present work is dedicated to an investigation of the point defects in the lead molybdate single crystal grown from a molybdenum enriched melt.

Single crystals of the molybdenum rich $PbMoO_4$ were studied by electron paramagnetic resonance (EPR) and wavelength resolved thermally stimulated luminescence (TSL) methods. Prior to 420 nm light irradiation, EPR spectra were composed of two clearly resolved signals which were attributed to Mn^{2+} and Bi^{2+}, accidental impurity ions. Light irradiation caused five new EPR signals to appear. A rigorous data analysis has shown them all to originate from Mo^{5+} related electron traps and their spin Hamiltonian parameters have been determined. One of these molybdenum centers has been deduced to be a self-trapped electron similarly to what observed in the nominally pure $PbMoO_4$ [1]. It exhibits low thermal stability, limited to approximately 40 K and its EPR signal decay correlates well with the TSL glow peak at about 40 K. The very good matching between EPR and TSL data allowed to correlate some of the observed TSL glow peaks in the 70-140 K temperature range with the decay of two other EPR signals. The traps undergo first order recombination kinetics. The corresponding trap depths and frequency factors have been determined by applying the partial cleaning procedure and initial rise method. No TSL peaks were detected above 160 K, however, the remaining two EPR signals of the five ones mentioned above disappear completely at approximately 170-180 K. In this case, a charge transfer occurs through Mn^{2+} and Bi^{2+} impurity ions which partly participate in the charge capturing processes.

The TSL and RL emission maxima temperature dependencies are very different: the former exhibits a stepwise red shift from 525 nm at 10 K to 544 nm at 55 K and then from 544 nm at 116 K to 626 nm at 140 K, whereas the latter experiences an opposite and more limited effect, with just 20 nm blue shift in the 10-300 K temperature range. Several spectral components with different thermal stabilities in TSL and RL spectra were supposed to be the origin of this phenomenon.

[1] M. Buryi, V. Laguta, M. Fasoli, F. Moretti, M. Trubitsyn, M. Volnianskii, A. Vedda, M. Nikl, *J. Lumin.* **192** (2017) 767–774.

Growth and luminescence properties of the β- Ga_2O_3 single crystalline films

V. Gorbenko [1,*], Z. Galazka [2], T. Zorenko [1], K. Paprocki [1], S. Witkiewicz [1], Yu. Zorenko [1]

[1] *Institute of Physics, Kazimierz Wielki University in Bydgoszcz, Powstańców Wielkopolskich 2, 85-090 Bydgoszcz, Poland*

[2] *Leibniz Institute for Crystal Growth, Max-Born-Str. 2, 12489 Berlin, Germany*

[*] *corresponding author:* gorbenko@ukw.edu.pl

The possibility of growing high-quality gallium oxide (Ga_2O_3) single crystals (SCs) and single crystalline films (SCFs) has triggered a great interest on this material, as a very promising candidate for applications in new areas such as materials for scintillators and cathodoluminescence screens, in addition to electronic and optoelectronic applications.

The first results on growth of the undoped and doped with Tb^{3+} and Eu^{3+} ions Ga_2O_3 SCFs by the Liquid Phase Epitaxy (LPE) method on Czochralski-grown β-Ga_2O_3 substrates [1] from PbO-B_2O_3 flux are reported in this work. The structural quality of the β-Ga_2O_3 SCF was studied using X-ray diffraction. The optical and scintillation properties of β-Ga_2O_3 SCF were studied using the absorption, cathodoluminescence and photoluminescence spectra as well as the light yield (LY) and scintillation decay kinetics measurements under α–particles excitation in comparison with the properties of reference β-Ga_2O_3 substrates (Fig.1).

Typically SCFs of oxide compounds, grown from PbO based flux, contain Pb^{2+} ions, which act as the emission and trapping centers. Meanwhile, in rare-earth doped SCFs, these ions typically decrease the light yield of dopants. Significant influence of these ions on optical properties in the β-Ga_2O_3 SCFs is shown as well. The emission spectrum of β-Ga_2O_3 SC substrates is caused by the luminescence of localized excitons in the 381-391 nm band and the emission of oxygen vacancies in the 481 nm band (Fig.1a) [2]. Meanwhile, the luminescent properties of nominally undoped β-Ga_2O_3 SCFs are completely different in comparison with their SC counterparts. Namely, the luminescence spectra of Ga_2O_3 SCFs are caused by the emission of Pb^{2+} ions in the 408 nm band, related to the intrinsic $^3P_1 \rightarrow {}^1S_0$ transitions, and in the main visible (VIS) band, peaked at 623 nm, related to the emission of excitons localized around Pb^{2+} ions (Fig.1b). The ratio of intensity in the UV/VIS bands strongly depends on the SCF growth temperature.

The different nature of emission centers determines different scintillation properties of β-Ga_2O_3 substrates and SCFs. Under α–particles excitation from ^{239}Pu sources, the LY of β-Ga_2O_3 substrates and SCFs is equal to 50% and 18-24%, respectively. Scintillation decay kinetics of SCFs is significantly faster with the decay time in the 31-38 ns range than that in the SC counterpart (Fig.1 a) with the decay time in the 210-290 ns range. Due to such different scintillation decay kinetics, the epitaxial structures β-Ga_2O_3 SCF/β-Ga_2O_3 SC in principle can be used for the registration of different components of mixed ionization fluxes, namely α–particles and γ-quanta [3].

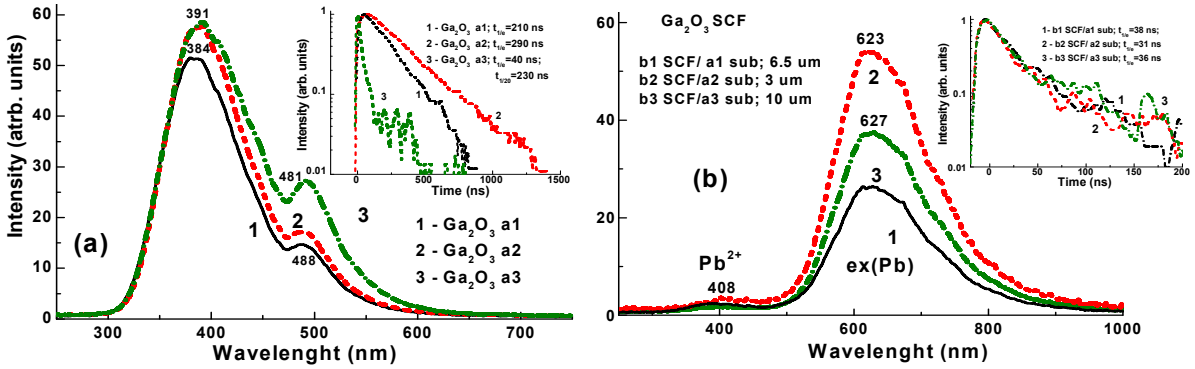

Fig.1 CL spectra of β-Ga_2O_3 substrates (a) and nominally undoped β-Ga_2O_3 SCFs (b), grown on these substrates.

Acknowledgments. This work was supported by the Polish NCN 2016/21/B/ST8/03200 project.

[1] Z. Galazka et al., ECS J. Solid State Sci. Technol. 6 (2017) Q3007-Q3011
[2] T. Yanagida, G. Okada, T. Kato, D. Nakauchi, e. a. Appl. Phys. Express 9 (2016) 042601.
[3] S. Witkiewicz-Lukaszek, V. Gorbenko, T. Zorenko, e. a., Cryst. Growth Des., 2018, Article ASAP

YAG:Ce Codoped with Ho^{3+}:Energy Transfer and Acceleration of Ce^{3+} Decay

Juraj Paterek [1,2,*], Martin Pokorny [1,3], Silviya Valkova [3], Silvia Sykorova [3], Jan Tous [3], Jindrich Houzvicka [3] and Martin Nikl [1]

[1]*Institute of Physics of the Czech Acamedy of Sciences, Cukrovarnicka 10/112, Prague 16200,Czech Republic*
[2]*Faculty of Nuclear Sciences and Physical Engineering, Czech Technical University in Prague, Brehová 7, Prague 16200, Czech Republic*
[3]*Crytur Ltd, Palackeho 175, Turnov 51119, Czech Republic*
[*]*Corresponding author*

Ce3+ activated YAG is a well known luminescent material that found application in many fields ranging from usage in CRTs at its beginning, to recent applications in white light-emitting diodes. Moreover, stable growth of YAG:Ce single crystal, its chemical and mechanical stability, radiation hardness, relatively good light yield and fast decay of Ce3+ makes this material an ideal scintillator suitable for several purposes in radiation detection, particularly in detection of charged particles. Performance of the material is degraded by slow components of lights originated in antisite defects [1, 2].

Modern application, e.g. particle detection in high energy physics or medical imaging, require very fast response and 60 ns decay of Ce3+ in YAG is no more sufficient for such purposes. We present a mechanism that enables further acceleration of inherent decay of the activator. The method is based on creating additional deexcitation channel by embedding a proper additional luminescence center into the system. Overlap of emission and absorption spectra of the centers enables a transfer of excitation energy away from Ce3+ by multipolar interaction which leads to higher rate of deexcitation of activator and its faster response.

In this work we report effect of introducing Ho^{3+} into YAG:Ce single crystal on photoluminescence properties with the main focus on acceleration of Ce^{3+} decay. Transfer of excitation energy is enabled through spectral overlap of Ce^{3+} 5d–4f emission and 4f–4f absorption lines of Ho^{3+} and provides a significant acceleration of Ce^{3+} decay (Fig. 1). The data were analyzed using Förster- Dexter model [3] in wide range of Ho^{3+} concentration. The extracted results can be used for precise decay time tailoring of YAG:Ce by Ho^{3+} codoping. Decay time of Ce^{3+} was shortened by 50% when 1-2 at.% of Ho^{3+} were introduced into material.

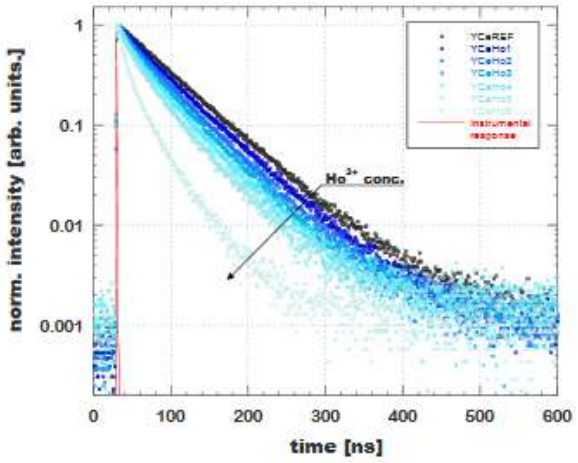

Figure 1: Ce^{3+} decay curve acceleration in dependence on Ho^{3+} concentration.

[1] Z. Xia and A. Meijerink, *Chem. Soc. Rev.* **46** (2017) 275
[2] M. Nikl and A. Yoshikawa, *Adv. Optical Mater.* **3** (2015) 463
[3] D. L. Dexter, *J. Chem. Phys.* **21** (1953) 836

Effect of Ca^{2+} and Si^{4+} co-doping on luminescence and scintillation properties of $Lu_3Al_5O_{12}$: Ce^{3+} epitaxial garnet films

Mamilla Rathaiah [1], Miroslav Kucera [1,*], Alena Beitlerova [2], Martin Nikl [2]

[1]*Charles University, Faculty of Mathematics and Physics, 12116 Prague, Czech Republic*
[2]*Institute of Physics ASCR, Cukrovarnicka 10, 16253 Prague, Czech Republic*
[*]*Corresponding author: kucera@karlov.mff.cuni.cz*

In detecting high energy radiation/particles, the Ce^{3+} doped garnets have been playing vital role due to their high density, broad transmission range, high solubility of active ions and high thermal and chemical stability. Transparent single crystalline films could provide better spatial resolution compared to powder phosphor screens due to eliminating light scattered by phosphor particles [1]. The films with high crystalline perfection are needed where number of impurity ions and defects has to be radically reduced. Liquid phase epitaxial (LPE) technique is a versatile method suitable for the growth of high quality scintillating materials in the form of single-crystalline films on suitable substrate, it is more flexible compared to growth of bulk single crystals by Czochralski or Bridgman methods [2]. The incorporation of divalent Mg^{2+} or Ca^{2+} ions into garnet lattice could alter the point defect structure through the charge compensation mechanism or/and affect the concentration of vacancies. As a consequence, the scintillation performance is directly affected [3].

In this work, a set of Ca^{2+} co-doped $Lu_3Al_5O_{12}$: Ce^{3+} (LuAG: Ce, Ca) epitaxial garnet films with Ca content 0 – 0.6% has been grown by the LPE from BaO-B_2O_3 flux. The optical, photoluminescence (PL), radioluminescence (RL), and PL and scintillation decays have been carried out. At high concentration of Ca^{2+} ions, the Ce^{3+} absorption at 340 and 450 nm has been decreased and completely disappears at Ca 0.6%, conversely the 200-330 nm absorption is increased due to $O^{2-} \rightarrow Ce^{4+}$ charge transfer transition. With increase of Ca co-doping, the PL emission has been quenched due to conversion of Ce^{3+} into Ce^{4+} ions as result of charge compensation, however, upon X-ray excitation the 5d-4f emission has been still observed likely due to participation of intermediate Ce^{4+} state in the scintillation process [3]. The PL and scintillation decay curves exhibit single exponential nature at low Ca-concentration, τ = 56 ns, but with increase of Ca^{2+} content the decays are considerably accelerated to 10 ns. Upon co-doping by Si^{4+} ions or by thermal annealing in reducing atmosphere of LuAG: Ce, Ca films, all the absorption, PL and RL emission, PL and scintillation decays are re-established due to $Ce^{4+} \rightarrow Ce^{3+}$ conversion through charge compensation process. Light yield exhibits strong dependence on Ca^{2+} and Si^{4+} concentrations. The results show that the prepared films could be useful for scintillation applications.

[1] J. M. Robertson and M.W. van Tol, *Thin Solid films* **114** (1984) 221.
[2] M. Kucera, K. Nitsch, M. Nikl, M. Hanus, S. Danis, *J. Cryst. Growth* **312** (2010) 1538.
[3] S. Liu, X. Feng, Z. Zhou, M. Nikl, Y. Shi, Y. Pan, *Phys. Status Solidi RRL* **8** (2014) 105.

Fabrication and Characterization of UV cured Polyvinyl Toluene based Plastic Scintillator for 3D Printing Applications

Sunghwan Kim [1,*], and Youl-Hun Seoung [2]

[1]*Cheongju University, Address1, Cheongju, Korea*
[*]*Corresponding author*

Plastic scintillator is widely used for radiation detection in medical, science, industry applications. It possesses good properties such as tissue equivalence, short decay time, cheap, chemical stability and so on. In general, plastic scintillator is made by thermal polymerization method, which take long time and difficult to produce in complex shape. In this study, we fabricated and characterized a UV-curable plastic scintillator by 3D printing technology. The resin for 3D printing is prepared by ourselves. It used co-polymers vinyl-toluene monomer, PPO (2,5-Diphenyloxazole, SigmaAldrich. Co.), POPOP [1,4-bis(5-phenyloxazol-2-yl) benzene, SigmaAldrich. Co.], and DHPA (dipentaerythritol hexaacrylate, SigmaAldrich. Co.). Irgacure 184 (BASF Co.) is used as photo-initiator. Using DLP 3D printer (http://attosystem.co.kr) and the prepared resin, a cylindrical plastic scintillator is printed. X-ray induced luminescence spectrum of the 3D printed scintillator is measured with an X-ray tube from a DRGEM having a W-anode. For the emission spectrum, QE65000 fiber optic spectrometer (Ocean Optics) is used. Figure 1 shows emission spectrum obtained between 380~480 nm peaking at 430 nm. The observed emission spectrum match well with the quantum efficiency curve of the modern photo-multiplier tubes. Decay time spectrum under gamma excitation is measured by using 400 MHz flash analog to digital converter. Signals from the PMT are fed directly into a 400 MHz FADC which is located in a VME (versa module eurocard) crate and read out by the Linux-operating personal computer through the VME-USB2 (universal serial bus) interface with a maximum data transfer rate of 10 Mbytes/s. The DAQ (data acquisition) system and the analysis program are written in the framework of the ROOT package. Decay time of the plastic scintillation is found to be ~15 ns.

Acknowledgments: These investigations have been supported by National Research Foundation of Korea (NRF) funded by the Ministry of Science and Technology, Korea (MEST) (No. 2016M2A2A6A03946565).

[1] M. Watanabe, M. Katsumata, H. Ono, et. al., *Nucl. Instr. Meth. in Phys.,* **770** (2015) 197.
[2] Jun Zhu, Yunyu Ding, Jiayi Zhu et. al., *Nucl. Instr. Meth. in Phys.,* **817** (2016) 30.
[3] Y. Mishnayot, M. Layani, I. Cooperstein, et. al., *Rev. Sci. Instrum.*, **85** (2014) 1.
[4] V. N. Salimgareeva, S. V. Kolesov, *Instr. Exp. Tech.,* **48** (2005) 273.

Structural and Electronic Properties of β-$NaYF_4$ and β-$NaYF_4$:Ce^{3+}

A. Platonenko [1*], A.I. Popov [1]

[1] *Institute of Solid State Physics, Kengaraga st. 8, Riga, Latvia*

Hexagonal $NaYF_4$ doped with rare-earth ions is one of the most popular up-conversion phosphor materials [1,2]. Due to low phonon energy and multisite structure, it has high luminescence efficiency [3], and also is considered as a potential material for scintillators. Disordered structure, where some lattice positions are occupied by either Na or Y atoms, makes theoretical computations of this material very complicated, thus only a few computational studies were published so far [4,5].

We present simulations on hexagonal β-$NaYF_4$ using density functional theory (DFT) approach combined with the linear combination of atomic orbitals (LCAO) as implemented in CRYSTAL14 computer code. Three possible space groups of this compound were discussed in literature: P-6, $P6_3/m$ and P-62m. Firstly, we have modelled disordered crystal structure of $NaYF_4$ within a large supercell containing 108 atoms. To get better agreement with experimental data, we tested different exchange-correlation functionals. Basic properties, such as lattice constant, band gap and total energies were calculated and compared for all three space groups and three exchange-correlation functionals-HSE06, PWGGA and PWGGA+13%HF. It was found that for all three functionals, the minimum of total energy corresponds to P-6 space group.

In the second part of our study, we have simulated P-6 β-$NaYF_4$, with introduced fluorine vacancies and $Ce_{Y/Na}^{3+}$ substitute ion, or both together. Several types of fluorine vacancies were simulated, taking into account that fluorine atoms have different nearest neighbours, which can result in rather different properties and formation energies of vacancy. For successful treatment of Ce^{3+} in β-$NaYF_4$, we performed a series of calculations, where Ce^{3+} ion was substituting Y or Na atom in different positions. The obtained structures were used for further calculations, where nearest to Ce^{3+} fluorine atom was removed, to simulate vacancy. For all defects, formation and incorporation energies were calculated.

[1] F. Wang, X. Liu, *Chem. Soc. Rev.*, **38** (2009) 976
[2] A. Sarakovskis, G. Krieke, *J. Eur. Ceram. Soc*. **35** (2015) 3665
[3] N. Menyuk, K. Dwight, and F. Pinaud, *Appl. Phys. Lett*. **21** (1972) 159
[4] B. Szefczyk, R. Roszak, and S. Roszak, *RSC Adv.* **4** (2014) 22526
[5] G. Yao, M. T. Berry, P. S. May, D. S. Kilin, *Int. J. Quantum Chem*, **112** (2012) 3889

Materials Theory and Informatics for the Discovery and Optimization of New Radiation Detector Materials

Ghanshyam Pilania [1,*], Martin Nikl [2], Christopher R. Stanek [1] and Blas P. Uberuaga [1]

[1] *Los Alamos National Laboratory, Los Alamos, NM 87545, USA*
[2] *Institute of Physics, Academy of Sciences of The Czech Republic, Cukrovarnicka 10, 16200 Prague 6, Czech Republic*
[*] *Corresponding author*

Historically, new radiation detector materials have been developed through Edisonian trialand-error, which is resource intensive and requires about a decade from discovery to deployment [1,2]. This process can be considerably expedited if we can effectively learn from past knowledge via employing state-of-the-art materials informatics techniques. This poster will highlight a unique co-design process to discover novel scintillator detector materials with a pre-specified property-portfolio. Our innovative strategy enables both rapid screening and subsequent optimization of detector materials while maintaining a close coupling between theory, simulation, experiments and physics-based machine learning. Promise of our approach has been demonstrated through preliminary proof-of-concept applications on garnets, perovskites and elpasolites with promising results [3,4].

[1] P. A. Rodnyi, Physical Processes in *Inorganic Scintillators* (CRC Press, Boca Raton, 1997).
[2] M. Nikl, A. Yoshikawa, K. Kamada, K. Nejezchleb, C.R. Stanek, J. A. Mares, K. Blazek, *Prog. Cryst. Growth Charact. Mater*. **59** (2013) 47.
[3] G. Pilania, S. K. Yadav, M. Nikl, B. P. Uberuaga, and C. R. Stanek, submitted to *Phys. Rev. Applied* (2018) under review.
[4] G. Pilania, K. J. McClellan, C. R. Stanek, and B. P. Uberuaga, submitted to *J. of Chem. Phys*. (2018) under review.

Simulation of Structural Evolution and Ion Diffusion in Li_xTiO_2 Nanosheet

Blessing N. Rikhotso [1,*], Malili G. Matshaba [1], Sayle D.C. [2] and Phuti E. Ngoepe [1]

[1]University of Limpopo, Materials Modelling Centre, Private Bag X 1106, Sovenga, 0727, South Africa

[2] University of Kent, School of Physical Sciences, Canterbury, Kent, CT2 7NZ, United Kingdom

**nkatekoblesing@gmail.com*

Nano-architectured Li_xTiO_2 are promising as anode materials for lithium rechargeable batteries due to their ability to accommodate more lithium atoms and their ability to withstand high temperatures at atomistic level during charging and discharging [1]. In the current study, we investigated how the nanosheet of Li_xTiO_2 (x = 0.03, 0.04 and 0.07) behave at high temperatures through the amorphisation and recrystallization method [2]. Recrystallisation of nanosheets, from amorphous precursors, was achieved and was followed by the cooling process towards 0K. Finally the nano-sheets were heated at temperature intervals of 100 K up to 1500 K. The variation of configuration energies with time, served as an indicators of the crystal growth of all nanostructures. Calculated Ti-O radial distribution functions, were used to confirm the stability interaction after cooling. Simulated X-Ray Diffraction (XRD) spectra, at low and above high temperatures, showed polymorphic structure in Li_xTiO_2 depicting domains of both rutile and brookite in accord with experiment. Nanosheet microstructures have pure straight and zigzag patterns (figure 1) that are consistent with our XRD patterns at all concentrations of lithium atoms and temperatures. The lithium transport was analysed using diffusion coefficient, calculated as a function of temperature in order to confirm the mobility above the given temperatures. An increase in temperature shows an increase in diffusivity of lithium at all lithium concentrations in nanosheet structuresThus rendering suitable anode material for Li ion batteries since it can withstand such temperatures.

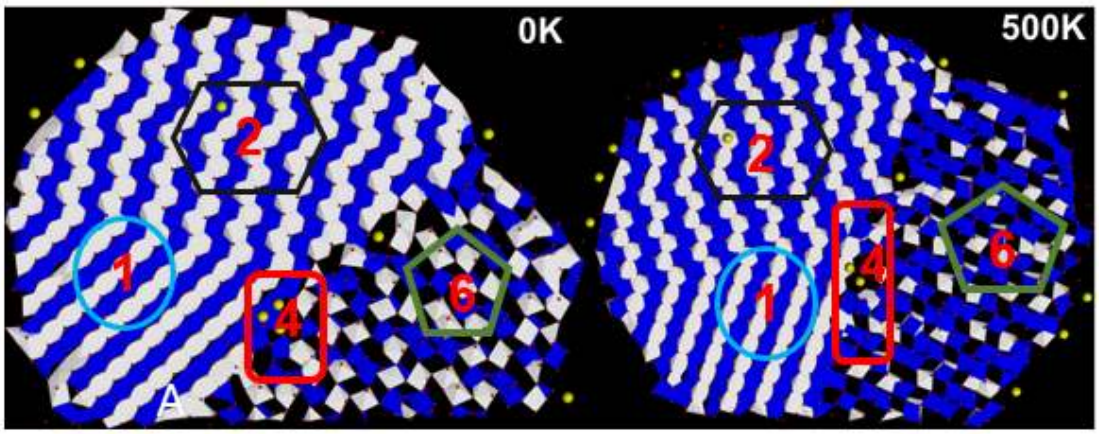

Figure 1: Lithiated snapshots of evolving microstructures of nanosheet ($Li_{0.02}TiO_2$) at 0K and 500K with different types of defects

[1] Bruce, P. G.; Scrosati, B.; Tarascon, J-M. *Angew. Chem. Int. Ed*. **47** (2008) 2930.

[2] Sayle, T.X.T.; Catlow, C.R.A.; Maphanga, R.R.; Ngoepe, P.E, Sayle D.C.; *J. Crys. Growth* **294** (2006) 1198

[3] Matshaba, M.G; Sayle D.C.; Sayle, T.X.T; Ngoepe, P.E, *J. Phys. Chem*. C. **26** (2016) 14001

Identification of antisite defects and transmuted impurities in gallium arsenide (GaAs) irradiated by fission neutrons

Der-Sheng Chao [1,*], Liang J.-H. [2]

[1]*Nuclear Science and Technology Development Center, National Tsing Hua University, Hsinchu 30013, Taiwan, ROC*

[2]*Institute of Nuclear Engineering and Science, National Tsing Hua University, Hsinchu 30013, Taiwan, ROC*

[*]*Corresponding author*

Neutron transmutation doping (NTD) is a useful method to homogeneously generate impurities in semiconductor materials by neutron irradiation in a nuclear reactor. In compound semiconductor GaAs, the isotopes of ^{69}Ga, ^{71}Ga, and ^{75}As can be converted into ^{70}Ge, ^{72}Ge, and ^{76}Se via neutron transmutation reactions, respectively. These transmuted atoms can contribute to donor-type carriers in GaAs crystal, provided that they occupy at proper lattice sites. However, in contrast to the elemental semiconductors such as Si and Ge, the neutron irradiation process would induce the lattice disorder as well as the antisite defects (e.g. Ga_{As}, Ge_{As}, and As_{Ga}) in GaAs due to the original lattice misplacement and the amphoteric Ge element. Since the existence of antisite defects disturbs the carrier activation and limits the effective carrier concentration, it is essential to understand the annealing behavior of antisite defects in the activation process of NTD-GaAs. Therefore, the purpose of this study is to identify the antisite defects and the transmuted impurities in neutron-irradiated GaAs using spectroscopic and electrical characterization methods.

Two kinds of GaAs wafers, i.e. undoped semi-insulating GaAs and Si-doped GaAs (ρ=2.74-4.24 Ω·cm), were employed as starting materials in this study. The NTD neutron irradiation experiments were carried out at the Tsing Hua Open-pool Reactor (THOR) under an operating power of 1.5 MW. After neutron irradiation, the isothermal annealing was performed to anneal the irradiated specimens in N_2 ambient at 300-800 ^{o}C for 1 hour. The neutron-irradiated GaAs specimens were then characterized by means of spectroscopic measurements of EPR, PL, and Raman before and after annealing. The EPR results revealed that the singlet spectrum assigned to gallium vacancies can be observed in NTD-GaAs specimens. From the PL spectra, the characteristic bands corresponding to the Ge_{As} and Ga_{As} antisite acceptors were found in the NTD-GaAs specimens annealed at the temperatures higher than 600 ^{o}C. The Raman spectra also showed a transverse optical (TO) phonon line from the coupled plasma-phonon modes, implying an increase in carrier concentration. Further investigation using Hall effect analyzer is currently in progress to verify the influence of antisite defects on the electrical properties of NTD-GaAs. In addition, the neutron irradiation damage effects on GaAs-based Schottky diodes were also investigated, showing a reduced current level which could be attributed to the variation of Schottky barrier height due to the decrease of carrier concentration in GaAs caused by neutron irradiation.

Radiation induced processes in spinel crystals doped with titanium

Vasyl T. Gritsyna [1,*], Yuriy G. Kazarinov [1,2], Volodymyr A. Kobyakov [1], Zakhar A. Bahniuk [1]

[1] *V.N. Karazin Kharkiv National University, 4, Svoboda Sq., Kharkiv, 61022 Ukraine*
[2] *NRC "Kharkov Institute of Physics and Technology" 1, Akademicheskaya St., Kharkiv, 61108 Ukraine*

The optical properties of non-stoichiometric magnesium aluminates spinel crystals ($MgO{\cdot}2.5Al_2O_3$) doped with titanium dioxide to concentration of 0.2 and 0.5 wt% and subjected to irradiation are investigated. The Verneuil grown boles of dimensions of 10-20 mm in diameter and 20-50 mm in length have non-uniform coloration in bluish. For investigations the boles were cut into slices of 1.5 mm in thickness along the direction of crystal growth and polished to optical finish. As-grown crystals demonstrates two absorption bands at about 800 and 470 nm and in UV range a strong absorption edge arising from 300 nm. Strong absorption in the UV range 200-300 nm has two slightly resolved bands at 215 and 260 nm and band at 280 nm for deeply colored spots.

After irradiation with UV-light and X-rays the absorption in the whole investigated spectral range decreases. There was observed also the temporal transformation of absorption bands in irradiated crystals. Thorough measurements of absorption band around 470 nm allow to disclose some resonance feature which is sensitive to different treatments. As can be seen from Figure for the as-grown crystals we observed antiresonance at wavelength of 477 nm, but annealing transforms into absorption resonance. The subsequent irradiation leads to increase of the resonant absorption peak. Such behavior is characteristic for Fano resonance on the Ti-Fe complexes near native defects creating local mechanical strength.

The spectra of photoluminescence excited at wavelength of 260 nm show wide not elemental blue emission band. The deconvolution of this peak into Gaussians curves reveals the existence of overlapping bands about 465 and 520 nm. The spectra of radio-luminescence measured at excitation by X-rays from (X-ray tube of Cu anode working at voltage of 40 kV and currant 0.4 mA) show the same bands and additional band around 620 nm.

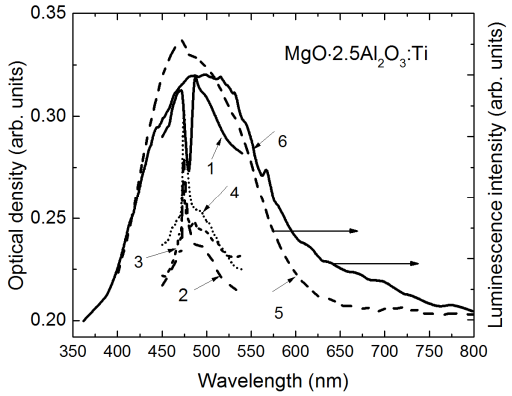

Absorption and luminescence spectra of titanium doped spinel crystals in the vicinity of blue emission band:
1 – absorption of as grown crystal;
2 – annealed to 660 C;
3 – UV-irradiated;
4 – the same X-ray irradiated;
5 – photoluminescence at excitation of 260 nm;
6 – radio-luminescence.

Therefore, we demonstrated the high sensitivity of optical properties of titanium doped spinel crystals to concentration of uncontrolled impurities (particularly, iron) and to different treatment, including irradiation. We speculate that some combination of impurity and doping ions creates the conditions leading to resonant phenomenon of the incident beam, absorption and emission photons at complex defects consisting of Ti-Fe ions and of native defects.

Modelling of photoluminescence from F_2 and F_3^+ colour centres in lithium fluoride irradiated at high doses by low-energy proton beams

Enrico Nichelatti [1,*], Massimo Piccinini [2], Alessandro Ampollini [2], Luigi Picardi [2], Concetta Ronsivalle [2], Francesca Bonfigli [2], Maria Aurora Vincenti [2] and Rosa Maria Montereali [2]

[1] *ENEA C.R. Casaccia, Fusion and Technologies for Nuclear Safety and Security, Via Anguillarese 301, 00123 Rome, Italy*
[2] *ENEA C.R. Frascati, Fusion and Technologies for Nuclear Safety and Security, Via E. Fermi 45, 00044 Frascati (RM), Italy*
[*] *enrico.nichelatti@enea.it*

Lithium fluoride (LiF) crystals and thin films were irradiated with a proton beam at a linear accelerator that is under development at ENEA C.R. Frascati. With nominal beam energies of 3 and 7 MeV, several irradiations were performed which delivered doses ranging from 10^3 to 10^7 Gy. The ionisation induced by the protons in the LiF samples induced the stable formation of point defects, known as colour centres (CCs), in the crystalline lattice. Two types of these CCs, the F_2 and F_3^+ ones, are optically active as they emit visible photoluminescence (PL) in the red and green, respectively, when optically pumped in the blue at wavelengths close to 450 nm. Their spectrally integrated PL intensity has been found to be proportional to the dose over at least three orders of magnitude, so that LiF solid-state dosimeters based on PL reading can be envisaged [1].
Recent measurements of the distinct F_2 and F_3^+ contributions to the PL spectrum showed a sub-linear behaviour of the PL intensity vs. absorbed dose curve for doses higher than ~10^5–10^6 Gy, especially as far as the green PL emitted by F_3^+ centres is concerned. While this phenomenon has been satisfactorily explained by means of a growth model that includes saturation of CC concentration [2], a further deviation from the linear (and sub-linear) growth was detected at even larger doses, say from ~10^6–10^7 Gy on, for which the PL intensity is seen to diminish for increasing dose. We try to explain such a behaviour by means of a model which includes the formation of quenching centres, and compare it with experimental PL spectra obtained for LiF samples that were irradiated at high doses.

[1] M. Piccinini, F. Ambrosini, A. Ampollini, L. Picardi, C. Ronsivalle, F. Bonfigli, S. Libera, E. Nichelatti, M. A. Vincenti, and R. M. Montereali, *Appl. Phys. Lett.* **106** (2015) 261108.
[2] M. Piccinini, E. Nichelatti, A. Ampollini, L. Picardi, C. Ronsivalle, F. Bonfigli, S. Libera, M. A. Vincenti, and R. M. Montereali, *Europhys. Lett.* **117** (2017) 37004.

ESR and luminescent properties of anion-deficient α-Al_2O_3 single crystals after high dose irradiation by pulsed electron beam

Daria V. Ananchenko*, Sergey V. Nikiforov and Sergey F. Konev

Ural Federal University, 21 Mira St., Ekaterinburg, Russia
**ananchenko.daria@mail.ru*

Anion-deficient α-Al_2O_3 single crystals are widely used for high-sensitivity luminescent detectors of ionizing radiation. It was shown [1] that after β-irradiation of Al_2O_3 single crystals with doses above 20 Gy, a resonance absorption line with g = 2.008 appears in the electron paramagnetic resonance (ESR) spectrum, the nature of this line is not clear at present. One of the effective sources of high-dose excitation is a pulsed electron beam of an accelerator [2]. This type of irradiation leads to the processes of intrinsic and impurity defects recharging in alumina and it is accompanied by filling of deep traps. ESR properties of Al_2O_3 crystals after irradiation with an electron beam have not been studied earlier. At the same time ESR study in combination with the measurement of TL and photoluminescence (PL) is necessary in the context of investigating the nature of radiation-induced defects in alumina. The purpose of the current work is a complex research of ESR, thermoluminescence (TL) and PL of alumina single crystals after irradiation with a pulse electron beam.

The samples of α-Al_2O_3 single crystals grown by using Stepanov's method in a strong reducing medium were investigated. The crystals were exposed at room temperature by an electron beam of an accelerator (pulse duration 2 ns, mean electron energy 130 ± 1 keV, and current density 60 A/cm^2, the mean absorbed dose 1.5 kGy/pulse). The irradiated samples were step-annealed with linear heating at a rate of 2 ˚C/s from room temperature to T=250-600 ˚C.

Irradiation of the crystals with a pulsed electron beam (10 kGy) leads to the appearance of ESR signal with $g_\perp$=2.008 (Fig. 1), similar to the absorption line [1], but less intensive. Along with this PL, emission of F^+-centers (330 nm) and F-centers (410 nm) decreases. ESR measurement results indicated that absorption line ($g_\perp$=2.008) remained stable under the stepped annealing at 250-600˚C and disappeared when the samples were held at T=600˚C for 3 min. The disappearance of ESR absorption line was accompanied by an increase in PL emission of F^+centers. One can hypothesize that disappearance of the resonance absorption line (g=2.008) is associated with a charge state conversion of radiation-induced defect as a result of the holes release from the deep trap at T=500-650˚C.

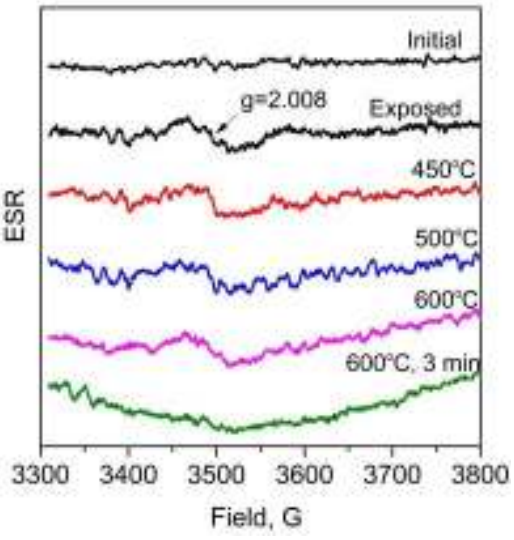

Figure 1. ESR spectra of Al_2O_3

[1] V. S. Kortov, D.V. Ananchenko, S. F. Konev and V. A. Pustovarov, *Nucl. Instrum. Methods Phys. Res., Sect. B* **407** (2017) 191.
[2] S.V. Nikiforov, V.S. Kortov, S.V. Zvonarev, E.V. Moiseykin and M.G. Kazantseva. *Rad. Meas.,* **71** (2014) 74.

Effect of the amounts of Li^+ additive on the luminescence properties of $LiBaPO_4$:Eu phosphors

Daniela A. Hora [1], Ariosvaldo J.S. Silva [1], Patresio A.M. Nascimento [1], David V. Sampaio [2], Benjamin J.A. Moulton [2], Ronaldo S. Silva [1], Marcos V. dos S. Rezende [3,*]

[1]*Universidade Federal de Sergipe, 49100-000, São Cristóvão, SE, Brazil*
[2]*Universidade Federal de São Carlo, 13565-905, São Carlos, SP, Brazil, São Carlos, SP, Brazil*
[3]*Universidade Federal de Sergipe, 49500-000, Itabaiana, SE, Brazil*
[*]*Corresponding author*

Lithium orthophosphates $LiBaPO_4$ have attracted much interest for their use in the luminescent devices due of their excellent properties such a stable structure, thermal stability, flat voltage profile, moderate phonon and exceptional optical damage threshold [1,2]. In general, luminescent properties are observed when lithium orthophosphates are doped with rare earth ions[3,4]. Recently, Eu-doped $LiBaPO_4$ phosphates have received much attention for application as new white light emission diodes (W-LEDs) phosphors [5]. In the literature, crystalline evolution, the effect of grain size, the influence of dopant concentration on the structural and optical properties has been studied. In this work, Eu-doped $LiBaPO_4$ phosphors were synthesized by sol–gel method using PVA as a chelating agent. The structures and photoluminescence (PL) properties of the as-prepared $LiBaPO_4$ phosphors were investigated by X-ray diffraction (XRD), X-ray Absorption spectroscopy (XAS) and PL spectroscopy. The synthesized samples were found to have single phase structure and the incorporation of dopant/ Li^+ additive did not affect the crystal structure. The luminescence properties of the Eu-doped $LiBaPO_4$ phosphors strongly depended on the amounts of the Li^+ additive. All the spectra exhibit transitions that are assigned to the Eu^{3+} and Eu^{2+} activators. A dominate band from Eu^{2+} are observed for the sample with greater Li^+ addiction. Therefore, we can conclude that Li^+ addiction contribute to the reduction $Eu^{3+} \rightarrow Eu^{2+}$.

Acknowledgment: Capes, CNPq e FINEP.

[1] R.-Y. Yang, K.-T. Chen, *Mater. Res. Bull.* **55** (2014) 246–253.
[2] R.-Y. Yang, H.-L. Lai, *J. Lumin.* **145** (2014) 49–54.
[3] D. Tu, Y. Liang, R. Liu, Z. Cheng, F. Yang, W. Yang, *J. Alloys Compd.* **509** (2011) 5596–5599.
[4] G. Ju, Y. Hu, Chen L., X. Wang, *J. Mater. Res.* **29** (2014) 519–526.
[5] J. Sun, X. Zhang, Z. Xia, H. Du, *J. Appl. Phys.* **111** (2012) 13101.

Energy Transfer in Dy^{3+}/Eu^{3+} Co-doped Glass-ceramics Containing Fluoride Nanocrystallites

M. Kemere*, U. Rogulis

Institute of Solid State Physics, University of Latvia, Kengaraga Street 8, Riga, Latvia
**Corresponding author*

The structure and optical properties of rare earth (RE) ions doped oxyfluoride glass-ceramics have been widely investigated for uses in sensors, scintillators, infrared detectors, lighting devices etc. [1-2]. Oxyfluoride glass-ceramics is a nanocomposite material that consists of a mechanically, chemically and thermally stable oxide glass matric and nanosized fluoride nanocrystals [3]. The advantage of fluoride nanocrystals, present in the material, is the possibility to alter and increase the luminescence intensity of dopant ions if they substitute cations in the fluoride nanocrystals. Dy^{3+} doped materials are widely used in optical devices, including white light phosphors [4]. Research shows, that adding of Eu^{3+} ions can improve the colour properties of the emitted light.

In the present study, luminescence of europium and dysprosium co-doped glass-ceramics containing SrF_2 and CaF_2 nanocrystallites has been investigated and analysed to tailor the local structure around RE ions with RE ions luminescence and energy transfer efficiency.

In the present study, oxyfluoride glasses with the compositions SiO_2-Al_2O_3-Na_2O-SrF_2 and SiO_2-Al_2O_3-CaO-CaF_2, activated with Dy^{3+} and Eu^{3+} ions (0-4 mol%) have been synthesized. The obtained glasses were annealed at 650, 680, 700 and 750 $^{\circ}$C temperature (1 to 4 hours) to obtain glass-ceramics containing SrF_2 or CaF_2 nanocrystallites. Luminescence emission, excitation and decay measurements at room temperatures and low temperatures have been performed as well as structure investigations (XRD, SEM techniques).

In the glass-ceramics containing SrF_2 nanocrystallites, luminescence lifetimes of Dy^{3+} ions have increased compared to the precursor glasses. This result indicates that a part of rare earth ions have been incorporated in SrF_2 nanocystallites The energy transfer efficiency processes in both series have been analysed. In the SrF_2 containing series, energy transfer efficiency in glass ceramics increases while in CaF_2 containing series it does not change. The colour properties of the emitted light and their validity for white light sources were analysed.

This work was carried out thanks to SIA “Mikrotik” donation. Donations are administred by the University of Latvia Foundation.

[1] D. Chen, W. Xiang, X. Liang, J. Zhong, H. Yu, M. Ding, H. Lu, Zh. Ji,, *J. Eur. Ceram. Soc.* **35(3)** (2015) 859-869.
[2] S. H. Lee, S. R. Bae, Y. G. Choi, W. J. Chung, *Opt. Mater.* **41** (2015) 71 -74.
[3] P. P. Fedorov, A. A. Luginina, A.I. Popov, *J. Fluorine Chem.* **172** (2015) 22-50.
[4] D. Rajesh, K. Brahmachary, Y.C. Ratnakaram, N. Kiran, A.P. Baker, G.G. Wang, *J. Alloy. Comp.* **646** (2015) 1096-1103.

Synthesis, Characterization and Properties of Multifferroic $Na_{0.5}Bi_{0.5-x}Eu_xTiO_3$ Perovskite Red Phosphor

T. Thomas [1], P. Kuruva [2], R. Palai [3] and W.M. Jadwisienczak [4,*]

[1]*Department of Metallurgical & Materials Engineering, IIT Madras, Chennai, India*
[2]*Department of Physics, National Taiwan Normal University, Taipei, Taiwan*
[3]*Department of Physics University of Puerto Rico, San Juan, PR, USA*
[4]*School of EECS, Ohio University, Athens, OH, USA*
**Corresponding author: jadwisie@ohio.edu*

In this paper we report on synthesis, optical, dielectric, ferroelectric, magnetodielectric, and magnetic properties in complex perovskite Europium-doped $Na_{0.5}Bi_{0.5}TiO_3$ (NBT:Eu) phosphors prepared by solid-state reaction. The as-synthesized NBT:Eu phosphors have Eu concentration between 1 to 20 at.% using A-site substitution in the general ABO_3 perovskite oxide are single phase, polycrystaline materials as determined by powder X-ray diffraction study [1]. The luminescence intensity monitored at 617 nm increases linearly with the Eu concentration increase up to 20 at.% without indication of typically observed concentration quenching effect. The photoluminescence (PL) and cathodo-luminescence (CL) spectra are dominated by sharp characteristic emission lines corresponding to Eu^{3+} intra-$4f^n$ shell transitions centered at 593 nm ($^5D_0 \rightarrow {}^7F_1$), 617 nm ($^5D_0 \rightarrow {}^7F_2$) and 700 nm ($^5D_0 \rightarrow {}^7F_4$), respectively. The PL excitation spectroscopy reveal that optically active Eu^{3+} ion centers can be effectively excited with photons between 325 nm to 550 nm via energy migration or direct resonant excitation processes. The electron paramagnetic resonance shows that characteristic electron spin resonance signal of Eu^{2+} ions are not observed in these phosphors. The temperature dependent PL and CL studies have shown that the luminescence of Eu^{3+} ions occupying centro-symmetric and non-centro-symmetric sites is very similar; however corresponding temperature thermal quenching mechanisms are different for photon- and electron-excited spectra. Dielectric permittivity, dielectric loss, impedance, and phase angle of NBT:Eu are studied as function of frequency and magnetic field [2]. Magnetic properties measurements shows a novel room temperature ferromagnetic like behavior, which is unusual, but can be explained by the local structural disordering or phase coexistence. Finally, we will discuss the defects in NBT:Eu and their effect on observed optical, electric and magnetic properties of this novel multifferroic material.

[1] R. Prusty, P. Kuruva, U. Ramamurty, Thomas T., *Sol. State Commun*., **173** (2013) 38-41.
[2] A. Kalaskar, B. Narayana Rao, Thomas T., and R. Ranjan, *J. Appl. Phys*. **117** (2015) 244106.

Free and bound excitons in ZnO at variable excitation density

Patrick Martin [1], Nikita Fedorov [1], Andrei Belsky [2,*], Andrey N. Vasil'ev [3]

[1]*Institute of Light and Matter, CNRS, University Lyon1, France*
[2]*CELIA, Université de Bordeaux, CNRS, CEA, 33405 Talence, France*
[3]*Skobeltsyn Institute of Nuclear Physics, Moscow State University 119991, Moscow, Russia*
**Corresponding author*

ZnO crystals and nanoparticles are promising subnanosecond scintillators. The intensity and kinetics of ZnO emission strongly depend on the fluence of excited photons both at ambient temperature and low temperatures. We perform systematic study of ZnO timeresolved luminescence under intense interband femtosecond excitation using 3rd harmonic of Ti:Sa laser (266 nm).

The dependence of emission spectra and decay kinetics in different bands at 10K can be analyzed using hypothesis based on "bound multiexciton-impurity complexes" [1]. For low intensities the emission of single bound exciton complexes (standard DX) and all phonon replicas have the same kinetics. When the intensity increases, double-exciton complexes appears. Such complexes should decay with conversion into single-exciton complexes. The radiation decay time for these complexes should be shorter than the decay time for singleexciton complex, roughly in two times, since each electron from this complex overlap with two holes. In the double-exciton complex the electron-phonon interaction should be also less than for single-exciton complex, since the electric fields in this complex are weaker in comparison with single-exciton one. Thus phonon replicas for double-exciton complex decay should be also weaker. Going further, three-exciton complexes should be faster and with additionally reduced phonon replicas. High intensities of excitation produce multiexciton complexes, without replicas. The energy of the transition in such complexes is slightly higher than that for single-exciton DX, but lower than for free exciton (FX). This is just what we see in emission spectra and kinetics when the excitation intensity increases.

Emission of FX dominates at T>140K. Systematic study of the luminescence intensity and decay characteristics when the density of created excitations at the center of the laser spot changes from 10^{18} to 10^{23} cm^{-3} can be performed using z-scan technique. The yield of luminescence strongly depends on the peak concentration of excitations, and the behavior of the yield differs from that for crystals with conventional excitons (see e.g. [2]). In contrary to conventional excitons, for which the yield is constant for low intensities, the yield of ZnO increases superlinearly with concentration of excitations up to 10^{21} cm^{-3}. For both types of excitons the yield drops for higher concentrations. Possible reasons of such anomalous nonlinear behavior of yield and kinetics are discussed.

[1] P. Belli, A. Incicchitti, and F. Cappella, *Int. Journal of Modern Physics A* **29** (2014) 1443011.
[2] Dmitry Spassky at al, *Excitation density effects in decay kinetics of $CaMoO_4$ and $ZnMoO_4$* (this conference)

Phase Transition, Structural Defects and Stress Development in Superficial and Buried Regions of Femtosecond Laser Modified Diamond

M.C. Rossi [1,*], S. Salvatori [2], G. Conte [3], T. Kononenko [4] and V. Valentini [5]

[1]*University of Roma Tre, Engineering Dept.,Via V. Volterra 62, 00146 Rome, Italy*
[2]*University Niccolò Cusano, Via don Carlo Gnocchi 3, 00166 Rome, Italy*
[3]*University of Roma Tre, Dept. of Science,Via della Vasca Navale 84, 00146 Rome, Italy*
[4]*A.M. Prokhorov General Physics Institute, Moscow, Russia*
[5]*Institute for Structure of Matter, CNR, Monterotondo (Rome), Italy*

Micro-Raman spectroscopy has been used to monitor structural defects and stress state developing in 3D graphitic electrodes realized by laser irradiation for the achievement of optimized carrier collection in ionizing radiation and particle diamond detectors [1].
Buried graphite pillars, 375±25 μm deep, 150±10 μm apart and 20 μm in diameter, were fabricated in a single-crystal 3×3×0.5 mm^3 CVD-diamond sample by means of a 400 fs pulsed VaryDisc50 laser (Dausinger+Giesen Gmbh) operating at 1030 nm and 200 kHz pulse repetition rate. The same conditions were also used for the realization of two series of graphitic strips on the surface (50 μm wide and 10 μm thick) allowing buried pillars connections. Details on the fabrication process of graphitic electrodes can be found in [2].
Micro-Raman measurements were performed in a confocal backscattering geometry by a DILOR XY spectrometer having spectral resolution of 1 cm^{-1}. The λ=514.5 nm laser line of an Ar-ion laser was focused down to a spot size of 1 μm.
Raman spectra of untreated regions exhibits the typical diamond peak at 1332 cm^{-1} which changes in intensity, width and position within the graphitic surface strips, where a G band at 1580 cm^{-1} is also detected suggesting a mixed composition of the laser modified material. Shifting of the diamond Raman peak is detected by scanning the laser spot between adjacent graphitic electrodes and along buried pillars, pointing out that phase transition from diamond to graphitic carbon is accompanied both by stress development and by structural disorder in the residual diamond tissue. In these regions, Raman spectra also exhibits a broad photoluminescence background signal, which is often observed in microcrystalline diamond. In particular, a splitting of the diamond Raman peak is detected at the pillars top surface, close to a crater, suggesting the occurrence of a laser-induced anisotropic stress.
From these results it is then tentatively suggested that charge transport in laser modified regions occurs through both graphitic carbon and disordered diamond paths, thereby affecting the 3D carrier collection.

[1] T. Kononenko, A. Bolshakov, V. Ralchenko, V. Konov, P. Allegrini, M. Pacilli, G. Conte, and E. Spiriti, *Applied Physics A,* **114** (2014) 297.
[2] G. Conte, P.Allegrini, M.Pacilli, S.Salvatori, T.Kononenko, A.Bolshakov, V. Ralchenko, V.Konov, *Nuclear Instruments and Methods in Physics Research A,* **799** (2015)10.

The influence of the level of H-termination on wetting properties of CVD diamond surface

L. Mosińska*, K. Fabisiak, P. Popielarski

Institute of Physics, Kazimierz Wielki University, Powstańców Wielkopolskich 2, 85-090 Bydgoszcz, Poland

The tailoring of diamond films properties was achieved by adjusting technological parameters of HF CVD process. The synthesized diamonds layers can acquire in this way suitable properties for particular application. Additionally very important problem is diamond surface termination as for example oxidation and hydrogenation, which strongly modify diamond surface electrical conductivity due to change its wettability. The wettability can be changed from hydrophilic to less hydrophilic or even up to hydrophobic.

The wetting properties of diamond surface is determined by contact angle method. The diamond surface termination, controlled by contact angle method, is studied in relation to its SEM pictures (morphology) and Raman spectroscopy (sp^2/sp^3 ratio and diamond quality).

The diamond surface termination is very important factor which is responsible for the electrochemical output in such application as Solution Gated Field Effect Transistor (SG FET).

The main goal is to show correlation between diamond morphology, quality, sp^2/sp^3 ratio and diamond surface wettability.

Morphological and Cathodoluminescence study of defects in diamond films grown by HF CVD technique

K. Paprocki*, P. Malinowski and K. Fabisiak

Institute of Physics, Kazimierz Wielki University, Powstańców Wielkopolskich 2, 85-090 Bydgoszcz, Poland

**Corresponding author: paprocki@ukw.edu.pl*

Defects and impurities in diamond films grown by chemical vapor deposition (CVD) were analyzed by cathodoluminescence spectroscopy (CL), Scanning Electron Microscopy (SEM) and X-ray diffraction (XRD).

The combination of CL and XRD makes it possible to correlate the film microstructure with the electronic structure due to defects. A correlation between the color luminescence centers and the diamond film preferred orientation (as estimated via texture coefficient TC_{hkl}) was derived. Depending on the diamond's film morphology and preferred orientation different CL spectra were observed.

Band A emission (2.88 eV) is the major emission band in the blue-green region and dominant in the spectra of all samples except that having <400> prefered orientation. It is believed that band A emission originates from donor-acceptor pairs localized around dislocation by electron-hole recombination. When preferred orientation change on <400> the A band is very weak and dominant peak is observed in red region at about 2.055 eV observed also in HPHT diamonds. For sample showing mixed character above bands are observed simultaneously.

Author Index